UNIVERSITY OF CALIFORNIA
RIVERSIDE

Genome-Wide Analysis of MicroRNA and Messenger RNA Expression Profiles During Fruit Development in Grafted Citrus

A Dissertation submitted in partial satisfaction
of the requirements for the degree of

Doctor of Philosophy

in

Plant Biology

by

Rachel Julie Rattner

June 2019

Dissertation Committee:
Dr. Mikeal Roose, Chairperson
Dr. Linda Walling
Dr. Hailing Jin

The Dissertation of Rachel Julie Rattner is approved:

Committee Chairperson

University of California, Riverside

ACKNOWLEDGEMENTS

I would like to thank my advisor, Dr. Mikeal Roose, as well as all past and present members of the Roose lab, particularly Dr. Claire Federici, Dr. Chandrika Ramadugu, Dr. Sai Zadgaonkar, Yoko Eck, Andrew Soto, Karene Trunnelle, and Michelle Lu. You have helped me with everything from fruit quality data collection and sample preparation to experimental design and general advice throughout my time in graduate school. I appreciate your support and friendships along the way.

I thank the members of my dissertation committee, Dr. Linda Walling and Dr. Hailing Jin for their insights and direction during my time at UCR. Your assistance in the development of my project was essential to its success. I also thank the additional members of my qualifying exam committee for their guidance in the first two years of my PhD training: Dr. Norman Ellstrand, Dr. Timothy Close, and Dr. Howard Judelson.

Finally, I would like to thank my friends and family who have made my time in graduate school and Riverside enjoyable. To my roller derby friends who became my family in Riverside. To my parents, for encouraging and fostering of my love of STEM fields for as long as I can remember. You have always been supportive of all my decisions to further my career, even when it meant moving across the country. To my brother, for being a great role model and always pushing me to better myself. Special thanks to my partner, Jon Norris, who has provided an endless supply of love and support, uplifting me when I needed it the most. Your kindness and laughter have helped me more than you know.

ABSTRACT OF THE DISSERTATION

Genome-Wide Analysis of MicroRNA and Messenger RNA Expression Profiles During Fruit Development in Grafted Citrus

by

Rachel Julie Rattner

Doctor of Philosophy, Graduate Program in Plant Biology
University of California, Riverside, June 2019
Dr. Mikeal Roose, Chairperson

Citrus, one of the most economically important fruit crops in the world, is commercially propagated through grafting. Varying scion-rootstock combinations cause substantial effects on trees that often influence yield and fruit quality traits. Presently, the explanation for these differences has not been extensively studied at the molecular level. One potential reason for rootstock effects on fruit quality is the presence of small RNAs, molecules known to affect gene expression and plant development.

It was hypothesized that grafting diverse rootstocks influences small RNA populations in citrus, which can greatly impact fruit quality. By using mRNA-seq and small RNA-seq, an integrative analysis of microRNA and mRNA expression profiles was performed on grafted citrus. In this study, fruit and root samples were collected from sweet orange scions grafted onto four genetically differing rootstocks (trifoliate orange, Carrizo citrange, rough lemon, and sweet orange). Differentially expressed microRNA (DEM) and mRNA profiles were identified according to fold change analysis and the relationships between these molecules were identified.

A total of 1,633 unique genes in the fruit tissues and 11,368 in the root tissues were identified as differentially expressed between genotypes in at least one collection date during fruit development. A majority of the differences came from the comparisons between trifoliate and rough lemon rootstocks. GO and KEGG functional annotation analyses revealed that genes differentially expressed between trifoliate and rough lemon rootstocks were related to defense response, cell wall organization and biosynthesis, and carbohydrate metabolism. DEGs in fruit tissues grown on these rootstocks were related to transcription regulation and plant hormone signal transduction.

The small RNA sequencing data identified 603 known, conserved miRNAs. Of these, 188 were differentially expressed between trifoliate and rough lemon rootstocks. Reads that were not homologous to any known plant miRNAs were assessed as potentially novel small RNAs. 17 potential novel microRNAs were identified in citrus, ten of which were differentially expressed between genotypes. Quantitative reverse transcriptase-polymerase chain reaction (qRT-PCR) analysis confirmed the results from the sequencing data and revealed a negative correlation between several DEMs and their respective target genes, whose function may play a crucial role in citrus fruit development.

TABLE OF CONTENTS

LIST OF FIGURES

LIST OF TABLES

General Introduction

The importance of the citrus industry

The citrus industry is one of the most economically importance fruit producers in the world. There are about 140 countries growing citrus commercially and the total output of citrus globally was 124 million tons in 2016 according to the Food and Agriculture Organization (www.fao.org/faostat/). Oranges accounted for 75 million tons of that production and 43% of those oranges were produced in the United States. Citrus production in the United States was valued at $3.44 billion according to the United States Department of Agriculture[1]. The total production of citrus in the United States in the 2018 growing season was 6.1 million tons on a total of 679 thousand acres. California produced 58 percent of the United States total, producing 3.6 million tons of citrus on 278 thousand acres. Approximately 75 percent of California's citrus production is sold to the fresh market opposed to being processed into other commodities, such as juice. Oranges accounted for 64 percent of the total citrus produced in the United States and were valued at $1.8 billion[1]. In addition to their monetary value, citrus is also a source of nutrition for Americans. For example, oranges are an excellent source of vitamin C, vitamin A, calcium, iron, and potassium, which are all essential for a healthy diet[2].

Citrus fruit quality

Fruit quality is a measure of the desired traits in a certain kind of fruit. Fruit quality at the simplest level is the sum of all attributes that create customer appeal. Scientists turn fruit

quality into a complex matter, attempting to quantify many separate horticultural, environmental, physiological, and biochemical components of a fruit, which all contribute on some level to fruit quality. Although desired traits can vary between individuals, citrus fruit quality is often based upon size, shape, color, peel, uniformity, organic compounds, acidity, flavor, ease of peeling, and seed content of the fruits[3]. Each of these factors needs to be considered during citrus breeding programs. The relative importance of each quality component depends on its intended use (e.g. fresh or processed) and this can vary among producers and consumers. To producers, high yield, good appearance, ease of harvest, and long shelf life are the most important. Consumers, on the other hand, judge quality of fresh fruit based on the appearance (freshness) and firmness at the time of purchase. Subsequent purchases will be based on the flavor quality and nutritional value of the fresh fruit[4].

Maturity at harvest is the most important factor that determines final fruit quality. The main indicators of citrus maturity are coloration, sugar and acid levels, and percent juice. Maturity indices are used to decide when a product should be harvested to ensure an acceptable quality for the consumer. California's mandatory quality standards (California Food and Agriculture Code) for fresh fruits include objective indices of maturity to guarantee the minimum acceptability of their flavor quality to consumers. Enforcement of these standards is the responsibility of the fruit growers and is monitored by the Agriculture Commissioner in each county, representing the California Department of Food and Agriculture. In citrus, these indices differ by variety. Beginning in 2012, navel oranges are required to follow the California Standard to determine maturity, which

follows the formula [Brix - (Titratable Acid * 4)) * 16.5][5,6]. This formula was consistently a better indicator of flavor than the previous index (sugar:acid ratio of 8)[4].

Grafting and rootstock-scion combinations

Citrus plants grown for fruit production are rarely grown from seed. Virtually all commercial citrus is propagated by grafting and the rootstock has a significant impact on the physiological traits of the citrus scion cultivars. Grafting is the process by which a part of one plant (in citrus usually a bud) is attached to a cut made on a plant with a healthy root system. The plant with the healthy root system is called the rootstock, and the part of the plant being attached to this system is called the scion[7]. The scion confers the properties that are desired by the breeder or grower, while the rootstock nourishes the plant. One of the many advantages of grafting is shortening of the juvenile phase, allowing for the trees to produce fruit many years earlier than producing from seed[8].

Due to the large variation in growing conditions and climate in California, different citrus rootstocks are required to improve fruit quality in numerous diverse climates, as well as resist various pests and diseases[9]. Rootstocks impart certain traits onto the scion and the effects of rootstocks can be large. Castle reviewed rootstock effects on fruit quality in citrus[3]. In the review, he states that citrus rootstocks affect many external and internal fruit characteristics including size, shape, peel thickness, juice content, and juice soluble solids concentration. The most significant impacts are on growth and vigor, tree nutrition, stress resistance, and fruit quality[10–13]. The magnitude of rootstock effects on fruit quality factors ranges from 4% to 24%, depending on the scion-rootstock combination[12].

In the present study, four rootstocks were chosen from a rootstock trial with Washington navel orange scion in Riverside, CA to assess for various fruit quality traits; Argentina sweet orange, Schaub rough lemon, Carrizo citrange, and Rich 16-6 trifoliate orange. These rootstocks have imparted significant phenotypic differences on overall growth and fruit quality in many previous studies[10,14–21]. Generally speaking, rough lemon rootstocks produce the highest yield and fruit size, but this fruit is often of lower quality (lower acidity and lower levels of total soluble solids). Trifoliate orange rootstock, on the other hand, produces high quality fruit, with high yield on smaller trees. Carrizo citrange rootstocks produce intermediate yield with good fruit quality. Sweet orange rootstocks produce good quality fruit but are very susceptible to various citrus diseases, so sweet orange is rarely used as a rootstock for commercial growth.

A general explanation for the effects that varying rootstocks have on quality is their ability to uptake and utilize water and nutritional elements that play crucial roles in citrus quality and productivity. These effects have been well documented in a variety of crops, including pepper, tomato, pear, grape, watermelon, apple, and citrus[3,22–29]. However, these studies still leave many unanswered questions about the mechanisms by which rootstocks impart these traits, especially at the regulatory level.

Transcriptome studies in citrus

In order to elucidate effects of rootstocks, previous studies in apple[30], grape[31], sweet cherry[32], and other fruit crops have examined transcriptome changes in various

rootstock-scion combinations. In citrus, gene expression profiling has been used to understand rootstock effects and responses to biotic and abiotic factors[33–35]. These studies look at transcriptome changes in grafted citrus in response to fungal inoculation, cold stress, and boron deficiency. In these studies transcriptomes of leaves from the same scion grafted onto differing rootstocks were subjected to RNA-seq in order to observe rootstock responses to biotic and abiotic stressors. In another study, expression studies of leaves from mandarin grafted onto various rootstocks were analyzed in order to explain rootstock effects on the growth of scions[15].

Additionally, many transcriptomic studies have also been performed in citrus to explain mechanisms of fruit ripening and development in commonly grown citrus cultivars[36–46]. Many of these studies take advantage of the many citrus bud mutations (bud sports) with altered aspects of fruit quality in order to compare gene expression to that in the non-mutant ancestor cultivar. Several of the papers utilize late ripening mutants to assess genes that are important for ripening. Genes involved in hormone-signaling pathways are the main variations associated with ripening in the majority of these reports. Others use mutations in acid and sugar accumulation to explain the molecular mechanisms underlying those processes. Yet to date, none of these reports have linked the genetic effects of citrus rootstocks to fruit quality.

There have been some previous studies showing changes in the transcriptome of various rootstock genotypes, especially in response to biotic and abiotic stressors. These types of changes have been shown in Arabidopsis, corn, mulberry, tomato, and poplar[47–51]. Though when it comes to root transcriptome studies in citrus, knowledge is

extremely limited. A small number of studies have been performed that evaluated trifoliate, trifoliate hybrid, and mandarin root transcriptomes in response to citrus diseases, but these studies each assessed only one genotype[52–54]. Even in an RNA-seq based approach to establish a reference transcriptome for citrus, 28 samples were used for the study and only two were obtained from roots[55]. The root samples collected for this study were sour orange and trifoliate genotypes, but samples were grouped by organ to perform differential expression and subsequent analyses. To our knowledge, there have been no comparative studies of citrus root transcriptomes between genotypes during fruit development.

Small RNA expression profiles in grafted crops

As highlighted above, RNA sequencing has become a very powerful and widely used technology to profile the transcriptome. This has provided valuable information for gene identification and defining their potential roles in the grafting process as well as during fruit development and maturation. However, additional regulators need to be discovered to better understand the regulatory network that controls these processes.

One regulatory factor that could contribute to rootstock effects on the scion are plant small RNAs. One type of small RNA, microRNAs (miRNAs), are 21-24 nucleotide RNAs that are products of genes in plants[56,57]. Generally, miRNA genes are transcribed into primary transcripts (pri-miRNA), which are processed into the stem-loop precursor (pre-miRNA) molecule by a DCL (Dicer-like) protein. These pre-miRNAs are further processed by DCL1 into a miRNA and miRNA* duplex[58]. In plants, the mature miRNA

sequence can bind to transcripts of target mRNAs based on perfect or near-perfect complementarity, leading either to cleavage-induced degradation of the mRNA or translational inhibition[59,60].

Increasing evidence has shown that the miRNAs in plants and animals consist of a set of conserved, ancient miRNAs, as well as many recently evolved species-specific miRNAs[61,62]. The availability of next generation sequencing technologies provides high-throughput tools to discover species-specific miRNAs in a variety of plants, such as *Arabidopsis thaliana*[63], *Oryza sativa* (rice)[64], *Populus trichocarpa* (poplar)[65], *Triticum aestivum* (wheat)[66], *Zea mays* (corn)[67], *Medicago tuncatula* (legume)[68], *Lycopersicon esculentum* (tomato)[69], *Gossypium hirsutum* (cotton)[70,71], *Taxus chinensis* (yew)[72,73], *Vitis vinifera* (grape)[74] and *Citrus trifoliata* (trifoliate orange)[75].

Plant miRNAs act as master regulators and control genes involved in various biological and metabolic processes and are thus imperative to proper plant development[76–78]. Recently, there has been an emergence of studies demonstrating miRNAs have a critical role in the regulation of fruit development and maturation. For example, in strawberry, miR159 acts as a ripening regulator by targeting a MYB transcription factor, which plays a critical role during the transition from development to ripening[79]. Additionally, miR73 was found to be involved in regulation of strawberry fruit ripening by targeting a gene that affects the abscisic acid-signaling pathway[80]. Application of this high-throughput technology to miRNA-related research has identified numerous miRNAs involved in fruit development and maturation in many fruit producing species, including apple[81], grape[82], peach[83], blueberry[84], date palm[85] and tomato[69]. In citrus, many miRNAs

have been identified in different tissues, such as leaf, flower, fruit, and callus[86–89]. A comparative study was performed between a spontaneous late-ripening sweet orange mutant and the wild-type sweet orange cultivar to better understand the role of miRNAs in citrus fruit ripening. In this study, csi-miR156k, csi-miR159, and csi-miR166d were found to suppress specific transcription factors (GAMYBs, SPLs, and ATHBs) that are supposed to be important regulators involved in citrus fruit development and ripening[90].

While grafting is known to induce many phenotypic differences, including those involved in fruit quality, there have been very few studies to assess the involvement of miRNAs in the regulation of graft-induced physiological events. Comparisons of miRNA expression profiles in various rootstock-scion combinations have been investigated in a few crops such as grapevine, watermelon, cucumber and tomato[91–95]. In general, it was found that grafted plants exhibit differential expression of miRNAs compared to non-grafted plants. Furthermore, expression profiles of miRNAs were altered when plants were grafted onto differing rootstocks, suggesting they play a role in regulating biological and metabolic processes resulting from grafting. In citrus, the hypothesis that changes in activity of specific miRNAs is one of the mechanisms involved in the physiological effects of grafting was tested by determining the expression of miRNAs in different scion-rootstock combinations. Changes in expression of the miRNAs tested was associated with the reduction of juvenility and micronutrient requirements of the grafted plants[96]. However, the precise mechanisms could not be elucidated. Taken together, it is hypothesized that miRNAs in diverse citrus rootstocks are differentially expressed in response to grafting and can influence processes related to fruit development and ripening.

Dissertation project

My dissertation study was originated with the goal of identifying small RNAs that are likely causing changes in fruit quality in grafted citrus. To do this, an integrated study of miRNA and mRNA transcriptomes of sweet orange scions grafted onto varying rootstocks was performed. Transcriptomes and miRNomes of fruit and root tissues from four different scion-rootstock combinations at four time points throughout fruit development were obtained. These results were correlated with the changes in fruit quality observed when fruit are grown on these genetically diverse rootstocks. Trifoliate orange, known for its high-quality fruit and tolerance to various biotic and abiotic stressors was compared to rough lemon which historically produces high yield and large fruit that are lacking in flavor. In Chapter 1, I report a detailed analysis of the temporal changes and genotypic differences in gene and miRNA expression in root tissue of different rootstocks. To the best of my knowledge, this is the first comparison of root transcriptomes performed in citrus. In Chapter 2, expression data from fruit of trees grafted onto the four different rootstocks was assessed. Changes in expression throughout development were linked to fruit quality variation. Additionally, the role of miRNAs in regulating the biological and metabolic processes that were affected in each of these chapters was investigated. The results provide a global examination of the molecular mechanisms underlying graft-induced changes in citrus fruit development and ripening.

References

1. Citrus Fruits 2018 Summary 08/28/2018. 35 (2018).

2. *USDA National Nutrient Database for Standard Reference, Legacy*. (US Department of Agriculture, Agricultural Research Service, Nutrient Data Laboratory, 2018).

3. Castle, W. S. Rootstock as a fruit quality factor in citrus and deciduous tree crops. *New Zealand Journal of Crop and Horticultural Science* **23**, 383–394 (1995).

4. Kader, A. A. Fruit maturity, ripening, and quality relationships. *Acta Horticulturae* 203–208 (1999). doi:10.17660/ActaHortic.1999.485.27

5. California Citrus Mutual. The California Standard. *California Citrus Mutual* Available at: https://www.cacitrusmutual.com/marketing/the-california-standard/. (Accessed: 27th March 2019)

6. Obenland, D. *et al.* Determinants of flavor acceptability during the maturation of navel oranges. *Postharvest Biology and Technology* **52**, 156–163 (2009).

7. Elam, P. Budding & grafting citrus & avocados in the home garden. (1997). doi:10.3733/ucanr.8001

8. Wareing, P. F. Problems of juvenility and flowering in trees. *Journal of the Linnean Society of London, Botany* **56**, 282–289 (1959).

9. Bitters, W. P. Citrus rootstocks: their characters and reactions (an unpublished manuscript) ca. 1986. 236 (1986).

10. Martínez-Cuenca, M.-R., Primo-Capella, A. & Forner-Giner, M. A. Influence of rootstock on citrus tree growth: effects on photosynthesis and carbohydrate distribution, plant size, yield, fruit quality, and dwarfing genotypes. *Plant Growth* (2016). doi:10.5772/64825

11. Simpson, C. R. *et al.* Growth response of grafted and ungrafted citrus trees to saline irrigation. *Scientia Horticulturae* **169**, 199–205 (2014).

12. Castle, W. S. A career perspective on citrus rootstocks, their development, and commercialization. *HortScience* **45**, 11–15 (2010).

13. Zhang, X., Breksa, A. P., Mishchuk, D. O. & Slupsky, C. M. Elevation, rootstock, and soil depth affect the nutritional quality of mandarin oranges. *J. Agric. Food Chem.* **59**, 2672–2679 (2011).

14. Al-Jaleel, A. & Zekri, M. Effects of rootstocks on yield and fruit quality of 'Parent Washington Navel' trees. *Proceedings of the Florida State Horticultural Society* **116**, 270–275 (2003).

15. Liu, X.-Y., Li, J., Liu, M.-M., Yao, Q. & Chen, J.-Z. Transcriptome profiling to understand the effect of citrus rootstocks on the growth of 'Shatangju' mandarin. *PLOS ONE* **12**, e0169897 (2017).

16. Roose, M. L. Citrus rootstock breeding and evaluation. *Annual Report* 3 Available at: https://www.citrusresearch.org/wp-content/uploads/2008-Michael-L-Roose-Rootstock-Breeding-Evaluation.pdf. (Accessed: 27th March 2019)

17. Roose, M. L., Cole, D. A., Atkin, D. & Kupper, R. S. Yield and tree size of four citrus cultivars on 21 rootstocks in California. *Journal of the American Society for Horticultural Science* (1989).

18. Roose, M. Lane Late navel orange replant trial at Lindcove, Available at https://plantbiology.ucr.edu/faculty/LLLC-full-Summary-4-09-final.pdf. (Accessed: 27th March 2019)

19. Rouse, R. E. Citrus fruit quality and yield of six Valencia clones on 16 rootstocks in the Immokalee foundation grove. *Proceedings of the Florida State Horticultural Society* **113**, 112–114 (2000).

20. Sinclair, W. & Bartholomew, E. Effects of rootstock and environment on the composition of oranges and grapefruit. *Hilgardia* **16**, 125–176 (1944).

21. Rootstocks effects on fruit quality. *Factors affecting fruit quality. Lake Alfred: University of Florida* 24–34 (1988).

22. Cohen, S. & Naor, A. The effect of three rootstocks on water use, canopy conductance and hydraulic parameters of apple trees and predicting canopy from hydraulic conductance. *Plant, Cell & Environment* **25**, 17–28 (2002).

23. Ikinci, A., Bolat, I., Ercisli, S. & Kodad, O. Influence of rootstocks on growth, yield, fruit quality and leaf mineral element contents of pear cv. 'Santa Maria' in semi-arid conditions. *Biol Res* **47**, (2014).

24. Jaskani, M. J. *et al.* Effect of rootstock types on leaf nutrient composition in three commercial citrus scion cultivars of Pakistan under the ASLP Citrus Project. *Acta Horticulturae* 131–136 (2016). doi:10.17660/ActaHortic.2016.1128.18

25. Lambert, J., Anderson, M. & Wolpert, J. Vineyard nutrient needs vary with rootstocks and soils. *California Agriculture* **62**, 202–207 (2008).

26. Ropokis, A., Ntatsi, G., Kittas, C., Katsoulas, N. & Savvas, D. Impact of cultivar and grafting on nutrient and water uptake by sweet pepper (*Capsicum annuum* L.)

grown hydroponically under Mediterranean climatic conditions. *Front Plant Sci* **9**, (2018).

27. Savvas, D. *et al.* Impact of grafting and rootstock on nutrient-to-water uptake ratios during the first month after planting of hydroponically grown tomato. *The Journal of Horticultural Science and Biotechnology* **92**, 294–302 (2017).

28. Yetisir, H. & Erhan, A. Rootstocks effect on plant nutrition concentration in different organ of grafted watermelon. **2013**, (2013).

29. Toplu, C., Kaplankran, M., Demirkeser, T. H. & Yldz, E. The effects of citrus rootstocks on Valencia Late and Rhode Red Valencia oranges for some plant nutrient elements. *African Journal Of Biotechnology* (2008). Available at: https://eurekamag.com/research/033/791/033791269.php. (Accessed: 28th March 2019)

30. Jensen, P. J. *et al.* Rootstock-regulated gene expression patterns in apple tree scions. *Tree Genetics & Genomes* **6**, 57–72 (2010).

31. Cookson, S. J. & Ollat, N. Grafting with rootstocks induces extensive transcriptional re-programming in the shoot apical meristem of grapevine. *BMC Plant Biology* **13**, 147 (2013).

32. Prassinos, C., Ko, J.-H., Lang, G., Iezzoni, A. F. & Han, K.-H. Rootstock-induced dwarfing in cherries is caused by differential cessation of terminal meristem growth and is triggered by rootstock-specific gene regulation. *Tree Physiol* **29**, 927–936 (2009).

33. Gao, X., Zhao, S., Xu, Q.-L. & Xiao, J.-X. Transcriptome responses of grafted *Citrus sinensis* plants to inoculation with the arbuscular mycorrhizal fungus G*lomus versiforme*. *Trees* **30**, 1073–1082 (2016).

34. Huang, Y., Si, Y. & Dane, F. Impact of grafting on cold responsive gene expression in Satsuma mandarin (*Citrus unshiu*). *Euphytica* **177**, 25–32 (2011).

35. Liu, X. *et al.* Transcriptome changes associated with boron deficiency in leaves of two citrus scion-rootstock combinations. *Front. Plant Sci.* **8**, (2017).

36. Huang, D., Zhao, Y., Cao, M., Qiao, L. & Zheng, Z.-L. Integrated systems biology analysis of transcriptomes reveals candidate genes for acidity control in developing fruits of sweet orange (*Citrus sinensis* L. Osbeck). *Front. Plant Sci.* **7**, (2016).

37. Lin, Q. *et al.* Transcriptome and metabolome analyses of sugar and organic acid metabolism in Ponkan (*Citrus reticulata*) fruit during fruit maturation. *Gene* **554**, 64–74 (2015).

38. Liu, Q. *et al.* Transcriptome analysis of a spontaneous mutant in sweet orange [*Citrus sinensis* (L.) Osbeck] during fruit development. *J Exp Bot* **60**, 801–813 (2009).

39. Lu, X. *et al.* Comparative transcriptome analysis reveals a global insight into molecular processes regulating citrate accumulation in sweet orange (*Citrus sinensis*). *Physiologia Plantarum* **158**, 463–482 (2016).

40. Qiao, L., Cao, M., Zheng, J., Zhao, Y. & Zheng, Z.-L. Gene coexpression network analysis of fruit transcriptomes uncovers a possible mechanistically distinct class of sugar/acid ratio-associated genes in sweet orange. *BMC Plant Biol* **17**, (2017).

41. Wang, L., Hua, Q., Ma, Y., Hu, G. & Qin, Y. Comparative transcriptome analyses of a late-maturing mandarin mutant and its original cultivar reveals gene expression profiling associated with citrus fruit maturation. *PeerJ* **5**, (2017).

42. Wu, J. *et al.* An integrative analysis of the transcriptome and proteome of the pulp of a spontaneous late-ripening sweet orange mutant and its wild type improves our understanding of fruit ripening in citrus. *J Exp Bot* **65**, 1651–1671 (2014).

43. Wu, J., Fu, L. & Yi, H. Genome-wide identification of the transcription factors involved in citrus fruit ripening from the transcriptomes of a late-ripening sweet orange mutant and its wild type. *PLOS ONE* **11**, e0154330 (2016).

44. Yu, K. *et al.* Transcriptome changes during fruit development and ripening of sweet orange (*Citrus sinensis*). *BMC Genomics* **13**, 10 (2012).

45. Yun, Z. *et al.* Comparative transcriptomics and proteomics analysis of citrus fruit, to improve understanding of the effect of low temperature on maintaining fruit quality during lengthy post-harvest storage. *J Exp Bot* **63**, 2873–2893 (2012).

46. Zhang, Y.-J. *et al.* Comparative transcriptome analyses between a spontaneous late-ripening sweet orange mutant and its wild type suggest the functions of ABA, sucrose and JA during citrus fruit ripening. *PLOS ONE* **9**, e116056 (2014).

47. Checker, V. G., Saeed, B. & Khurana, P. Analysis of expressed sequence tags from mulberry (*Morus indica*) roots and implications for comparative transcriptomics and marker identification. *Tree Genetics & Genomes* **8**, 1437–1450 (2012).

48. Cohen, D. *et al.* Comparative transcriptomics of drought responses in Populus: a meta-analysis of genome-wide expression profiling in mature leaves and root apices across two genotypes. *BMC Genomics* **11**, 630 (2010).

49. Jansen, L. *et al.* Comparative transcriptomics as a tool for the identification of root branching genes in maize. *Plant Biotechnology Journal* **11**, 1092–1102 (2013).

50. Ntatsi, G. *et al.* Rootstock sub-optimal temperature tolerance determines transcriptomic responses after long-term root cooling in rootstocks and scions of grafted tomato plants. *Front. Plant Sci.* **8**, (2017).

51. Weber, M., Harada, E., Vess, C., Roepenack-Lahaye, E. v & Clemens, S. Comparative microarray analysis of *Arabidopsis thaliana* and *Arabidopsis halleri* roots identifies nicotianamine synthase, a ZIP transporter and other genes as potential metal hyperaccumulation factors. *The Plant Journal* **37**, 269–281 (2004).

52. An, J. *et al.* Comparative transcriptome analysis of *Poncirus trifoliata* identifies a core set of genes involved in arbuscular mycorrhizal symbiosis. *J Exp Bot* **69**, 5255–5264 (2018).

53. Zhang, Y., Barthe, G., Grosser, J. W. & Wang, N. Transcriptome analysis of root response to citrus blight based on the newly assembled Swingle citrumelo draft genome. *BMC Genomics* **17**, 485 (2016).

54. Zhong, Y. *et al.* Comparative transcriptome and iTRAQ proteome analyses of citrus root responses to *Candidatus* Liberibacter asiaticus infection. *PLOS ONE* **10**, e0126973 (2015).

55. Terol, J., Tadeo, F., Ventimilla, D. & Talon, M. An RNA-Seq-based reference transcriptome for Citrus. *Plant Biotechnology Journal* **14**, 938–950 (2016).

56. Reinhart, B. J., Weinstein, E. G., Rhoades, M. W., Bartel, B. & Bartel, D. P. MicroRNAs in plants. *Genes Dev.* **16**, 1616–1626 (2002).

57. Bartel, D. P. MicroRNAs: genomics, biogenesis, mechanism, and function. *Cell* **116**, 281–297 (2004).

58. Voinnet, O. Origin, biogenesis, and activity of plant microRNAs. *Cell* **136**, 669–687 (2009).

59. Bartel, D. P. MicroRNAs: target recognition and regulatory functions. *Cell* **136**, 215–233 (2009).

60. Brousse, C. *et al.* A non-canonical plant microRNA target site. *Nucleic Acids Res.* **42**, 5270–5279 (2014).

61. Zhang, B., Pan, X., Cannon, C. H., Cobb, G. P. & Anderson, T. A. Conservation and divergence of plant microRNA genes. *The Plant Journal* **46**, 243–259 (2006).

62. Rajagopalan, R., Vaucheret, H., Trejo, J. & Bartel, D. P. A diverse and evolutionarily fluid set of microRNAs in Arabidopsis thaliana. *Genes Dev.* **20**, 3407–3425 (2006).

63. Fahlgren, N. *et al.* High-throughput sequencing of Arabidopsis microRNAs: evidence for frequent birth and death of MIRNA genes. *PLOS ONE* **2**, e219 (2007).

64. Sunkar, R., Zhou, X., Zheng, Y., Zhang, W. & Zhu, J.-K. Identification of novel and candidate miRNAs in rice by high throughput sequencing. *BMC Plant Biology* **8**, 25 (2008).

65. Klevebring, D. *et al.* Genome-wide profiling of Populus small RNAs. *BMC Genomics* **10**, 620 (2009).

66. Wei, B. *et al.* Novel microRNAs uncovered by deep sequencing of small RNA transcriptomes in bread wheat (*Triticum aestivum* L.) and *Brachypodium distachyon* (L.) Beauv. *Funct. Integr. Genomics* **9**, 499–511 (2009).

67. Zhang, L. *et al.* A genome-wide characterization of microRNA genes in maize. *PLoS Genet.* **5**, e1000716 (2009).

68. Szittya, G. *et al.* High-throughput sequencing of *Medicago truncatula* short RNAs identifies eight new miRNA families. *BMC Genomics* **9**, 593 (2008).

69. Moxon, S. *et al.* Deep sequencing of tomato short RNAs identifies microRNAs targeting genes involved in fruit ripening. *Genome Res.* **18**, 1602–1609 (2008).

70. Ruan, M.-B., Zhao, Y.-T., Meng, Z.-H., Wang, X.-J. & Yang, W.-C. Conserved miRNA analysis in *Gossypium hirsutum* through small RNA sequencing. *Genomics* **94**, 263–268 (2009).

71. Wang, Z.-M. *et al.* A comparative miRNAome analysis reveals seven fiber initiation-related and 36 novel miRNAs in developing cotton ovules. *Molecular Plant* **5**, 889–900 (2012).

72. Qiu, D. *et al.* High throughput sequencing technology reveals that the taxoid elicitor methyl jasmonate regulates microRNA expression in Chinese yew (*Taxus chinensis*). *Gene* **436**, 37–44 (2009).

73. Zhang, M. *et al.* High-throughput sequencing reveals miRNA effects on the primary and secondary production properties in long-term subcultured Taxus cells. *Front Plant Sci* **6**, (2015).

74. Chitarra, W. *et al.* miRVIT: a novel miRNA database and Its application to uncover Vitis responses to Flavescence dorée infection. *Front. Plant Sci.* **9**, (2018).

75. Song, C. *et al.* Deep sequencing discovery of novel and conserved microRNAs in trifoliate orange (*Citrus trifoliata*). *BMC Genomics* **11**, 431 (2010).

76. Chen, X. Small RNAs and their roles in plant development. *Annu. Rev. Cell Dev. Biol.* **25**, 21–44 (2009).

77. Jones-Rhoades, M. W., Bartel, D. P. & Bartel, B. MicroRNAS and their regulatory roles in plants. *Annu Rev Plant Biol* **57**, 19–53 (2006).

78. Lelandais-Brière, C. *et al.* Small RNA diversity in plants and its impact in development. *Curr Genomics* **11**, 14–23 (2010).

79. Csukasi, F. *et al.* Two strawberry miR159 family members display developmental-specific expression patterns in the fruit receptacle and cooperatively regulate Fa-GAMYB. *New Phytol.* **195**, 47–57 (2012).

80. Li, D. *et al.* Developmental and stress regulation on expression of a novel miRNA, Fan-miR73, and its target ABI5 in strawberry. *Scientific Reports* **6**, 28385 (2016).

81. Qu, D. *et al.* Identification of microRNAs and their targets associated with fruit-bagging and subsequent sunlight re-exposure in the 'Granny Smith' apple exocarp using high-throughput sequencing. *Front Plant Sci* **7**, 27 (2016).

82. Paim Pinto, D. L. *et al.* The influence of genotype and environment on small RNA profiles in grapevine berry. *Front Plant Sci* **7**, (2016).

83. Zhu, H. *et al.* Unique expression, processing regulation, and regulatory network of peach (*Prunus persica*) miRNAs. *BMC Plant Biol.* **12**, 149 (2012).

84. Hou, Y. *et al.* Comparative analysis of fruit ripening-related miRNAs and their targets in blueberry using small RNA and degradome sequencing. *Int J Mol Sci* **18**, (2017).

85. Xin, C. *et al.* Profiling microRNA expression during multi-staged date palm (*Phoenix dactylifera* L.) fruit development. *Genomics* **105**, 242–251 (2015).

86. Liu, Y. *et al.* Genome-wide comparison of microRNAs and their targeted transcripts among leaf, flower and fruit of sweet orange. *BMC Genomics* **15**, 695 (2014).

87. Wu, X.-M. *et al.* Genomewide analysis of small RNAs in nonembryogenic and embryogenic tissues of citrus: microRNA- and siRNA-mediated transcript cleavage involved in somatic embryogenesis. *Plant Biotechnology Journal* **13**, 383–394 (2015).

88. Xu, Q. *et al.* Discovery and comparative profiling of microRNAs in a sweet orange red-flesh mutant and its wild type. *BMC Genomics* **11**, 246 (2010).

89. Zhang, J.-Z. *et al.* Identification of miRNAs and their target genes using deep sequencing and degradome analysis in trifoliate orange [*Poncirus trifoliate* (L.) Raf]. *Mol Biotechnol* **51**, 44–57 (2012).

90. Wu, J., Zheng, S., Feng, G. & Yi, H. Comparative analysis of miRNAs and their target transcripts between a spontaneous late-ripening sweet orange mutant and its wild-type using small RNA and degradome sequencing. *Front Plant Sci* **7**, 1416 (2016).

91. Khaldun, A. B. M. *et al.* Comparative profiling of miRNAs and target gene identification in distant-grafting between tomato and Lycium (goji berry). *Front. Plant Sci.* **7**, (2016).

92. Li, C. *et al.* Grafting-responsive miRNAs in cucumber and pumpkin seedlings identified by high-throughput sequencing at whole genome level. *Physiologia Plantarum* **151**, 406–422 (2014).

93. Li, C., Li, Y., Bai, L., He, C. & Yu, X. Dynamic expression of miRNAs and their targets in the response to drought stress of grafted cucumber seedlings. *Horticultural Plant Journal* **2**, 41–49 (2016).

94. Liu, N., Yang, J., Guo, S., Xu, Y. & Zhang, M. Genome-wide identification and comparative analysis of conserved and novel microRNAs in grafted watermelon by high-throughput sequencing. *PLOS ONE* **8**, e57359 (2013).

95. Pagliarani, C. *et al.* The accumulation of miRNAs differentially modulated by drought stress is affected by grafting in grapevine. *Plant Physiol.* **173**, 2180–2195 (2017).

96. Tzarfati, R., Ben-Dor, S., Sela, I. & Goldschmidt, E. E. Graft-induced changes in microRNA expression patterns in citrus leaf petioles. *The Open Plant Science Journal* **7**, (2013).

Chapter 1. Combined Messenger RNA and Small RNA Transcriptome Profiling of Fruit Juice Vesicles of *Citrus sinensis* Scions Grafted onto Genetically Diverse Citrus Rootstocks to Understand Their Effects on Fruit Quality

Abstract

Citrus, one of the most economically important crops in the world, is commercially propagated by grafting. Citrus rootstocks have well-known effects on tree size, fruit size, and many aspects of fruit quality. Citrus rootstocks can have an influence on traits such as size, juice content, peel thickness, organic compounds, acidity, and flavor. The effects of rootstocks on fruit quality are well documented but understanding of the molecular mechanisms underlying these differences is lacking, especially regulatory mechanisms. Therefore, fruit quality, and transcriptome and miRNome data from fruit grown on four genetically divergent rootstocks was collected. Generally, fruit grown on rough lemon produced the highest yield and fruit size, but fruit was of lower quality, containing lower acidity and lower levels of total soluble solids. On the other hand, trifoliate orange produced smaller, high quality fruit with high yield on smaller trees.

Differentially expressed genes (DEGs) and differentially expressed miRNAs (DEMs) were identified between the fruit grown on different citrus rootstock genotypes. Functional analysis revealed that the ‘GO’ term ‘DNA-binding transcription factor activity’ was significantly enriched. Additionally, KEGG pathway analysis revealed that genes

involved in plant-hormone signal transduction, carotenoid biosynthesis, and fructose and mannose metabolism were enriched among those differing in expression between these fruits. Many of the genes differentially expressed (DE) between genotypes had roles in controlling the hormone signaling pathways in fruit, which have implications in altering fruit size. Additionally, genes potentially involved in control of the accumulation of sugars and acids were DE between fruit grown on different rootstocks. Furthermore, miRNA-mRNA interaction pairs were identified to understand potential regulatory mechanisms of these genes.

Introduction

Citrus is grown in more than 140 countries and is one of the most economically important crops in the world. The total production of citrus in the United States in the 2018 growing season was 6.1 million tons on a total of 679 thousand acres. California produced 58 percent of the United States total, producing 3.6 million tons of citrus on 278 thousand acres. Approximately 75 percent of California's citrus production is sold to the fresh market opposed to being processed into other commodities, such as juice. Oranges accounted for 64 percent of the total citrus produced in the United States and were valued at $1.8 billion, according to the United States Department of Agriculture[1].

Citrus trees are rarely grown from seed and virtually all commercial citrus is propagated by grafting. This reduces the juvenile phase, allowing for the trees to produce fruit many years earlier than those grown from seed[2]. Rootstocks impart certain traits onto the scion and the effects of rootstocks can be large. The most significant impacts are on

growth and vigor, tree nutrition, stress resistance, and fruit quality[3–6]. In citrus, phenotypic differences in fruit quality have been well documented[3,7–14]. However, understanding of the molecular mechanisms underlying these differences is lacking, especially regulatory mechanisms.

Previous studies in apple[15], grape[16–19], sweet cherry[20], and other fruit crops have examined transcriptome changes in various rootstock-scion combinations. In citrus, gene expression profiling has been used to understand rootstock effects on growth of trees and responses to biotic and abiotic factors. Many transcriptomic studies have also been performed in citrus to elucidate fruit ripening and development in commonly grown citrus cultivars[21–31]. To date, none of these reports have linked the genetic effects of citrus rootstocks to fruit quality.

Fruit growth and development and the mechanisms underlying fruit quality are complex. Signal transduction systems regulate many aspects of fruit ripening[32]. During citrus development, the ABA-signal pathway may act as a central regulator of ripening, combined with other hormones, including auxin and ethylene[31,33–35]. A recent study showed that ABA is a positive regulator of citrus ripening and exogenously applied ABA regulates citrus fruit maturation, suggesting that ABA metabolism plays a crucial role in citrus fruit development and ripening[35]. Previous studies identified Protein phosphatase 2C family (PP2C) proteins as negative regulators of ABA signaling[36–38]. PP2C dephosphorylates and inactivates a SNF1-related kinases family 2 (SnRK2) protein, which is a positive regulator of ABA-response pathways. Plants with an inactive form of PP2C were hypersensitive to ABA, causing increased activation of ABA-responsive

genes[38,39]. ABA-signaling response has also been linked with drought-stress tolerance[40]. This study suggested that ABA accumulation is associated with a decrease in relative water content and Romero et al. suggest that ABA increases caused by dehydration upregulate levels of PP2C[34].

Auxin, another phytohormone important for fleshy fruit development, regulates many growth and development processes. The auxin-signaling pathway regulates transcription of hundreds of auxin-inducible genes. Promoters of these auxin-responsive genes contain auxin-responsive elements (AuxRE), which bind the auxin-response factor (ARF) family of transcription factors[41]. ARF activity is regulated in part by Aux/IAA genes, which are transcriptional repressors of the auxin response. In the absence of auxin, Aux/IAA proteins dimerize with ARFs and recruit corepressors of the TOPLESS (TPL) family, which in turn recruit chromatin-remodeling proteins that stabilize the repressed state[42]. When auxin is present, it acts as a “glue” between Aux/IAAs and F-box proteins that are part of a ubiquitin protein ligase complex. This causes polyubiquitination and subsequent degradation of Aux/IAAs, which releases its repression, leading to the activation of auxin-regulated genes[43]. Together with ABA and other hormones, auxin regulates several aspects of fruit development, including fruit set, fruit size, and ripening related events[44–46].

Additionally, prior studies have indicated that small RNAs may play a regulatory role in fruit development and ripening. Small RNAs are a type of single-stranded, non-coding RNA that is typically 20-24 nucleotides in length, of which microRNAs (miRNAs) are the most extensively researched class and are known to post-transcriptionally downregulate the expression of target mRNAs through mRNA cleavage or translational inhibition[47–50].

In strawberry, miR159 was shown to act as a ripening regulator by targeting a MYB transcription factor, which plays a crucial role in the ripening process[51]. Several examples of miRNA involvement in fruit development and maturation have been described in a variety of crop species, including apple, grape, peach, blueberry, date palm, and tomato[52–57]. miRNAs that suppress specific transcription factors that are thought to be regulators of citrus fruit development and ripening have also been identified[58]. However, the expression profiles of miRNAs in various scion-rootstock combinations and their subsequent impact on fruit quality have not yet been evaluated.

In this study, trees grafted on four rootstocks were chosen from a rootstock trial at the University of California, Riverside to assess for various fruit quality traits; Argentina sweet orange, Schaub rough lemon, Carrizo citrange, and Rich 16-6 trifoliate orange. In general, rough lemon rootstocks produce the highest yield and fruit size, but fruit is of lower quality, containing lower acidity and lower levels of total soluble solids, also known as the “dilution effect”[59]. On the other hand, trees on trifoliate orange produce smaller, high quality fruit with high yield on often smaller trees. Carrizo citrange rootstocks produce intermediate yield with good fruit quality. Sweet orange rootstocks produce good quality fruit, but trees are very susceptible to various citrus diseases. An RNA-seq approach was implemented to investigate differences in gene expression in fruit due to genetically varying rootstocks, with the aim of identifying genes that could potentially play a role in improvement of fruit quality. Furthermore, miRNA expression profiles were obtained for each of the rootstocks to identify potential regulatory mechanisms associated with their target genes.

Materials and Methods

Plant materials

The citrus cultivar, ‘Washington’ navel sweet orange (*Citrus sinensis* (L.) Osbeck) scion was previously grafted onto the following rootstocks: Argentina sweet orange (*Citrus sinensis* (L.) Osbeck), Schaub rough lemon (*Citrus jambhiri* Lush), Carrizo citrange (*Citrus sinensis* 'Washington' sweet orange X *Poncirus trifoliata*), and Rich 16-6 trifoliate (*Poncirus trifoliata* (L.) Raf.). The grafted trees were part of a rootstock trial conducted at the Citrus Research Center and Agricultural Experiment Station (CRC-AES) at the University of California, Riverside that included 28 rootstocks. Trees were planted in 2011 in a randomized block design with ten replications. Trees were planted on berms, irrigated with minisprinklers according to soil moisture sensors, and treated with fertilizers and pesticides according to standard commercial practices.

For sequencing, fruit from two biological replicate trees was collected at four time points throughout the 2014-2015 growing season (July, September, November, and January). Juice vesicles were collected, taking care to exclude rind and segment membranes. Juice vesicles from three representative fruit collected from different sides of the tree were pooled, immediately frozen on dry ice in the field, and kept at -80°C for RNA extraction.

Fruit quality analysis

Fruit were harvested in January at the end of the 2016 growing season when fruit were ripe. Total yield was recorded. Ten fresh fruit per tree were collected and analyzed for

the following traits: weight, height, width, rind color, rind texture, peel thickness, internal texture and taste. The juice was then pooled from all ten fruit and percent juice, total titratable acid (% by weight), and total soluble solids (%) for each pool were calculated at the UC ANR Lindcove Research and Extension Center. The average for each trait of the ten fruit per tree were considered one biological replicate and ten biological replicate trees were sampled for statistical analyses.

Statistical differences in fruit quality between fruit from trees on different rootstocks were evaluated using an analysis of variance (ANOVA) test and Chi-squared test. The differences among treatment means were evaluated by Fisher's Least Significant Difference (LSD) test and Duncan's Multiple Range Test. Data were considered to be statistically significant when $P < 0.05$.

RNA extraction, library construction, and sequencing

The juice vesicles of three representative fruit per tree from two biological replicates of each of the four rootstock genotypes at the four collection time points were subjected to RNA-seq (32 samples total). Samples were ground in liquid nitrogen and total RNA was extracted from ~200 mg tissue using the ZR Plant RNA MiniPrep™ kit (Zymo Research) per manufacturer's instructions. An Agilent Bioanalyzer (Agilent Technologies) was used to confirm the integrity of the total RNA. The RNA with a RIN (RNA Integrity Number) value greater than seven qualified for RNA-seq.

For messenger RNA-seq, sequencing libraries were created using TruSeq Stranded mRNA Library Preparation Kit (Illumina) according to the manufacturer's protocol. For

small RNA-seq, sequencing libraries were created using TruSeq Small RNA Library Preparation Kit (Illumina) according to the manufacturer's protocol. Each library was prepared for multiplexing with a unique indexed primer. Quantification of all libraries was performed with Nanodrop and Qubit fluorometer. The library size distribution and quality were measured with an Agilent Bioanalyzer. Multiplexed libraries were sequenced in a single lane on an Illumina NextSeq 500 instrument at the University of California, Riverside Genomics Core facility. An average of 11 samples were sequenced per lane.

Illumina Sequence Analysis

The data analysis was carried out using the RNA-seq workflow module of the systemPipeR package available on Bioconductor[60]. RNA-seq reads were demultiplexed and preprocessed by quality filtering and trimming of adaptors. Quality reports were created with the FastQC function. *Citrus clementina v 1.0* genome assembly and annotations were downloaded from JGI's portal (https://phytozome.jgi.doe.gov/pz/portal.html). Sequencing reads were then mapped against the *Citrus clementina v 1.0* reference genome using the Bowtie2 alignment suite[61] for small RNAs and HISAT2 alignment suite[62] for messenger RNAs. Messenger RNA raw reads were counted in a strand-specific manner. Known miRNA gene coordinates, required for counting, were acquired by downloading all known plant miRNAs from the plant miRNA database (PMRD)[63], aligning these sequences to the *Citrus clementina v 1.0* reference genome using Bowtie2 with perfect alignment, and extracting the alignment coordinates. Small RNA raw reads were then counted at the known miRNA locations using the summarizeOverlaps function. Sample-wise correlation

analysis was performed using rlog transformed expression values generated by the DESeq2 package[64].

Identification of novel miRNAs

Sequences that aligned to the *Citrus clementina v 1.0* reference genome but did not match any known plant miRNAs were used to predict novel miRNAs. Novel miRNAs were predicted using three miRNA prediction tools (Shortstack[65], miRA[66], and miR-PREFeR[67]). These three programs assess the expression patterns, Dicer cleavage site, and secondary structure of miRNA precursors to predict novel miRNAs from small RNA-seq data. *Citrus clementina* reference genome was input as the reference for determining flanking sequences to predict secondary structures of the miRNA precursors. ShortStack was run with default settings with the exception of the following changes: --dicermin 20; --dicermax 24; --foldsize 400. miRA was run with default settings with the exception of the following changes: cluster_gap_size = 100; min_precursor_length= 0; max_precursor_length= 400; max_pvalue = 0.05; max_duplex_length = 26. miR-PREFeR was run with default settings with the exception of the following changes: PRECURSOR_LEN = 400; READS_DEPTH_CUTOFF = 30; NUM_OF_CORE = 10; MIN_MATURE_LEN = 20; MAX_MATURE_LEN = 24. To avoid false positive results, only miRNAs that were predicted by all three programs were considered to be real novel miRNAs and were included in downstream analyses.

Differential expression analysis of miRNAs and mRNAs

Normalization, fold-change calculations, and statistical analysis of differentially expressed genes (DEGs) and differentially expressed miRNAs (DEMs) were performed using the DESeq2 package. The adjusted p-value (aka false discovery rate (FDR)) was calculated by the DESeq2 package using the Benjamini-Hochberg procedure. DEGs and DEMs were considered as those with a fold change $\geq$ 2 and FDR of $\leq$ 0.05 for comparisons between two genotypes at a single time point. Protein-coding genes with an average of 5 reads per kilobase of transcript per million mapped reads (RPKM) and miRNAs with an average of 5 reads per million (RPM) were included in downstream analyses. Dendrograms, heatmaps, and Venn diagrams were created using R packages DESeq2, ComplexHeatmap[68], and ggplot2[69]. Heatmaps displaying gene expression represent normalized expression values (RPKM), with red representing increased expression and blue representing decreased expression.

GO and KEGG pathway analysis

Gene Ontology (GO) functional annotation enrichment analysis was conducted using the GO Term Enrichment Tool in PlantRegMap[70] (http://plantregmap.cbi.pku.edu.cn/go.php) using *Citrus clementina* genome annotation IDs as input. Pathway analysis was performed using the Gene-list Enrichment Tool in KOBAS 3.0[71] (http://kobas.cbi.pku.edu.cn/anno_iden.php) using *Citrus clementina* Entrez Gene IDs as input. GO terms and KEGG pathways with p value $\leq$ 0.05 were considered significantly enriched.

Prediction of miRNAs targeting differentially expressed genes and expression correlation analysis

Coding sequences of DEGs were downloaded from the website Phytozome Biomart (http://www.phytozome.net/biomart/martview/). DEG sequences along with a list of miRNAs discovered in the *Citrus clementina* reference genome were submitted to the psRNATarget program[72] (https://plantgrn.noble.org/psRNATarget/analysis) with default parameters in order to predict miRNAs targeting DEGs. An in-house R script was used to identify combinations of differentially expressed mRNAs and the miRNAs that target them based on the expected negative correlation between fold changes of miRNAs and their predicted targets.

Quantitative RT-PCR validation of differentially expressed genes and miRNAs

Several combinations of miRNAs and target DEGs found to be negatively correlated were quantified by real-time PCR (qRT-PCR). qRT-PCR was conducted to detect relative expression of these selected miRNAs and target mRNAs. Total RNA (including sRNAs) from each sample was first polyadenylated and reverse transcribed to cDNA using Mir-X miRNA First-Strand Synthesis and SYBR qRT-PCR Kit (Takara Bio Inc) according to the manufacturer's protocol. The 10-µl cDNA reaction was diluted one to ten to a produce a final volume of 100 µl. cDNA was amplified on a BioRad CFX-96 real time system (Bio-Rad). The gene-specific primers were designed using IDT PrimerQuest software[73] and are listed in Supplemental Table 1.1. Reference gene expression stability

across genotype and developmental stage was calculated by NormFinder and Bestkeeper software[74,75].

For miRNA qPCR, *U6* served as the reference gene. Reactions of 15-µl were prepared containing 1.5 µL cDNA, 7.5 µL 2x TB Green Advantage qPCR premix (Takara Bio), 0.3 µL each primer (0.1 mM) and 5.4 µL molecular grade water. PCR cycling conditions were as follows: 95 °C for 5 min, 40 cycles of 95 °C for 10 s, and 60 °C for 25 s. For mRNA qPCR, *GAPDH* served as the reference gene. Reactions of 10-µl were prepared containing 1 µL cDNA, 5 µL SSO Advanced Universal SYBR Green Supermix (Bio-Rad), 0.2 µL each primer (0.1 mM) and 3.6 µL molecular grade water. PCR cycling conditions were as follows: 95°C for 5 min, 40 cycles of 95°C for 20 s, and 60°C for 40 s. A melting curve analysis beginning at 65°C and increasing by increments of 0.5°C every 5 seconds to 90°C was added at the end of each PCR to evaluated the specificity of the amplified product. For each sample two biological replicates were used, and all reactions were performed in triplicate for technical replication. No template controls (NTC) were run in duplicate for each primer pair. The relative expression levels of miRNAs and the predicted target genes was calculated using the Pfaffl method in order to correct for PCR efficiencies[76]. Statistical significance was calculated using Student's t-test with two independent biological replicates, each representing an average of three technical replicates.

Results

Determination of rootstock effects on fruit quality

To determine the effect of rootstocks on fruit quality, *Citrus sinensis* (sweet orange) scions were previously grafted onto various rootstocks as part of a rootstock trial planted at the University of California in 2011. In this study, four rootstocks were chosen from the trial to assess for various fruit quality traits; Argentina sweet orange (SO), Schaub rough lemon (RL), Carrizo citrange (CZ), and Rich 16-6 trifoliate orange (TF). Data for the following fruit quality traits was collected in Feb 2016 at the end of the growing season: weight, height, width, rind color, rind texture, peel thickness, internal texture, juice weight, percent juice, total soluble solids (TSS) and titratable acid (percent acid) levels.

Rootstocks had a significant effect on the yield, peel thickness, rind color, rind texture, sugar and acid levels (Table 1.1). The total yield and average fruit weights of sweet orange fruit grown on rough lemon were significantly larger than when sweet orange was grafted onto sweet orange, Carrizo citrange, or trifoliate orange rootstocks. Additionally, the rind thickness of fruit grown on Schaub rough lemon was significantly greater than that of fruit grown on the other three rootstocks. Fruit from trees grafted onto Carrizo citrange contained the highest levels of total soluble solids, followed closely by Argentine sweet orange and Rich trifoliate orange rootstocks. Sugar levels in fruit grown on Schaub rough lemon were the lowest and were significantly lower than the other three. Similar trends were seen in titratable acid levels, where Schaub rough lemon rootstocks produced significantly lower levels of acid than sweet orange, Carrizo, and trifoliate

orange (Figure 1.1). Schaub rough lemon rootstock also produced a rougher rind and Argentine sweet orange rootstock produced a lighter colored rind (data not shown).

Table 1.1. Citrus rootstock effects on Parent Washington Navel Orange (*Citrus sinensis*) yield and quality (2016) for trees grown in Riverside, CA

Rootstock	Average Fruit weight (g)	Rind thickness (mm)	Juice content (%)	Total soluble solids (%)	Acid (%)	Total yield (lb/tree)
Argentine sweet orange	227.66	31.40	36.68	12.76	0.74	35.73
Carrizo citrange	230.24	30.56	39.19	13.13	0.75	42.92
Rich 16-6 trifoliate orange	237.29	30.40	39.20	12.50	0.72	42.80
Schaub rough lemon	251.80*	34.11*	38.31	10.50*	0.61*	70.44*
LSD (0.05)	17.77	1.76	3.06	0.53	0.03	14.74

The data are means of ten biological replicates. * indicates significant difference at $P < 0.05$ by Fisher's LSD test.

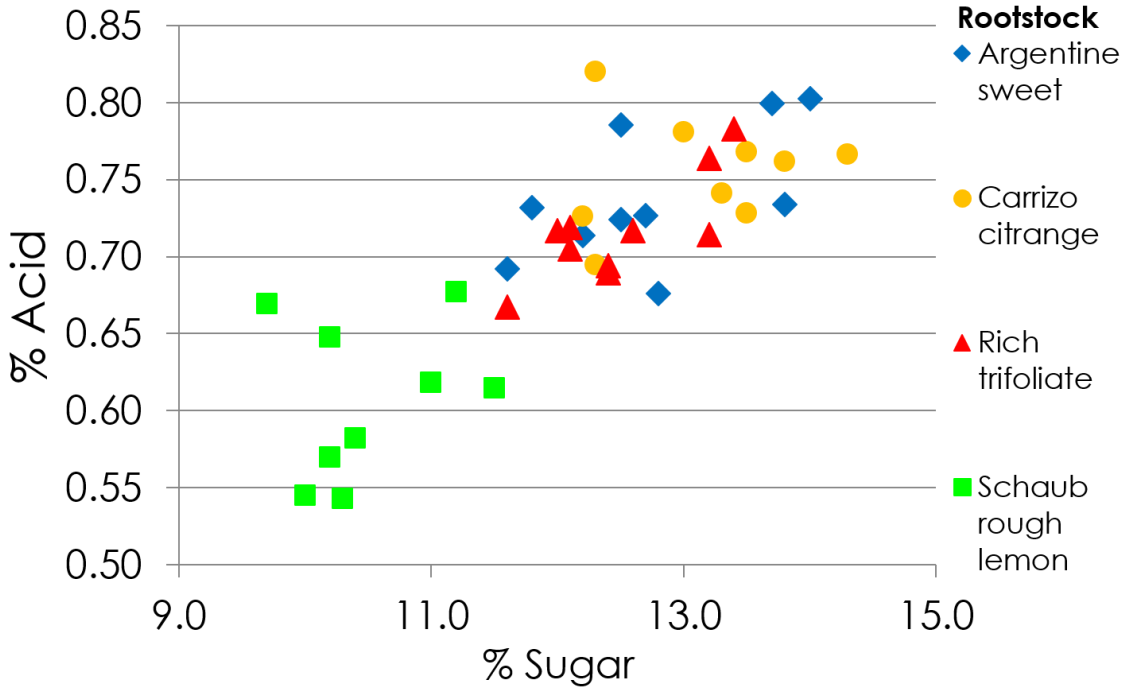

Figure 1.1. Sugar to acid ratio in fruit grown on four rootstocks. Each point represents one biological replicate.

High-throughput sequencing of mRNAs and sRNAs in fruit grafted onto various rootstocks

In order to profile the expression of genes and small RNAs in fruit from trees grafted onto different rootstocks, total RNA was extracted from juice vesicles collected from fruit grown on each of the four rootstocks listed above at four time points throughout the 2014-2015 growing season. Fruit were collected in July (Time 1), September (Time 2), November (Time 3), and January (Time 4) (Figure 1.2). These timepoints were chosen because they correlated with the phases of citrus fruit growth[77]. Time 1 was collected during cell division (phase I), time 2 was collected during early cell enlargement (phase

II), time 3 was collected during late cell enlargement (phase II), and time 4 was collected during maturation and ripening (phase III).

Poly-A enriched fractions (mRNA) and small RNA fractions that were size selected were used to construct libraries for Illumina sequencing. Sequencing statistics in Table 1.2 are an average of the libraries sequenced for each genotype. After 3'-adaptor trimming, quality filtering, and removal of reads shorter than 18 nt and longer than 30 nt, there were an average of 14,820,293, 15,139,706, 13,536,108, and 14,815,164 clean small RNA reads in libraries from fruit grown on the four rootstocks (SO, CZ, RL, and TF, respectively) (Table 1.2). Of the clean small RNA reads, 12,889,578 (86.97%), 13,174,896 (86.93%), 11,777,403 (87.07%), and 12,987,114 (87.58%) were mappable and could be aligned to the *Citrus clementina v 1.0* reference genome, most of which were between 21 and 24 nt in length. For reads 18-30 nt, all libraries showed similar size distributions, with most reads belonging to the 24-nt class, followed by the reads of 21-nt (Figure 1.3). Using the Bowtie2 aligner, a total of 669 known conserved plant miRNAs could be mapped to the *Citrus clementina v 1.0* reference genome. Of these, 614 were retrieved in this study by deep sequencing of the fruit juice vesicle samples. Additionally, five novel miRNAs not homologous to those of any other plant species were predicted (Table 1.3, Supplemental Figure 1.1).

After adapter removal and quality filtering, there was an average of 47,927,451, 42,649,554, 50,809,049, and 49,813,049 clean mRNA reads in the libraries from fruit of the four rootstocks (SO, CZ, RL, and TF, respectively) (Table 1.2). Of the clean mRNA reads, 43,262,346 (90.27%), 38,845,224 (91.04%), 45,698,718 (89.95%), and 44,771,732 (89.80%) were mappable and could be aligned to the reference genome

using HISAT2. On average, 82.69% of clean reads could be aligned to annotated genes. Of the 24,533 annotated genes in the clementine gene models, 20,705 (87.12%) were detected by sequencing during fruit development. A hierarchical clustering tree of the samples reflected an age-specific structure, as samples organized into distinct clades based on time of collection (Figure 1.4).

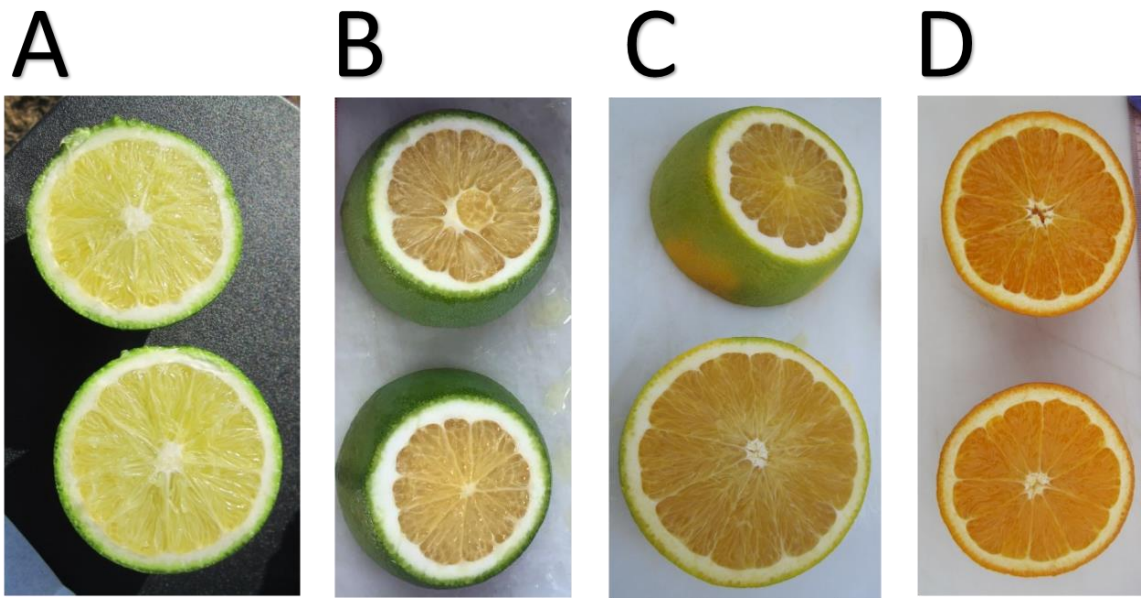

Figure 1.2. Fruit collected for sequencing at four timepoints throughout ripening and development. Fruit collected in (A) July, (B) September, (C) November and (D) January. Circumference of the fruit at the time of collection was ~18, 24, 26, and 27 cm, respectively.

Table 1.2. Summary statistics of the small RNA and mRNA sequencing results for fruit samples grafted onto four rootstock varieties

	Category	Sweet Orange Rootstock	Carrizo Rootstock	Rough Lemon Rootstock	Rich 16-6 Trifoliate Rootstock
Small RNA sequencing	Number clean reads	14,820,293	15,139,706	13,536,108	14,815,164
	Percent reads aligned to genome (%)	86.93	86.93	87.07	87.57
	Percent reads aligned to known miRNAs (%)	12.81	15.14	17.77	18.61
mRNA sequencing	Number clean reads	47,927,451	42,649,554	50,809,049	49,813,049
	Percent reads aligned to genome (%)	90.27	91.05	89.95	89.80
	Percent reads aligned to transcripts (%)	82.65	83.34	82.66	82.10

Table 1.3. Novel miRNA candidates detected in fruit tissue and aligned to the *Citrus clementina* reference genome

Novel miRNA	Mature Sequence	Scaffold	Start position	End position
Ccl_n01	UUUUGUUGCAUGAUGCUGAUAA	1	21925381	21925483
Ccl_n02	UCGCAGGGGAGAUGGGACCAAC	6	24421055	24421129
Ccl_n03	UCUCAGGUCGCCCCUGUGGGA	2	8093626	8093757
Ccl_n04	CACGCGGCCAUCUCUCAUUGA	3	31161588	31161667
Ccl_n05	AUCGGAUCAGGUUGUAAAUUC	7	13469344	13469433

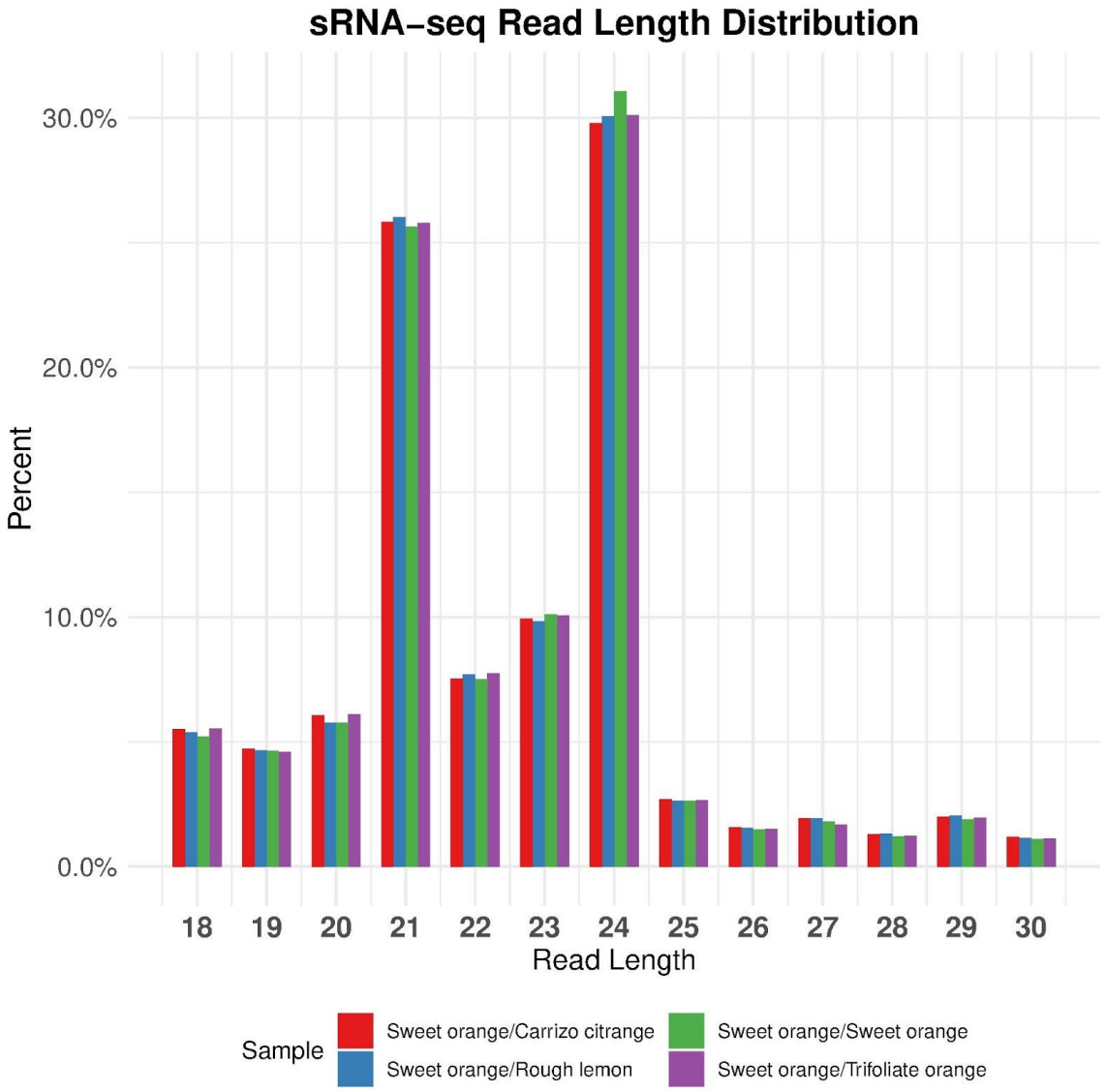

Figure 1.3. Read length (nt) distribution of small RNA libraries of sweet orange fruit grafted onto various rootstocks. Legend is listed as Scion/Rootstock.

A.

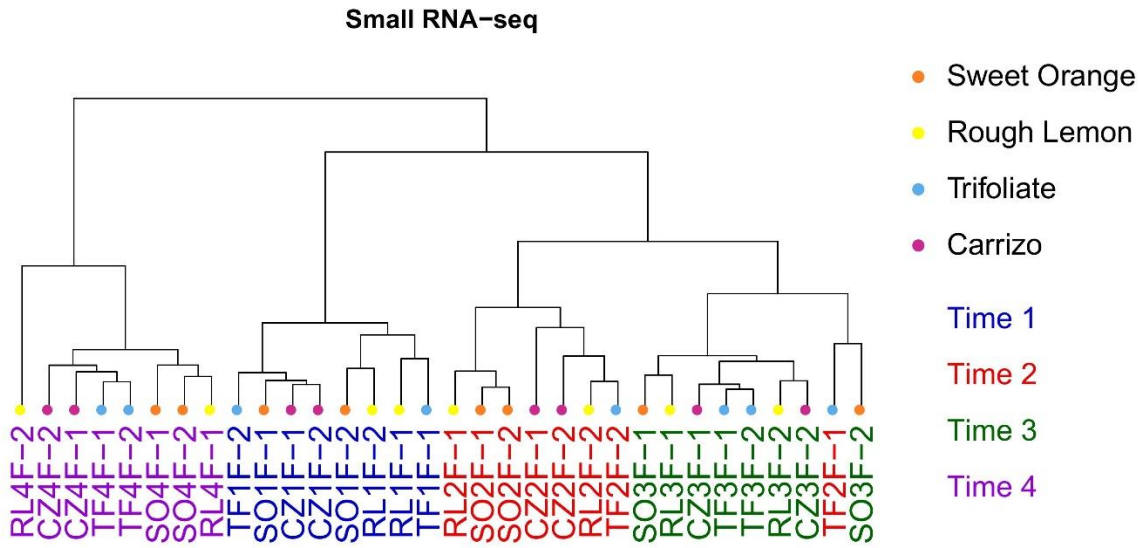

B.

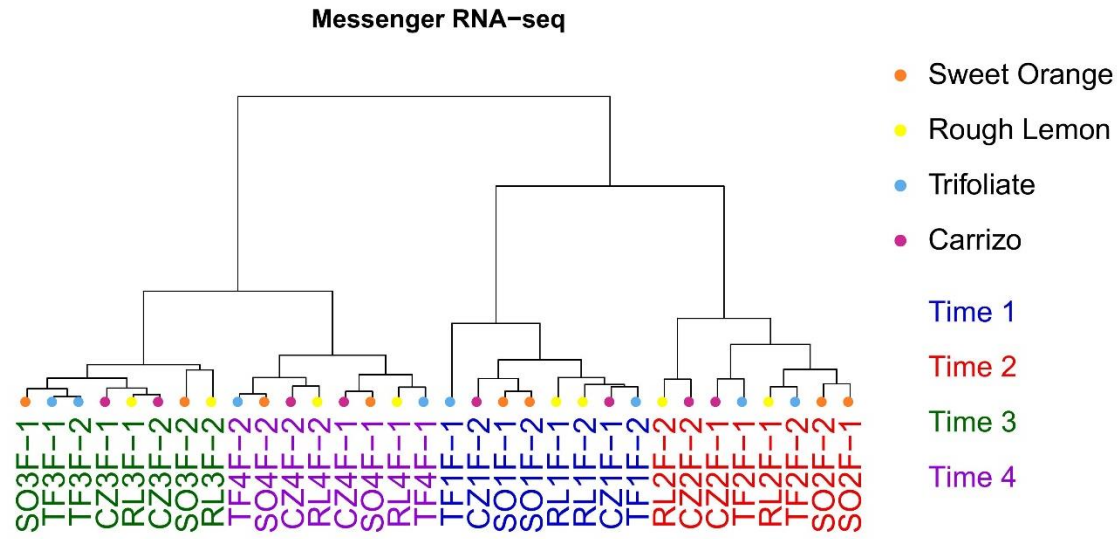

Figure 1.4. Hierarchical clustering of samples. Clustering of samples based on small RNA expression (A) or mRNA expression (B) represented by a dendrogram. Distance between samples is measured as 1 - Spearman's correlation coefficient. SO = sweet orange rootstock; CZ = Carrizo rootstock; RL = rough lemon rootstock; TF = trifoliate rootstock; F = fruit sample. Numbers directly after rootstock names indicate time point of collection, while numbers after dash indicate biological replicates.

Differential expression of genes in fruit grafted onto different rootstocks

In this study, RNA-seq generated reads that mapped to 19,359, 19,124, 19,336, and 19,374 citrus genes in samples from fruit of trees grafted onto sweet orange, Carrizo citrange, rough lemon, and trifoliate orange rootstocks, respectively. With criterium of at least 2-fold difference and a p-value less than 0.05 ($|log2FC| \geq 1$, $p < 0.05$), a total of 1,633 differentially expressed genes (DEGs) were identified between genotypes at one or more time points (Figure 1.5A). There were 684 genes found to be DE between rough lemon and sweet orange rootstocks, 388 DEGs between Carrizo citrange and sweet orange, 361 DEGs between trifoliate orange and sweet orange, 178 DEGs between rough lemon and Carrizo citrange, 395 DEGs between trifoliate orange and Carrizo citrange, and 855 DEGs between trifoliate and rough lemon. None of these DEGs overlapped in all 6 comparisons (Figure 1.5B). The majority of the DEGs were specific to one pairwise comparison, but the largest overlap of was a group of 122 DEGs that were commonly shared between RL-SO, CZ-SO, TF-RL, and TF-CZ. Due to the large number of DEGs observed between fruit grafted onto trifoliate orange and rough lemon rootstocks and the fact that the largest phenotypic differences in fruit quality traits were generally seen when comparing fruit grown on these rootstocks, we primarily focused on this contrast for the remainder of this study. DEGs uniquely belonging to this comparison are more likely to play a role in the phenotypic changes seen when fruit are grown on trifoliate orange versus rough lemon rootstock.

A.

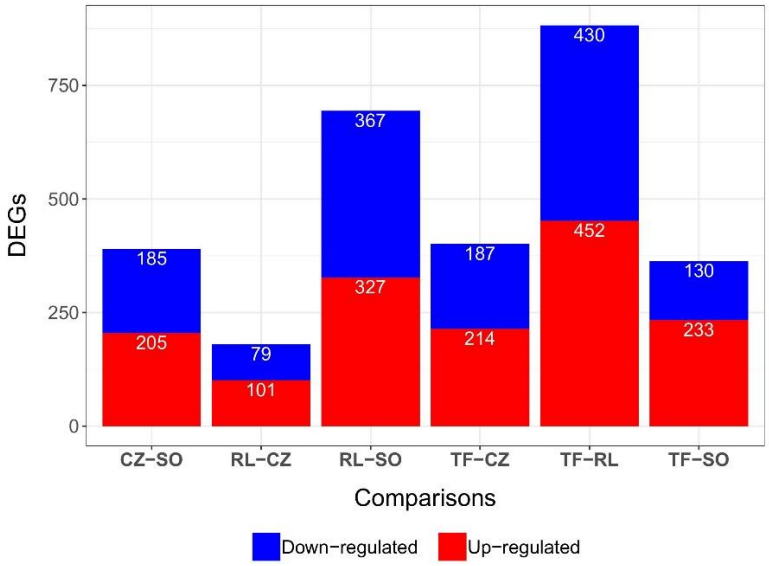

B.

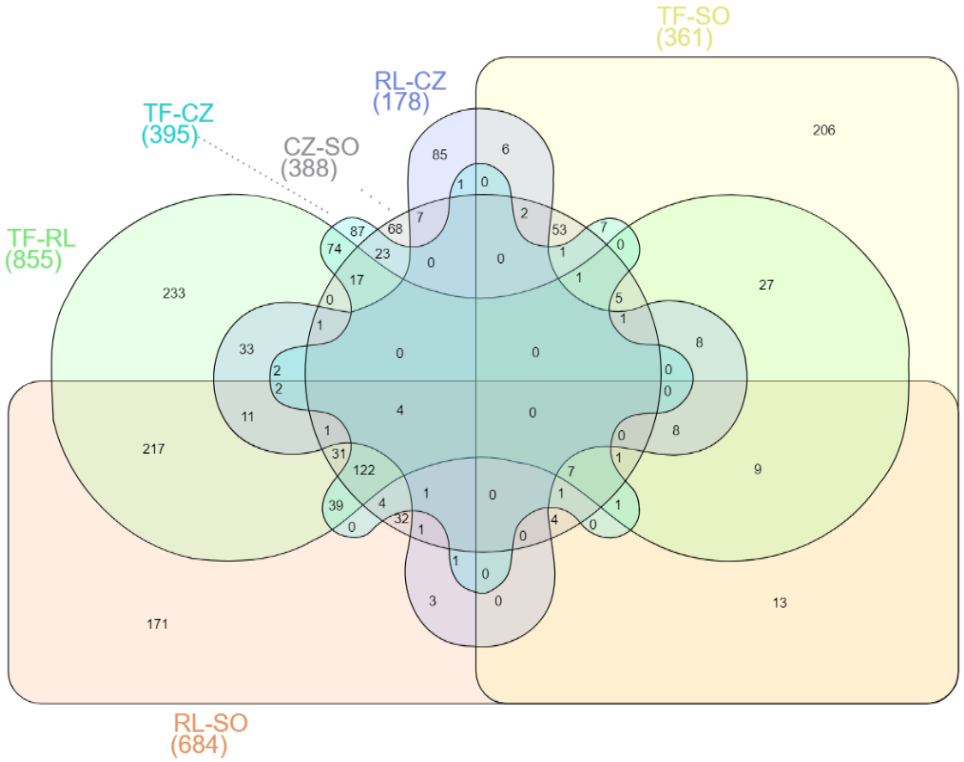

Figure 1.5. Differential gene expression analysis of fruit grafted onto various rootstocks. (A) The number of differentially expressed genes (DEGs) for all pairwise comparisons (P <0.05); red, DEGs with up-regulated expression; blue, DEGs with down-regulated expression. SO = fruit from tree grafted on sweet orange rootstock; CZ = fruit from tree grafted on Carrizo rootstock; RL = fruit from tree grafted on rough lemon rootstock; TF = fruit from tree grafted on trifoliate rootstock (B) Venn diagram of overlapping DEGs among various pairwise comparisons.

Functional classification of DEGs

Gene Ontology (GO) and pathway enrichment analyses were conducted to explore the functions of genes that were DE in trees on different rootstocks. GO categorization showed that the molecular function GO terms ‘DNA-binding transcription factor activity’ and ‘transferase activity’ were significantly enriched (Figure 1.6). Genes associated with photosynthesis and located in the photosynthetic membrane were also enriched (p-value < 0.05). KEGG pathway analysis revealed that genes for plant-hormone signal transduction, carotenoid biosynthesis, and fructose and mannose metabolism were significantly enriched (p-value < 0.05) when comparing fruit grown on trifoliate to rough lemon rootstocks (Figure 1.7). The hormone-signaling-related pathway included DEGs involved in auxin, gibberellin (GA), abscisic acid (ABA), ethylene (ET), and jasmonic acid (JA) signaling (Figure 1.8). Visualization of fold changes using MapMan software revealed that several genes in the ABA and GA pathways were down-regulated in fruit grown on rough lemon compared to trifoliate rootstocks. Genes in the ethylene and auxin pathways were both up and down regulated (Figure 1.9A). Many genes involved in other cellular responses, as well as transporters were also DE (Figure 1.9B, C).

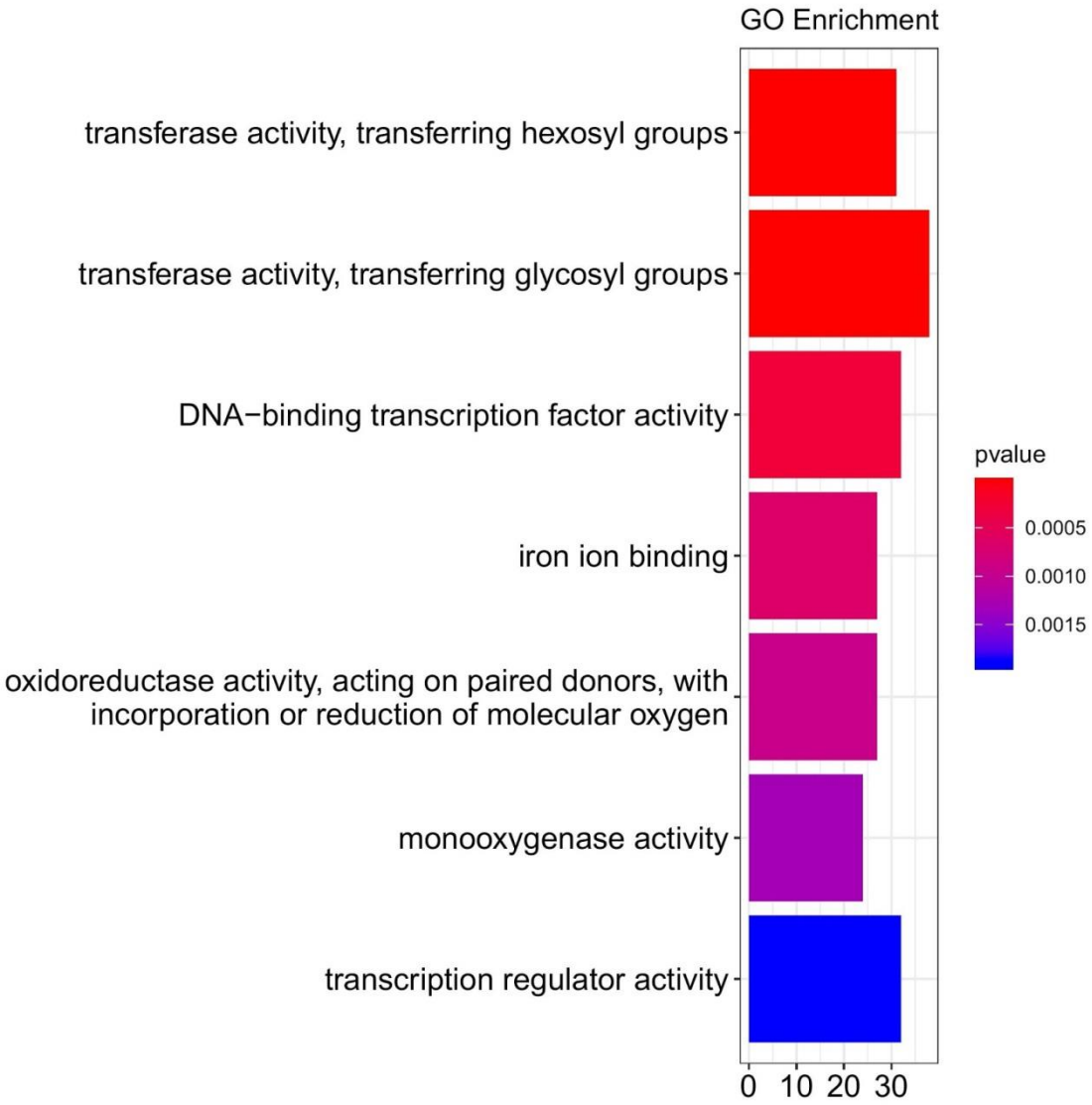

Figure 1.6. Gene ontology analysis of differentially expressed genes in fruit grafted onto trifoliate orange vs rough lemon rootstock.

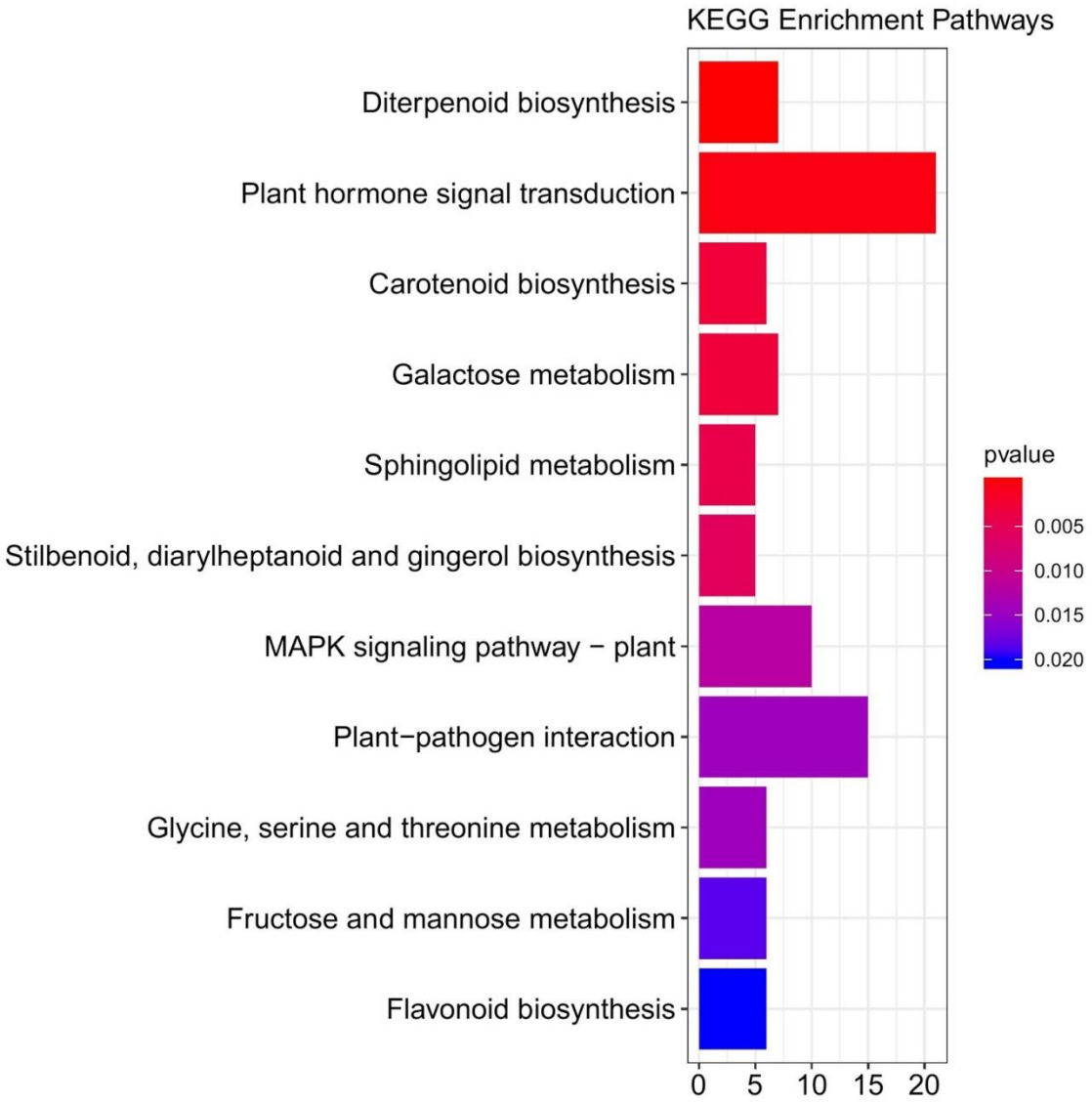

Figure 1.7. KEGG pathway enrichment of differentially expressed genes in fruit grafted onto trifoliate orange compared to rough lemon rootstock.

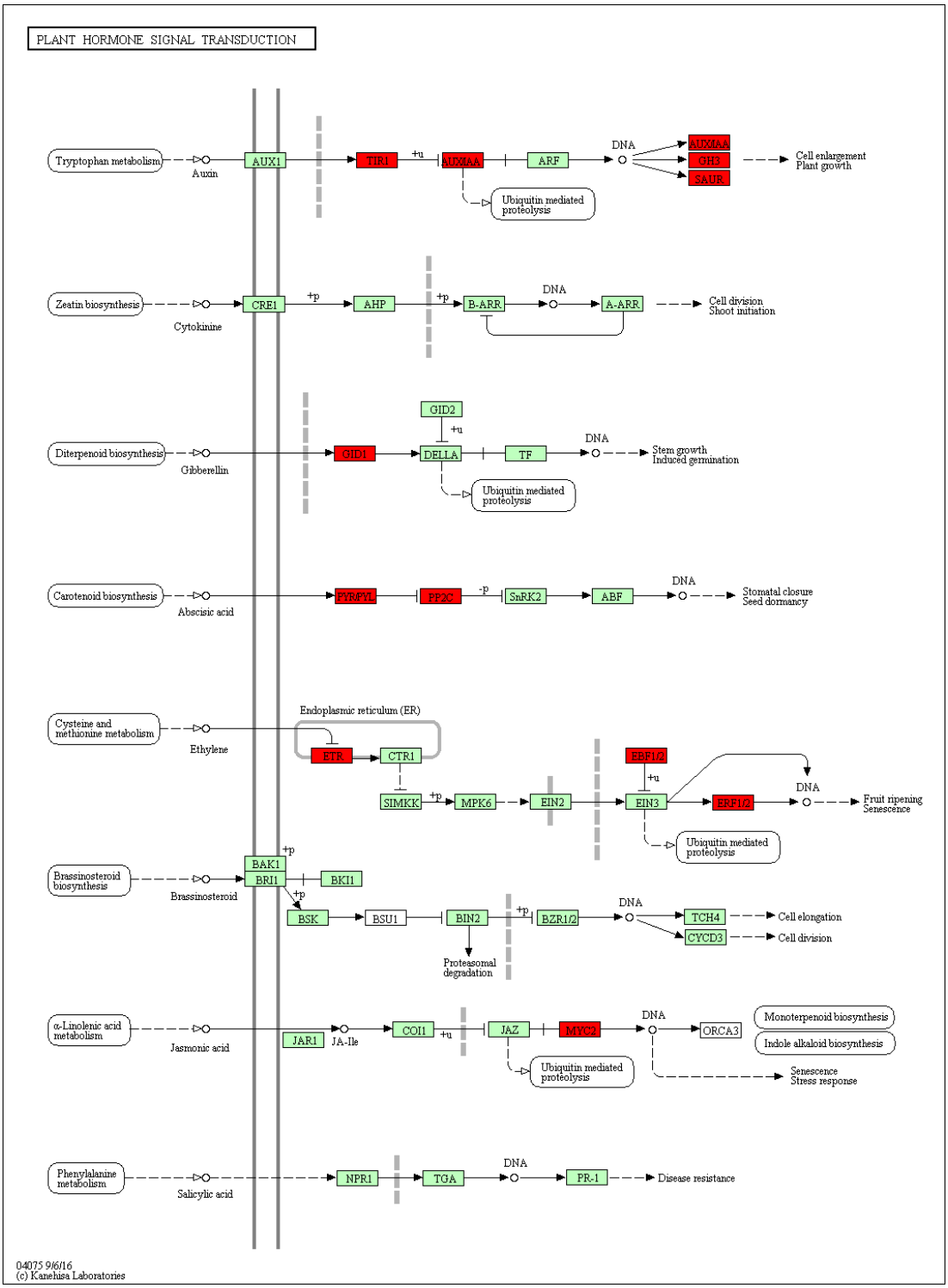

Figure 1.8. Schematic of the 'Plant hormone signal transduction' pathway. DEGs from the comparison of citrus fruit from trees grafted on trifoliate versus rough lemon rootstock highlighted in red. The map is from the Kyoto Encyclopedia of Genes and Genomes (KEGG).

A.

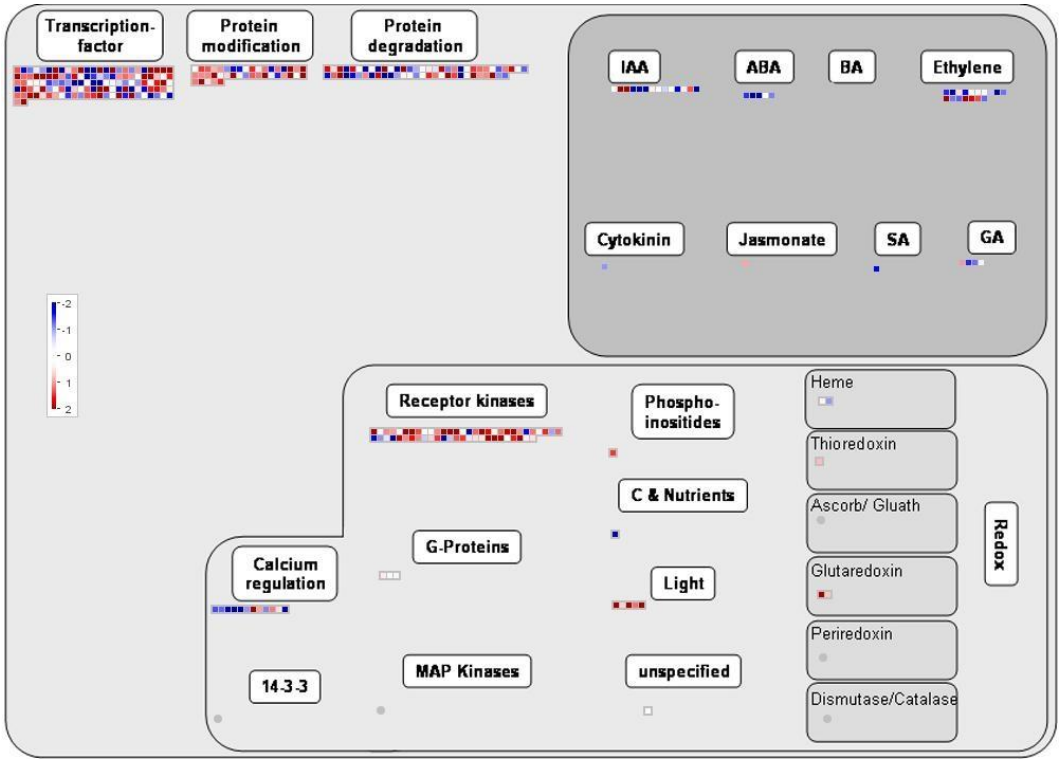
Transcription-factor
Protein modification
Protein degradation
IAA
ABA
BA
Ethylene
Cytokinin
Jasmonate
SA
GA
-2
-1
0
1
2
Receptor kinases
Phospho-inositides
Heme
Thioredoxin
C & Nutrients
Ascorb/ Gluath
Redox
Calcium regulation
G-Proteins
Light
Glutaredoxin
Periredoxin
14-3-3
MAP Kinases
unspecified
Dismutase/Catalase

B.

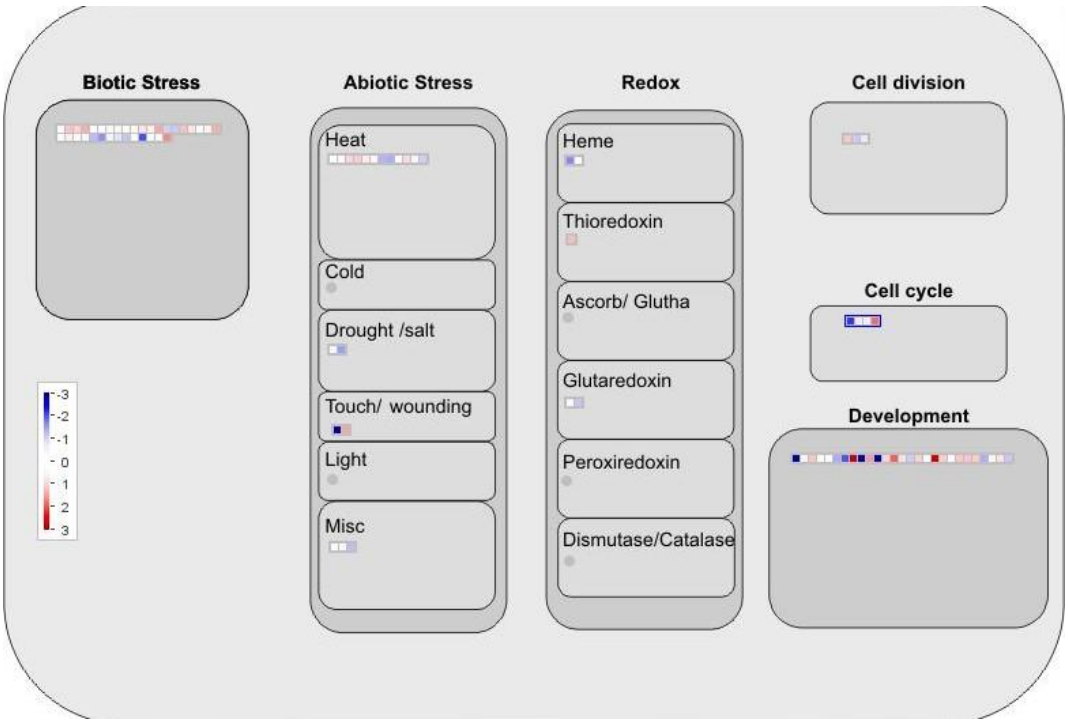
Biotic Stress
Abiotic Stress
Redox
Cell division
Heat
Heme
Thioredoxin
Cold
Cell cycle
Ascorb/ Glutha
Drought /salt
Glutaredoxin
Touch/ wounding
Development
Peroxiredoxin
Light
Misc
Dismutase/Catalase
-3
-2
-1
0
1
2
3

C.

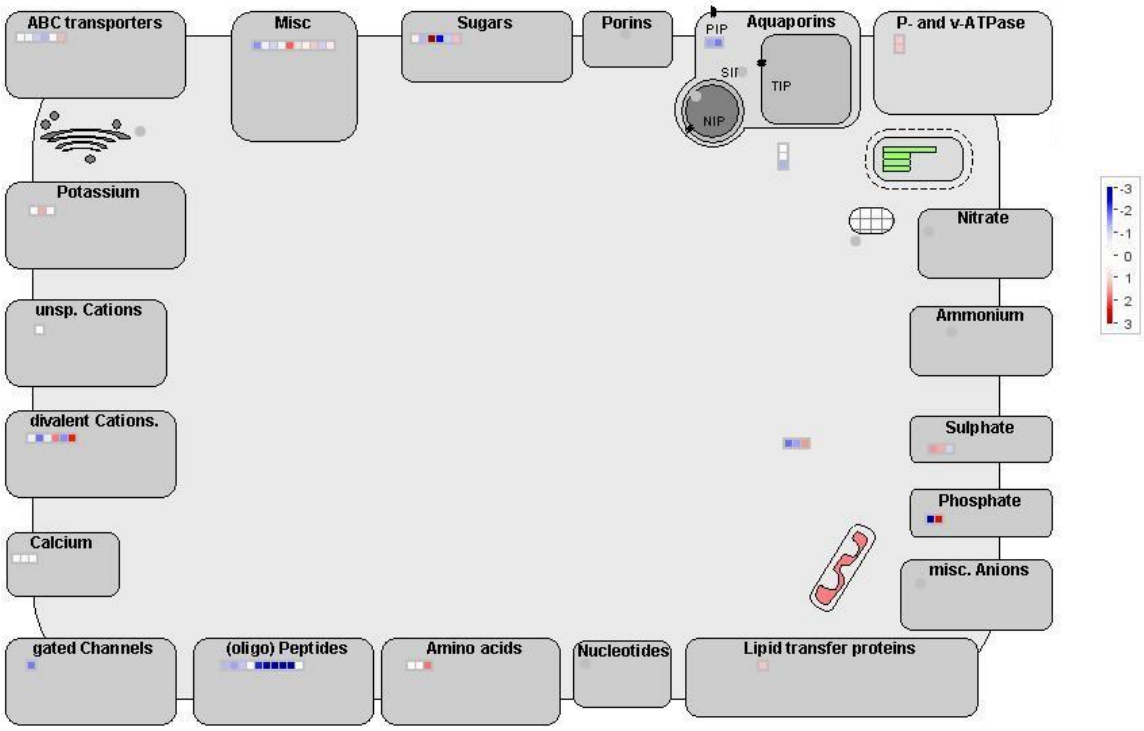

Figure 1.9. Relative expression levels of DEGs involved in (A) regulation and hormone signaling, (B) cellular response, and (C) transport. Genes that were up-regulated in fruit grown on trifoliate orange rootstock compared to rough lemon rootstock are represented in red and down-regulated genes are represented in blue. The map is from MapMan Application Software.

Transcriptional changes of fruit quality related genes

Among the identified DEGs, there were many genes that have potential roles in fruit quality. Over 130 citrus genes were DE in this study that have been previously linked to fruit development and ripening (Supplemental Table 1.2)[23,25–29,31,78–80]. Of these DEGs, 8, 6, and 22 belonged to starch-related, fructose-related, and hormone-signaling proteins, respectively. Additionally, 25 of these DEGs were annotated as transcription factors (Figure 1.10). Most of the significant differences in transcriptional changes occurred at the second and third time points, and many of the expression levels changed from time two to time three (ie. a gene was up-regulated at time two in trifoliate orange compared to rough lemon rootstock and down-regulated at time three or vice versa). Figure 1.11, which shows all DEGs between genotypes, displays this trend.

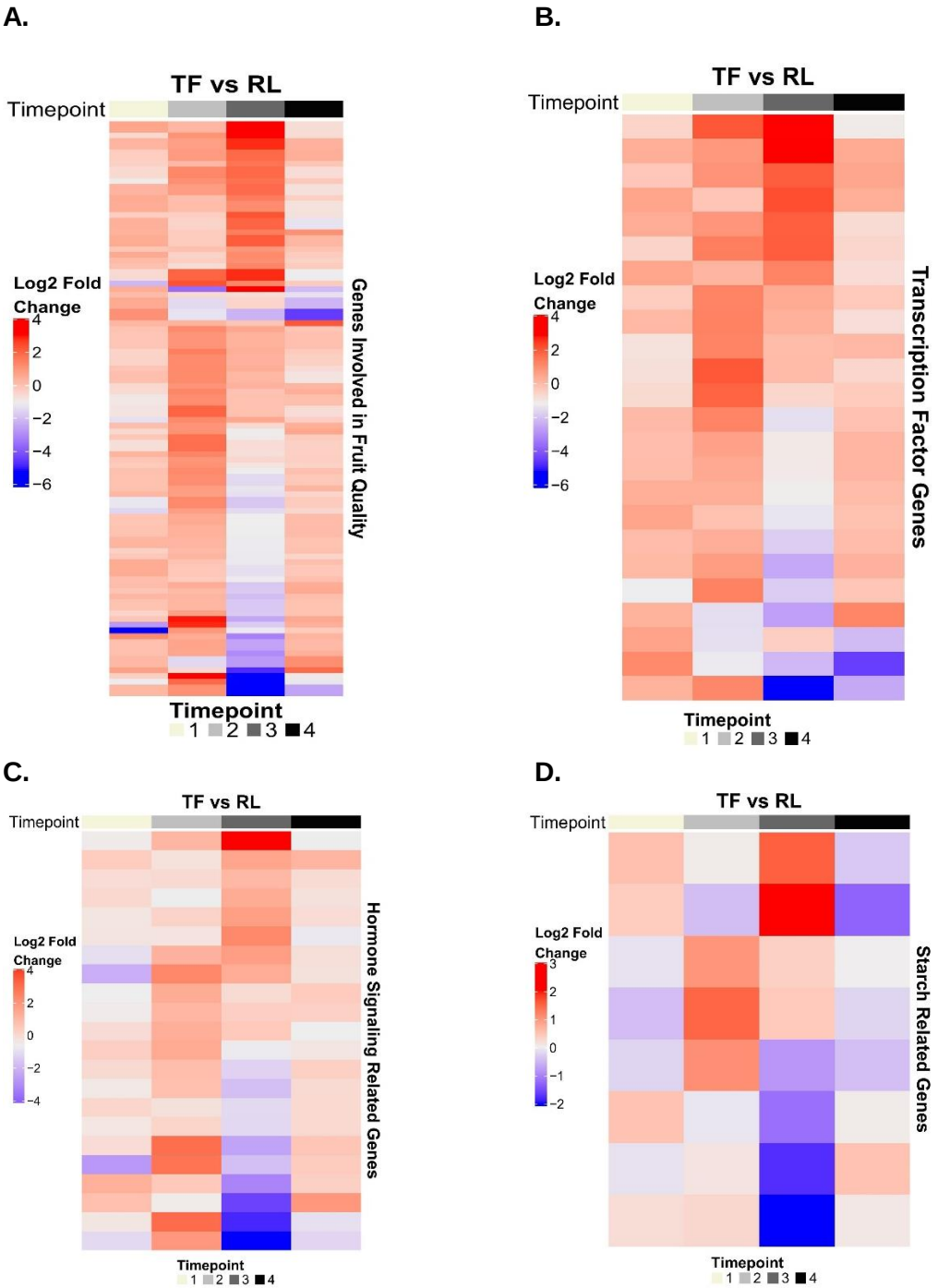

Figure 1.10. Heatmaps of differentially expressed genes (DEGs) and transcription factors related to fruit quality in fruit tissue. DEGS were observed between fruit grown on trees grafted to trifoliate orange vs rough lemon rootstocks at each time point (1, 2, 3, and 4). (A) All genes correlated to fruit quality (n=101). (B) Transcription factor genes (n=24). (C) hormone signaling genes (n=22). (D) Starch-related genes (n=8).

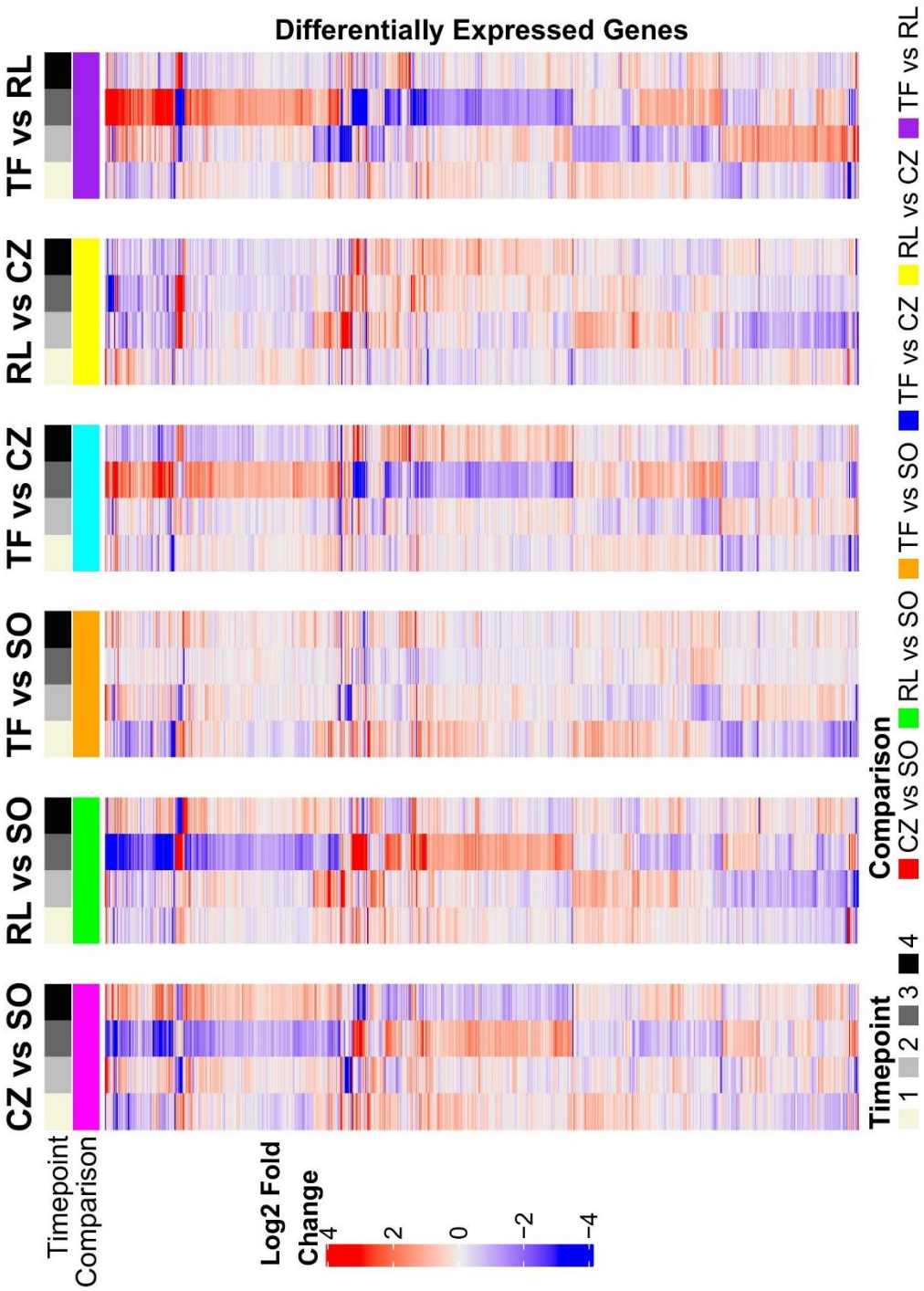

Figure 1.11. Heatmaps of all differentially expressed genes (DEGs) between different genotype comparisons in fruit tissue at each time point (1, 2, 3, and 4).

miRNA–mRNA interaction

To further understand the genetic influence of rootstocks on fruit quality, we focused on the expression changes of miRNAs and their target genes. miRNAs are post-transcriptional regulators that cause downregulation of target genes[47]. Therefore, if a target gene is down-regulated by a miRNA, a negative correlation between miRNA expression and the target mRNA expression is expected. No statistically significant differentially expressed miRNAs (DEMs) were observed in our fruit small RNA seq data, so we instead predicted miRNAs that are potentially targeting DEGs found in fruit tissues. This approach was taken due to the complex regulatory networks that are known to exist in plants and other higher organisms. One miRNA may regulate many genes as its targets, while one gene may be targeted by many miRNAs[81–83]. Both of these scenarios were observed in citrus roots in response to dehydration and salt stress[84]. To evaluate these potential relationships in this study, the psRNATarget program (https://plantgrn.noble.org/psRNATarget/analysis?function=3) was utilized, which accepts a list of known plant miRNAs in citrus and the coding sequence of the DEGs reported here to predict miRNAs according to the criteria described by Meyers et al.[85].

Over 15,000 miRNA-mRNA interactions were predicted using psRNATarget. The RNA-seq data was then utilized with an in-house R-script in order to select potential interacting pairs with an expected negative correlation in gene expression. After removal of genes that did not have any functional annotation, there were 366 combinations of miRNA-mRNA pairs that showed reciprocal expression patterns. Comparing these genes with the enriched GO terms and KEGG pathways led to several candidate

miRNA-mRNA interactions that could be causing changes in fruit traits when differentially expressed between rootstocks. These genes included transcriptional regulators, hormone signal transduction genes, transporters, and sugar metabolism genes.

Validation of the sequencing data by quantitative RT-PCR

Based on the interacting pairs predicted and their relevance to fruit quality, 10 pairs of miRNAs and target mRNAs were selected for validation via qRT-PCR analysis (Table 1.4). Samples collected at timepoints two and three were chosen for validation due to the larger differences in expression levels of genes in fruit grown on trifoliate orange compared to rough lemon rootstocks at those times. For qRT-PCR, two biological replicates and three technical replicates were analyzed to quantify expression of each gene.

Three miRNAs (Csi-miR1863, Ctr-miR319, and Csi-miR845) were up-regulated at both timepoints, while their target genes were down-regulated, two miRNAs (Csi-miR390a and Csi-miR171a) were down-regulated at both timepoints, while their target genes were up-regulated, and the remaining five miRNAs validated were down-regulated at one time point and up-regulated at the other (with inverse target gene expression) (Figure 1.12). The correlation between the relative expression level detected by qRT-PCR and by RNA-sequencing was calculated. Pearson correlation values were highly significant with $r = 0.94$, which strongly supported the sequencing data (Figure 1.13). However, certain miRNA-mRNA pairs did not have the expected fold changes from one time point to the next. For example, Csi-miR171a shows an increased fold change from September to

November. This should correlate with a decreased fold change from September to November in the target gene (ATHAM3), but instead, we see an increase in the target mRNA expression from September to November. Only this pair and Csi-miR1863 - AT-EXP1 show this inconsistency. The results for the remaining eight pairs were consistent with their expected expression levels. Figure 1.12 shows that seven of the miRNAs had increased expression levels in November compared with September, while three miRNAs decreased in expression from the during fruit development.

Table 1.4. Deep sequencing and qRT-PCR relative expression of selected miRNAs and their predicted target genes.

sRNA	Predicted target gene (*C. clementina* locus name)	Arabidopsis Homology	Arabidopsis gene name and description	RNA-seq				qRT-PCR				RNA-seq - qPCR Correlation	sRNA-mRNA Correlation
				Fold change of sRNA		Fold change of target gene		Fold change of sRNA		Fold change of target gene			
				Time 2	Time 3	Time 2	Time 3	Time 2	Time 3	Time 2	Time 3		
Csi-miR164a	Ciclev10012379m.g	AT2G37170.1	PIP2B - plasma membrane intrinsic protein 2	-0.507	0.562 *	0.626	-1.745 *	-0.307	0.049 *	0.282	-0.776 *	0.982	-0.995
Csi-miR1863	Ciclev10021897m.g	AT1G69530.2	AT-EXP1 -expansin A1	0.895	0.055	-0.134	-1.434 *	0.31	0.021	-0.279 *	-0.407 *	0.912	0.597
Csi-miR1023	Ciclev10018566m.g	AT1G68710.1	ATPase E1-E2 type family protein / haloacid dehalogenase-like hydrolase family protein	1.051 *	-0.013	-0.718 *	1.127 *	0.257	-0.437	-0.371	1.233 *	0.817	-0.886
Csi-miR390a	Ciclev10002290m.g	AT3G04730.1	IAA16 - indoleacetic acid-induced protein 16	-0.585	-0.516	1.284 *	0.491	-0.538 *	-0.174	0.692	0.628 *	0.925	-0.42
Csi-miR833.1	Ciclev10002239m.g	AT3G50060.1	MYB77 - myb domain protein 77	-0.767 *	0.174	1.135	-5.152 *	-0.191	0.217 *	0.907 *	-3.419 *	0.998	-0.84
Ctr-miR319	Ciclev10026743m.g	AT1G72430.1	SAUR-like auxin-responsive protein family	0.195	0.564	-1.434	-2.984 *	0.105	0.314 *	-1.120 *	-2.033 *	0.998	-0.954
Csi-miR845	Ciclev10020137m.g	AT4G11090.1	TBL23 - TRICHOME BIREFRINGENCE-LIKE 23	1.173 *	0.275	-1.096 *	-0.093	0.192	0.01	-1.320 *	-0.332 *	0.947	-0.431
Csi-miR1092.2b	Ciclev10019134m.g	AT1G12240.1	ATBETAFRUCT4,VAC-INV - Glycosyl hydrolases family 32 protein	-0.222	0.539 *	0.312	-1.953 *	-0.465 *	0.25	0.064	-1.708 *	0.998	-0.937
Csi-miR171a	Ciclev10019083m.g	AT4G00150.1	ATHAM3 - GRAS family transcription factor	-0.774	-0.293	0.238	1.054 *	-0.503 *	-0.174	0.181	1.185 *	0.987	0.782
Csi_n01	Ciclev10004981m.g	AT5G51760.1	AHG1 - Protein phosphatase 2C family protein	-0.501	0.319	0.789	-1.695 *	-0.163	0.727 *	0.187	-1.040 *	0.886	-0.912

Both fold change of sRNAs and target genes are the ratio of the expression levels in fruits grown on trifoliate rootstock compared to fruits grown on rough lemon rootstock. The value for fold change in qRT-PCR experiments is an average of two biological replicates with three technical replicates; * indicates a significant difference at $P < 0.05$ when comparing the two genotypes at a given time point.

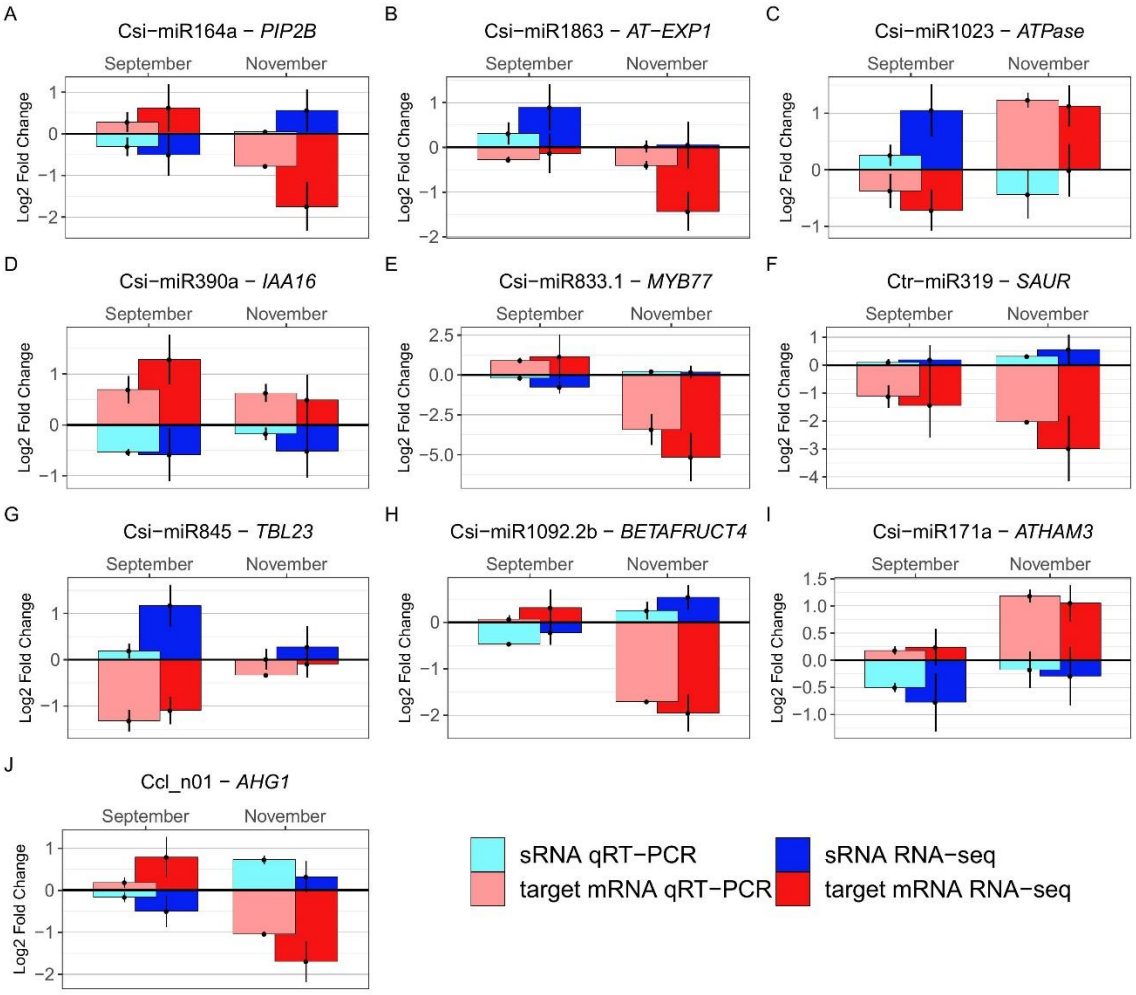

Figure 1.12. qRT-PCR validation of differential expression patterns of genes and miRNAs in fruit tissues from trees grafted onto trifoliate orange and rough lemon rootstocks. Relative expression levels of genes in fruit grown on trifoliate compared to rough lemon rootstocks is shown. qPCR log2 fold changes are represented by light blue and pink for miRNA and mRNA expression, respectively. The corresponding RNA-seq data is represented by dark blue and red for miRNA-mRNA pair. *GAPDH* and *U6* were used as the reference genes for mRNA and miRNA, respectively. The error bars indicate standard error of the means of two biological replicates and three technical replicates. (A) Csi-miR164a - *PIP2B*, (plasma membrane intrinsic protein 2); (B) Csi-miR1863 - *AT-EXP1*, (expansin A1); (C) Csi-miR1023 - *ATPase*, (ATPase E1-E2 type family protein); (D) Csi-miR390a - *IAA16*, (indoleacetic acid-induced protein 16); (E) Csi-miR833.1 - *MYB77*, (myb domain protein 77); (F) Ctr-miR319 - *SAUR*, (SAUR-like auxin-responsive protein family); (G) Csi-miR845 - *TBL23*, (trichome birefringence-like 23); (H) Csi-miR1092.2b - *BETAFRUCT4*, (VAC-INV - Glycosyl hydrolases family 32 protein); (I) Csi-miR171a - *ATHAM3*, (GRAS family transcription factor); (J) Ccl_n06 - *AHG1*, (Protein phosphatase 2C family protein).

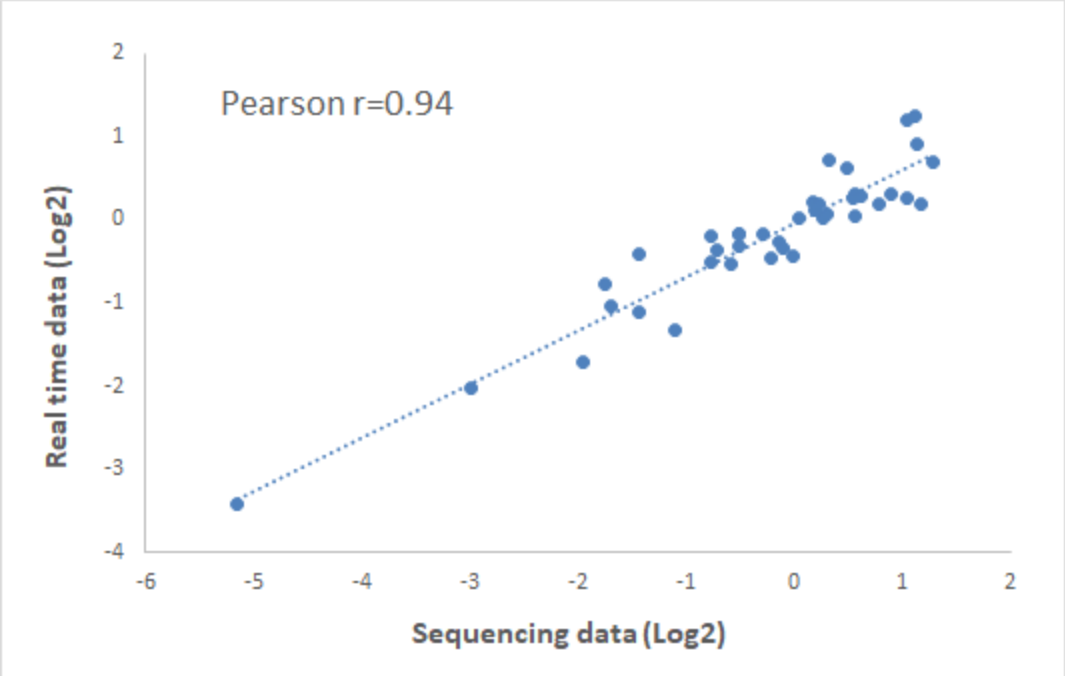

Figure 1.13. Correlation of September to November gene expression ratios between sequencing data and quantitative RT-PCR data. Pearson correlation scatter plot of comparisons of ratios measured by sequencing and quantitative RT-PCR in mRNAs and miRNAs. 20 genes, including 10 mRNAs and 10 miRNAs, were subjected to quantitative real-time PCR analysis. RNA-seq data (fold changes in gene expression) were plotted against qRT-PCR data (fold-changes in gene expression). Both the x and y-axes are shown in log2 scale. r indicates the Pearson correlation coefficient.

Discussion

The objective of this study was to correlate changes in gene expression of grafted citrus trees to effects in fruit quality due to varying rootstocks. In this study, four rootstocks were chosen from a rootstock trial with Washington navel orange scion in Riverside, CA to assess for various fruit quality traits; Argentina sweet orange, Schaub rough lemon, Carrizo citrange, and Rich 16-6 trifoliate orange. Fruit quality data was collected from fruit grown on each of the four rootstocks at the end of the growing season when fruit were ripe. In the present study, weight, height, width, rind color, rind texture, peel

thickness, internal texture, juice weight, percent juice, total soluble solid (TSS) and titratable acid (percent acid) levels were measured. The total yield and average fruit weights were markedly higher in navel orange fruit from trees grafted onto rough lemon compared to sweet orange, Carrizo citrange, or trifoliate orange rootstocks. The rind thickness was also greatest on rough lemon rootstocks compared with the other rootstock-scion combinations. The most substantial differences could be seen in total soluble solids and acid levels. The highest levels of sugars and acids were found in fruit grown on Carrizo citrange. Trifoliate orange and sweet orange rootstocks produced fruit with only slightly lower sugar and acid levels, while rough lemon produced fruit with significantly lower levels (Figure 1.1). This is consistent with the previously mentioned reports of rootstock effects on fruit quality[3,7-14]. Presently, there is very little understanding of how rootstocks influence citrus fruit quality, especially at the level of gene regulation. In this study, an integrated mRNA and miRNA high throughput sequencing analysis in fruit grafted onto genetically diverse rootstocks was performed to help resolve potential mechanisms of rootstock-scion effects on fruit quality.

Transcriptome sequencing and DEG screening of ‘Washington’ navel sweet orange fruit on different rootstocks

In the present study, RNA-seq was used to investigate transcriptome differences in the fruit of ‘Washington’ navel sweet orange grafted onto different rootstocks and explore genes that may influence fruit quality traits. Juice vesicles from fruit grafted onto four genetically diverse rootstocks at four different fruit development periods were sequenced. The RNA-seq approach detected a similar number of genes in all samples

(an average of ~19,300 genes were represented in each rootstock-scion combination). A large number of these genes were identified as differentially expressed over the course of fruit development, which is consistent with previous studies of transcriptome changes during fruit ripening in sweet orange (Yu et al., 2012). However, most genes (54.7%) showed similar temporal expression patterns among all rootstock genotypes. Furthermore, only ~15% of the genes were genotype-specific (Supplemental Figure 1.2). Therefore, the remainder of this study focused on DEGs identified between these rootstock genotypes during fruit development.

A total 684, 388, 361, 178, 395, and 885 genes were significantly differentially expressed between RL vs SO, CZ vs SO, TF vs SO, RL vs CZ, TF vs CZ and TF vs RL rootstocks respectively (RL=rough lemon, SO=sweet orange, CZ=Carrizo, TF=trifoliate). The majority of the differentially expressed genes are observed in comparisons involving rough lemon rootstocks, especially compared to trifoliate orange. This is consistent with the observed differences in fruit quality traits, as fruit of trees grafted on rough lemon rootstock showed consistent significant differences from fruit of trees grafted on the other three rootstocks in many of the traits measured (Figure 1.1, Table 1.1). These results suggest that rough lemon and trifoliate rootstocks show the greatest effects on the scion and are good candidates to identify graft-related genes playing a role in fruit quality.

The largest and most significant changes in gene expression between rootstocks were observed at time points two and three (September and November, respectively). Among the DEGs were several genes with functions involved in fruit quality traits, such as those

relating to starch and sucrose metabolism, fructose metabolism, and hormone signaling-related genes. KEGG pathway analysis displayed plant hormone signal transduction, carotenoid biosynthesis, and fructose and mannose metabolism pathways to be significantly enriched. Several genes involved in various hormone-signaling pathways were DE, mainly genes in the abscisic acid (ABA) and auxin-response pathways. Several genes involved in these pathways were chosen to validate the RNA-seq data by qRT-PCR due to their potential biological significance regarding rootstock effects on fruit quality.

Role of hormonal signaling pathway genes in scion-rootstock interactions

ABA has been known to be a regulator of fruit ripening and response to abiotic stress in non-climacteric fruit[86]. AHG1, a homolog of Arabidopsis PP2C family protein, was DE in this study. PP2C is a negative regulator of the ABA hormone-signaling pathway. This gene was slightly up-regulated when comparing fruit of trees grafted on trifoliate to fruit of trees grafted on rough lemon rootstock at time two and significantly down-regulated at time three (Table 1.4, Figure 1.12J). Upregulation of *AHG1* is in accordance with previous studies showing this gene being induced by water stress[34], which may have occurred in September. The downregulation of this gene later in the season could be correlated with increased fruit maturation in fruit grown on trifoliate rootstocks. This is in agreement with a study in tomato where suppression of *PP2C* expression led to increased ABA accumulation and higher levels of ABA-signaling genes that increase the expression of ABA-mediated ripening-related genes[87].

Auxin signal transduction is mediated by Aux/IAA and ARF genes[88]. Aux/IAA proteins are negative regulators of the auxin signal transduction pathway. In this study, a gene encoding an Aux/IAA protein, *IAA16,* was up-regulated in fruit grown on trifoliate compared to rough lemon rootstocks at time two and three (Table 1.4, Figure 1.12D). A previous study revealed that a gain-of-function mutation in *IAA16* displayed reduced response to auxin and ABA, which led to reduced plant growth[89]. Silencing of related Aux/IAA genes increased fruit size in tomato due to auxin control of cell expansion and elongation[90,91]. In addition to Aux/IAA, another early auxin-response gene, *SAUR78*, was DE in this study. This gene was down-regulated in fruit grown on trees grafted onto trifoliate compared to rough lemon rootstocks at time two and three (Table 1.4, Figure 1.12F). Small Auxin Up RNA (SAUR) genes are a group of auxin-inducible proteins. *SAUR78* overexpression lines in Arabidopsis increased plant growth through interaction with ethylene receptor[92]. Other SAUR genes have also been shown to promote cell expansion[93–95]. Furthermore, a *MYB77* gene encoding a transcription factor was DE in this study, displaying a slight increase in expression in fruit grown on trifoliate rootstock at time two, but a large decrease in expression at time three (Table 1.4, Figure 1.12E). This gene was previously described as a regulator of the auxin signal transduction pathway[96]. This protein was shown to interact with ARFs to promote plant growth. Interestingly, the effects of MYB77 in Arabidopsis were found to be increased by endogenous exposure to ABA and further promote plant growth[97]. While these two studies were performed in roots, this transcription factor was shown to be involved in citrus fruit ripening, where it was highly correlated with ABA and suggested to have a similar function in response to the hormone[28].

Although there were not statistically significantly differences seen in other genes in the auxin- and ABA-signaling pathways, trends could be observed during hierarchical clustering of these genes. Many of the genes within a family shared common expression levels and generally follow the predicted regulatory patterns in their respective pathways (Figure 1.8, Supplemental Figure 1.3). Taken together, the changes in ABA- and auxin-responsive genes suggest a potential mechanism for induced ripening by trifoliate rootstock and larger fruit produced when rough lemon is used as a rootstock.

Differential expression of other fruit-ripening related genes

The expansion phase of citrus fruit development involves cell enlargement and water accumulation. Given the changes in hormone-signaling pathways that likely lead to changes in fruit size, other genes related to fruit growth, such as transporters and genes related to cell wall metabolism were investigated. This led to the identification of two DEGs that could be influencing fruit size. The first, a *Plasma membrane Intrinsic Protein 2 (PIP2B)* gene encoding an aquaporin was down-regulated in fruit grown on trifoliate rootstock (Table 1.4, Figure 1.12A). Water import in plants is mediated by aquaporins and essential for cell expansion[98]. These genes were highly expressed in expanding green grapes and one was identified as a candidate gene under the QTL for berry weight[99]. *PIP* genes were also associated with an increase in volume of fruit in apple and strawberry[100,101]. The second DEG, an expansin (*EXP1*), was also down-regulated in fruit grown on trifoliate rootstock (Table 1.4, Figure 1.12B). Expansins play various roles in fruit development, including cell elongation and cell wall softening[102]. A homolog of *EXP1* in tomato was expressed during green fruit cell division and expansion with maximum

accumulation of *EXP1* during the late phase of green fruit expansion and early maturation[103]. The increase in expression of these two genes in fruit grown on rough lemon rootstock could contribute to the larger fruit size observed.

In addition to cell division and cell expansion, during fruit development, fruit softening is also an important feature that relies on cell wall metabolism[104]. The *Trichome Birefringence-Like (TBL)* gene, which encodes a protein required for cellulose biosynthesis[105], was identified in our study as DE. Mutations in this gene caused a reduction in the amount of pectins and an increase in pectin methylesterase (PME) activity. PME catalyses the demethylesterification of pectin, which may undergo depolymerisation by glycosidases. *TBL23* was up-regulated in fruit grown on trifoliate rootstock compared to rough lemon (Table 1.4, Figure 1.12G), suggesting a potential role in fruit softening during citrus ripening.

Transcription factors also play an important role in plant development and fruit ripening. Several transcription factors were differentially expressed in this study. GO enrichment showed the molecular function GO term 'DNA-binding transcription factor activity' was significantly enriched. In addition to the *MYB77* transcription factor gene described earlier, a GRAS transcription factor gene, *HAM3*, was DE in this study. GRAS transcription factors were previously found to play a role in berry development and ripening in grapes, tomato, and citrus[28,106,107]. This transcription factor showed increased expression later in the season when fruit were grown on trifoliate rootstock, suggesting the rootstock influences its role in improved citrus fruit quality.

The largest phenotypic differences seen in mature fruit grown on trifoliate compared to rough lemon rootstock were in the levels of total soluble sugar and titratable acid in ripe fruit. The levels of sugars and acids and their ratio in fleshy fruits is one of the most important determinants of sensory traits such as taste and flavor[108,109]. Two genes were identified as differentially expressed that could play a role in the accumulation of these compounds. Firstly, a P-type ATPase was DE in fruit growing on trees grafted onto trifoliate versus rough lemon. This gene was down-regulated at time two, but up-regulated at time three (Table 1.4, Figure 1.12C). Studies have proposed a number of ATPases as proton pumps that are responsible for organic acid accumulation in citrus fruit[21,24,110,111]. The reduced expression of this ATPase gene later in the season in fruit grown on rough lemon rootstocks could contribute to the lower accumulation of titratable acid levels in these fruits. This ATPase gene identified in this study was not identified in the previous citrus studies, but the regulation of acid accumulation is a complex, as can be seen in other fruits, such as papaya and apple[112,113]. It is possible this is a graft-induced effect observed with these specific rootstocks, which were not examined in the previous studies.

Secondly, a homolog of Arabidopsis *BETAFRUCT4* was down-regulated in fruit of trees grown on trifoliate rootstock compared to rough lemon at time three (Table 1.4, Figure 1.12H). This gene encodes a vacuolar invertase. Decreased expression of vacuolar invertases has been associated with increased sucrose content and accelerated ripening[114–117]. Interestingly, by using an antisense acid invertase gene in transgenic

tomato to reduce acid invertase activity, fruit displayed higher levels of sucrose, as well as smaller fruit[118]. We see similar trends in sugar accumulation and alterations in fruit size in this study. Klann et al. suggested that the water influx that drives fruit expansion is closely related to the concentration of osmotically active soluble sugars and therefore, all genotypes accumulate water until they reach a similar threshold of soluble sugar concentration[118]. This could also contribute to the increased size of fruit grown on rough lemon fruit compared to trifoliate rootstocks.

Role of miRNAs in rootstock-scion interactions

This study did not identify any statistically significant differentially expressed miRNAs (DEMs) from our fruit small RNA seq data. Therefore, potential miRNAs that target DEGs were predicted. An in-house R-script was used to select for miRNA-mRNA interaction pairs with an expected negative correlation in gene expression. These pairs were identified for the ten genes described above. All ten miRNA genes and their target mRNAs were detected by qRT-PCR. Pearson correlation coefficient value between the relative expression level detected by qRT-PCR and by RNA-sequencing was highly significant with $r = 0.94$. Of the ten interaction pairs, eight followed expected fold changes between timepoints (for example a miRNA showing an increase in fold change from September to November should correlate with a decreased fold change in the target gene). Therefore, it is likely that these eight target mRNAs are being regulated to some extent by their respective miRNA.

Only two pairs (Csi-miR1863 - AT-EXP1 and Csi-miR171a - ATHAM3) do not follow the expected inverse relationship between timepoints, suggesting those mRNAs are not being regulated post transcriptionally by their miRNAs. This has been observed in previous integrated miRNA-mRNA studies[84,119]. There have also been reports of target genes having a negative or positive feedback regulation on their respective miRNA, which could be another explanation for the inconsistent correlations seen in this study[120,121].

Conclusion

In conclusion, the present study provides a dynamic view of the transcriptome of fruit from navel oranges grafted onto various rootstocks. The combination of decreased size along with the increased concentrations of sugars and acids in fruit from trees on trifoliate orange are typical effects of this rootstock on fruit quality and this study offers potential molecular mechanisms for these phenotypic differences. Ten candidate transcripts related to primary metabolism, hormone signaling, and transcription factor regulation and eight miRNAs likely regulating some of these genes were identified. The expression patterns of these miRNAs and genes indicated that the related biological pathways may be responsible for changes in fruit quality in scion-rootstock combinations and might be good targets for manipulation. These results enhance our understanding of rootstock effects in grafted citrus but require additional functional validation.

References

1. Citrus Fruits 2018 Summary 08/28/2018. 35 (2018).

2. Wareing, P. F. Problems of juvenility and flowering in trees. *Journal of the Linnean Society of London, Botany* **56**, 282–289 (1959).

3. Martínez-Cuenca, M.-R., Primo-Capella, A. & Forner-Giner, M. A. Influence of rootstock on citrus tree growth: effects on photosynthesis and carbohydrate distribution, plant size, yield, fruit quality, and dwarfing genotypes. *Plant Growth* (2016). doi:10.5772/64825

4. Simpson, C. R. *et al.* Growth response of grafted and ungrafted citrus trees to saline irrigation. *Scientia Horticulturae* **169**, 199–205 (2014).

5. Castle, W. S. A career perspective on citrus rootstocks, their development, and commercialization. *HortScience* **45**, 11–15 (2010).

6. Zhang, X., Breksa, A. P., Mishchuk, D. O. & Slupsky, C. M. Elevation, rootstock, and soil depth affect the nutritional quality of mandarin oranges. *J. Agric. Food Chem.* **59**, 2672–2679 (2011).

7. Al-Jaleel, A. & Zekri, M. Effects of rootstocks on yield and fruit quality of 'Parent Washington Navel' trees. *Proceedings of the Florida State Horticultural Society* **116**, 270–275 (2003).

8. Liu, X. *et al.* Transcriptome changes associated with boron deficiency in leaves of two citrus scion-rootstock combinations. *Front. Plant Sci.* **8**, (2017).

9. Roose, M. L. Citrus rootstock breeding and evaluation. *Annual Report* 3 (2008).

10. Roose, M. Lane Late navel orange replant trial at Lindcove. (2009).

11. Roose, M. L., Cole, D. A., Atkin, D. & Kupper, R. S. Yield and tree size of four citrus cultivars on 21 rootstocks in California. *Journal of the American Society for Horticultural Science* (1989).

12. Rouse, R. E. Citrus fruit quality and yield of six Valencia clones on 16 rootstocks in the Immokalee foundation grove. *Proceedings of the Florida State Horticultural Society* **113**, 112–114 (2000).

13. Sinclair, W. & Bartholomew, E. Effects of rootstock and environment on the composition of oranges and grapefruit. *Hilgardia* **16**, 125–176 (1944).

14. Rootstocks effects on fruit quality. *Factors affecting fruit quality. Lake Alfred: University of Florida* 24–34 (1988).

15. Jensen, P. J. *et al.* Rootstock-regulated gene expression patterns in apple tree scions. *Tree Genetics & Genomes* **6**, 57–72 (2010).

16. Gao, X., Zhao, S., Xu, Q.-L. & Xiao, J.-X. Transcriptome responses of grafted Citrus sinensis plants to inoculation with the arbuscular mycorrhizal fungus Glomus versiforme. *Trees* **30**, 1073–1082 (2016).

17. Huang, Y., Si, Y. & Dane, F. Impact of grafting on cold responsive gene expression in Satsuma mandarin (Citrus unshiu). *Euphytica* **177**, 25–32 (2011).

18. Licciardello, C. *et al.* A transcriptomic analysis of sensitive and tolerant citrus rootstocks under natural iron deficiency conditions. *Journal of the American Society for Horticultural Science* **138**, 487–498 (2013).

19. Liu, X.-Y., Li, J., Liu, M.-M., Yao, Q. & Chen, J.-Z. Transcriptome profiling to understand the effect of citrus rootstocks on the growth of 'Shatangju' mandarin. *PLOS ONE* **12**, e0169897 (2017).

20. Prassinos, C., Ko, J.-H., Lang, G., Iezzoni, A. F. & Han, K.-H. Rootstock-induced dwarfing in cherries is caused by differential cessation of terminal meristem growth and is triggered by rootstock-specific gene regulation. *Tree Physiol* **29**, 927–936 (2009).

21. Huang, D., Zhao, Y., Cao, M., Qiao, L. & Zheng, Z.-L. Integrated systems biology analysis of transcriptomes reveals candidate genes for acidity control in developing fruits of sweet orange (Citrus sinensis L. Osbeck). *Front. Plant Sci.* **7**, (2016).

22. Lin, Q. *et al.* Transcriptome and metabolome analyses of sugar and organic acid metabolism in Ponkan (Citrus reticulata) fruit during fruit maturation. *Gene* **554**, 64–74 (2015).

23. Liu, Q. *et al.* Transcriptome analysis of a spontaneous mutant in sweet orange [Citrus sinensis (L.) Osbeck] during fruit development. *J Exp Bot* **60**, 801–813 (2009).

24. Lu, X. *et al.* Comparative transcriptome analysis reveals a global insight into molecular processes regulating citrate accumulation in sweet orange (Citrus sinensis). *Physiologia Plantarum* **158**, 463–482 (2016).

25. Qiao, L., Cao, M., Zheng, J., Zhao, Y. & Zheng, Z.-L. Gene coexpression network analysis of fruit transcriptomes uncovers a possible mechanistically distinct class of sugar/acid ratio-associated genes in sweet orange. *BMC Plant Biol* **17**, (2017).

26. Wang, L., Hua, Q., Ma, Y., Hu, G. & Qin, Y. Comparative transcriptome analyses of a late-maturing mandarin mutant and its original cultivar reveals gene expression profiling associated with citrus fruit maturation. *PeerJ* **5**, (2017).

27. Wu, J. *et al.* An integrative analysis of the transcriptome and proteome of the pulp of a spontaneous late-ripening sweet orange mutant and its wild type improves our understanding of fruit ripening in citrus. *J Exp Bot* **65**, 1651–1671 (2014).

28. Wu, J., Fu, L. & Yi, H. Genome-wide identification of the transcription factors involved in citrus fruit ripening from the transcriptomes of a late-ripening sweet orange mutant and its wild type. *PLOS ONE* **11**, e0154330 (2016).

29. Yu, K. *et al.* Transcriptome changes during fruit development and ripening of sweet orange (Citrus sinensis). *BMC Genomics* **13**, 10 (2012).

30. Yun, Z. *et al.* Comparative transcriptomics and proteomics analysis of citrus fruit, to improve understanding of the effect of low temperature on maintaining fruit quality during lengthy post-harvest storage. *J Exp Bot* **63**, 2873–2893 (2012).

31. Zhang, Y.-J. *et al.* Comparative transcriptome analyses between a spontaneous late-ripening sweet orange mutant and its wild type suggest the functions of ABA, sucrose and JA during citrus fruit ripening. *PLOS ONE* **9**, e116056 (2014).

32. Adams-Phillips, L., Barry, C. & Giovannoni, J. Signal transduction systems regulating fruit ripening. *Trends in Plant Science* **9**, 331–338 (2004).

33. Kumar, R., Khurana, A. & Sharma, A. K. Role of plant hormones and their interplay in development and ripening of fleshy fruits. *J. Exp. Bot.* **65**, 4561–4575 (2014).

34. Romero, P., Lafuente, M. T. & Rodrigo, M. J. The Citrus ABA signalosome: identification and transcriptional regulation during sweet orange fruit ripening and leaf dehydration. *J Exp Bot* **63**, 4931–4945 (2012).

35. Wang, X., Yin, W., Wu, J., Chai, L. & Yi, H. Effects of exogenous abscisic acid on the expression of citrus fruit ripening-related genes and fruit ripening. *Scientia Horticulturae* **201**, 175–183 (2016).

36. Jia, H. *et al.* Type 2C protein phosphatase ABI1 is a negative regulator of strawberry fruit ripening. *J Exp Bot* **64**, 1677–1687 (2013).

37. Merlot, S., Gosti, F., Guerrier, D., Vavasseur, A. & Giraudat, J. The ABI1 and ABI2 protein phosphatases 2C act in a negative feedback regulatory loop of the abscisic acid signalling pathway. *The Plant Journal* **25**, 295–303 (2001).

38. Umezawa, T. *et al.* Type 2C protein phosphatases directly regulate abscisic acid-activated protein kinases in Arabidopsis. *PNAS* **106**, 17588–17593 (2009).

39. Yoshida, R. *et al.* The regulatory domain of SRK2E/OST1/SnRK2.6 interacts with ABI1 and integrates abscisic acid (ABA) and osmotic stress signals controlling stomatal closure in Arabidopsis. *J. Biol. Chem.* **281**, 5310–5318 (2006).

40. Sack, L., John, G. P. & Buckley, T. N. ABA accumulation in dehydrating leaves is associated with decline in cell volume, not turgor pressure. *Plant Physiol* **176**, 489–495 (2018).

41. Chapman, E. J. & Estelle, M. Mechanism of auxin-regulated gene expression in plants. *Annual Review of Genetics* **43**, 265–285 (2009).

42. Szemenyei, H., Hannon, M. & Long, J. A. TOPLESS mediates auxin-dependent transcriptional repression during Arabidopsis embryogenesis. *Science* **319**, 1384–1386 (2008).

43. Leyser, O. Auxin Signaling. *Plant Physiology* **176**, 465–479 (2018).

44. Given, N. K., Venis, M. A. & Gierson, D. Hormonal regulation of ripening in the strawberry, a non-climacteric fruit. *Planta* **174**, 402–406 (1988).

45. Gorguet, B., van Heusden, A. W. & Lindhout, P. Parthenocarpic fruit development in tomato. *Plant Biol (Stuttg)* **7**, 131–139 (2005).

46. Stern, R. A., Flaishman, M., Applebaum, S. & Ben-Arie, R. Effect of synthetic auxins on fruit development of 'Bing' cherry (Prunus avium L.). *Scientia Horticulturae* **114**, 275–280 (2007).

47. Bartel, D. P. MicroRNAs: genomics, biogenesis, mechanism, and function. *Cell* **116**, 281–297 (2004).

48. Brousse, C. *et al.* A non-canonical plant microRNA target site. *Nucleic Acids Res.* **42**, 5270–5279 (2014).

49. Reinhart, B. J., Weinstein, E. G., Rhoades, M. W., Bartel, B. & Bartel, D. P. MicroRNAs in plants. *Genes Dev.* **16**, 1616–1626 (2002).

50. Voinnet, O. Origin, biogenesis, and activity of plant microRNAs. *Cell* **136**, 669–687 (2009).

51. Csukasi, F. *et al.* Two strawberry miR159 family members display developmental-specific expression patterns in the fruit receptacle and cooperatively regulate Fa-GAMYB. *New Phytol.* **195**, 47–57 (2012).

52. Hou, Y. *et al.* Comparative analysis of fruit ripening-related miRNAs and their targets in blueberry using small RNA and degradome sequencing. *Int J Mol Sci* **18**, (2017).

53. Moxon, S. *et al.* Deep sequencing of tomato short RNAs identifies microRNAs targeting genes involved in fruit ripening. *Genome Res.* **18**, 1602–1609 (2008).

54. Paim Pinto, D. L. *et al.* The influence of genotype and environment on small RNA profiles in grapevine berry. *Front Plant Sci* **7**, (2016).

55. Qu, D. *et al.* Identification of microRNAs and their targets associated with fruit-bagging and subsequent sunlight re-exposure in the 'Granny Smith' apple exocarp using high-throughput sequencing. *Front Plant Sci* **7**, 27 (2016).

56. Xin, C. *et al.* Profiling microRNA expression during multi-staged date palm (Phoenix dactylifera L.) fruit development. *Genomics* **105**, 242–251 (2015).

57. Zhu, H. *et al.* Unique expression, processing regulation, and regulatory network of peach (Prunus persica) miRNAs. *BMC Plant Biol.* **12**, 149 (2012).

58. Wu, J., Zheng, S., Feng, G. & Yi, H. Comparative analysis of miRNAs and their target transcripts between a spontaneous late-ripening sweet orange mutant and its wild-type using small RNA and degradome sequencing. *Front Plant Sci* **7**, 1416 (2016).

59. Barry, G. H., Castle, W. S. & Davies, F. S. Rootstocks and plant water relations affect sugar accumulation of citrus fruit via osmotic adjustment. *Journal of the American Society for Horticultural Science* **129**, 881–889 (2004).

60. Backman, T. W. H. & Girke, T. systemPipeR: NGS workflow and report generation environment. *BMC Bioinformatics* **17**, 388 (2016).

61. Langmead, B. & Salzberg, S. L. Fast gapped-read alignment with Bowtie 2. *Nature Methods* **9**, 357–359 (2012).

62. Kim, D., Langmead, B. & Salzberg, S. L. HISAT: a fast spliced aligner with low memory requirements. *Nature Methods* **12**, 357–360 (2015).

63. Zhang, Z. *et al.* PMRD: plant microRNA database. *Nucleic Acids Res* **38**, D806–D813 (2010).

64. Love, M. I., Huber, W. & Anders, S. Moderated estimation of fold change and dispersion for RNA-seq data with DESeq2. *Genome Biol* **15**, (2014).

65. Axtell, M. J. ShortStack: comprehensive annotation and quantification of small RNA genes. *RNA* **19**, 740–751 (2013).

66. Evers, M., Huttner, M., Dueck, A., Meister, G. & Engelmann, J. C. miRA: adaptable novel miRNA identification in plants using small RNA sequencing data. *BMC Bioinformatics* **16**, 370 (2015).

67. Lei, J. & Sun, Y. miR-PREFeR: an accurate, fast and easy-to-use plant miRNA prediction tool using small RNA-Seq data. *Bioinformatics* **30**, 2837–2839 (2014).

68. Gu, Z., Eils, R. & Schlesner, M. Complex heatmaps reveal patterns and correlations in multidimensional genomic data. *Bioinformatics* **32**, 2847–2849 (2016).

69. Wickham, H. ggplot2. *Wiley Interdisciplinary Reviews: Computational Statistics* **3**, 180–185 (2011).

70. Jin, J. *et al.* PlantTFDB 4.0: toward a central hub for transcription factors and regulatory interactions in plants. *Nucleic Acids Res* **45**, D1040–D1045 (2017).

71. Xie, C. *et al.* KOBAS 2.0: a web server for annotation and identification of enriched pathways and diseases. *Nucleic Acids Res* **39**, W316–W322 (2011).

72. Dai, X., Zhuang, Z. & Zhao, P. X. psRNATarget: a plant small RNA target analysis server (2017 release). *Nucleic Acids Res* **46**, W49–W54 (2018).

73. Owczarzy, R. *et al.* IDT SciTools: a suite for analysis and design of nucleic acid oligomers. *Nucleic Acids Research* **36**, W163–W169 (2008).

74. Pfaffl, M. W., Tichopad, A., Prgomet, C. & Neuvians, T. P. Determination of stable housekeeping genes, differentially regulated target genes and sample integrity: BestKeeper – Excel-based tool using pair-wise correlations. *Biotechnology Letters* **26**, 509–515 (2004).

75. Andersen, C. L., Jensen, J. L. & Ørntoft, T. F. Normalization of real-time quantitative reverse transcription-PCR data: a model-based variance estimation approach to identify genes suited for normalization, applied to bladder and colon cancer data sets. *Cancer Res* **64**, 5245–5250 (2004).

76. Pfaffl, M. W. A new mathematical model for relative quantification in real-time RT–PCR. *Nucleic Acids Res* **29**, e45–e45 (2001).

77. Tadeo, F. R. *et al.* Molecular physiology of development and quality of citrus. in *Advances in Botanical Research* **47**, 147–223 (Academic Press, 2008).

78. Ibáñez, A. M. *et al.* Transcriptome and metabolome analysis of Citrus fruit to elucidate puffing disorder. *Plant Science* **217–218**, 87–98 (2014).

79. Terol, J. *et al.* Analysis of 13000 unique Citrus clusters associated with fruit quality, production and salinity tolerance. *BMC Genomics* **8**, 31 (2007).

80. Wang, J. *et al.* Comparative transcriptome and proteome profiling of two Citrus sinensis cultivars during fruit development and ripening. *BMC Genomics* **18**, 984 (2017).

81. Samad, A. F. A. *et al.* MicroRNA and transcription factor: key players in plant regulatory network. *Front Plant Sci* **8**, (2017).

82. Hashimoto, Y., Akiyama, Y. & Yuasa, Y. Multiple-to-multiple relationships between microRNAs and target genes in gastric cancer. *PLOS ONE* **8**, e62589 (2013).

83. Peter, M. E. Targeting of mRNAs by multiple miRNAs: the next step. *Oncogene* **29**, 2161–2164 (2010).

84. Xie, R. *et al.* Combined analysis of mRNA and miRNA identifies dehydration and salinity responsive key molecular players in citrus roots. *Scientific Reports* **7**, (2017).

85. Meyers, B. C. *et al.* Criteria for annotation of plant microRNAs. *The Plant Cell* **20**, 3186–3190 (2008).

86. Leng, P., Yuan, B. & Guo, Y. The role of abscisic acid in fruit ripening and responses to abiotic stress. *J Exp Bot* **65**, 4577–4588 (2014).

87. Zhang, Y. *et al.* Suppressing type 2C protein phosphatases alters fruit ripening and the stress response in tomato. *Plant Cell Physiol* **59**, 142–154 (2018).

88. Pierre-Jerome, E., Moss, B. L. & Nemhauser, J. L. Tuning the auxin transcriptional response. *J Exp Bot* **64**, 2557–2563 (2013).

89. Rinaldi, M. A., Liu, J., Enders, T. A., Bartel, B. & Strader, L. C. A gain-of-function mutation in IAA16 confers reduced responses to auxin and abscisic acid and impedes plant growth and fertility. *Plant Mol. Biol.* **79**, 359–373 (2012).

90. Bassa, C., Mila, I., Bouzayen, M. & Audran-Delalande, C. Phenotypes associated with down-regulation of Sl-IAA27 support functional diversity among Aux/IAA family members in tomato. *Plant Cell Physiol* **53**, 1583–1595 (2012).

91. Su, L. *et al.* The auxin Sl-IAA17 transcriptional repressor controls fruit size via the regulation of endoreduplication-related cell expansion. *Plant Cell Physiol* **55**, 1969–1976 (2014).

92. Li, Z.-G. *et al.* Three SAUR proteins SAUR76, SAUR77 and SAUR78 promote plant growth in *Arabidopsis*. *Scientific Reports* **5**, 12477 (2015).

93. Chae, K. *et al.* Arabidopsis SMALL AUXIN UP RNA63 promotes hypocotyl and stamen filament elongation. *Plant J.* **71**, 684–697 (2012).

94. Kong, Y. *et al.* Tissue-specific expression of SMALL AUXIN UP RNA41 differentially regulates cell expansion and root meristem patterning in Arabidopsis. *Plant Cell Physiol.* **54**, 609–621 (2013).

95. Spartz, A. K. *et al.* SAUR inhibition of PP2C-D phosphatases activates plasma membrane H+-ATPases to promote cell expansion in Arabidopsis. *Plant Cell* **26**, 2129–2142 (2014).

96. Shin, R. *et al.* The Arabidopsis transcription factor MYB77 modulates auxin signal transduction. *Plant Cell* **19**, 2440–2453 (2007).

97. Zhao, Y. *et al.* The ABA receptor PYL8 promotes lateral root growth by enhancing MYB77-dependent transcription of auxin-responsive genes. *Sci. Signal.* **7**, ra53–ra53 (2014).

98. Maurel, C., Verdoucq, L., Luu, D.-T. & Santoni, V. Plant aquaporins: membrane channels with multiple integrated functions. *Annual Review of Plant Biology* **59**, 595–624 (2008).

99. Doligez, A. *et al.* New stable QTLs for berry weight do not colocalize with QTLs for seed traits in cultivated grapevine (Vitis vinifera L.). *BMC Plant Biology* **13**, 16 (2013).

100. Alleva, K. *et al.* Cloning, functional characterization, and co-expression studies of a novel aquaporin (FaPIP2;1) of strawberry fruit. *J Exp Bot* **61**, 3935–3945 (2010).

101. Hu, C.-G., Hao, Y.-J., Honda, C., Kita, M. & Moriguchi, T. Putative PIP1 genes isolated from apple: expression analyses during fruit development and under osmotic stress. *J Exp Bot* **54**, 2193–2194 (2003).

102. Marowa, P., Ding, A. & Kong, Y. Expansins: roles in plant growth and potential applications in crop improvement. *Plant Cell Rep* **35**, 949–965 (2016).

103. Brummell, D. A., Harpster, M. H. & Dunsmuir, P. Differential expression of expansin gene family members during growth and ripening of tomato fruit. *Plant Mol Biol* **39**, 161–169 (1999).

104. Brummell, D. A. & Harpster, M. H. Cell wall metabolism in fruit softening and quality and its manipulation in transgenic plants. in *Plant Cell Walls* (eds. Carpita, N. C., Campbell, M. & Tierney, M.) 311–340 (Springer Netherlands, 2001). doi:10.1007/978-94-010-0668-2_18

105. Bischoff, V. *et al.* TRICHOME BIREFRINGENCE and its homolog AT5G01360 encode plant-specific DUF231 proteins required for cellulose biosynthesis in Arabidopsis. *Plant Physiology* **153**, 590–602 (2010).

106. Grimplet, J., Agudelo-Romero, P., Teixeira, R. T., Martinez-Zapater, J. M. & Fortes, A. M. Structural and functional analysis of the GRAS gene family in grapevine indicates a role of GRAS proteins in the control of development and stress responses. *Front Plant Sci* **7**, (2016).

107. Huang, W., Xian, Z., Kang, X., Tang, N. & Li, Z. Genome-wide identification, phylogeny and expression analysis of GRAS gene family in tomato. *BMC Plant Biol* **15**, (2015).

108. Obenland, D. *et al.* Determinants of flavor acceptability during the maturation of navel oranges. *Postharvest Biology and Technology* **52**, 156–163 (2009).

109. Kader, A. A. Flavor quality of fruits and vegetables. *Journal of the Science of Food and Agriculture* **88**, 1863–1868 (2008).

110. Aprile, A. *et al.* Expression of the H+-ATPase AHA10 proton pump is associated with citric acid accumulation in lemon juice sac cells. *Funct Integr Genomics* **11**, 551–563 (2011).

111. Shi, C.-Y. *et al.* Citrus PH5-like H+-ATPase genes: identification and transcript analysis to investigate their possible relationship with citrate accumulation in fruits. *Front. Plant Sci.* **6**, (2015).

112. Ma, B. *et al.* A Ma10 gene encoding P-type ATPase is involved in fruit organic acid accumulation in apple. *Plant Biotechnol J* **17**, 674–686 (2019).

113. Azevedo, I. G. *et al.* P-type H+-ATPases activity, membrane integrity, and apoplastic pH during papaya fruit ripening. *Postharvest Biology and Technology* **48**, 242–247 (2008).

114. Lester, G. E., Arias, L. S. & Gomez-Lim, M. Muskmelon fruit soluble acid invertase and sucrose phosphate synthase activity and polypeptide profiles during growth and maturation. *Journal of the American Society for Horticultural Science* **126**, 33–36 (2001).

115. Ohyama, A. *et al.* Suppression of acid invertase activity by antisense RNA modifies the sugar composition of tomato fruit. *Plant Cell Physiol* **36**, 369–376 (1995).

116. Pan, Y.-Q., Luo, H.-L. & Li, Y.-R. Soluble acid invertase and sucrose phosphate synthase: key enzymes in regulating sucrose accumulation in sugarcane stalk. *Sugar Tech* **11**, 28–33 (2009).

117. Qin, G. *et al.* A tomato vacuolar invertase inhibitor mediates sucrose metabolism and influences fruit ripening. *Plant Physiology* **172**, 1596–1611 (2016).

118. Klann, E. M., Hall, B. & Bennett, A. B. Antisense acid invertase (TIV1) gene alters soluble sugar composition and size in transgenic tomato fruit. *Plant Physiology* **112**, 1321–1330 (1996).

119. Zheng, C. *et al.* Integrated RNA-Seq and sRNA-seq analysis identifies chilling and freezing responsive key molecular players and pathways in tea plant (Camellia sinensis). *PLOS ONE* **10**, e0125031 (2015).

120. Cho, J.-H., Dimri, M. & Dimri, G. P. MicroRNA-31 is a transcriptional target of histone deacetylase inhibitors and a regulator of cellular senescence. *J. Biol. Chem.* **290**, 10555–10567 (2015).

121. Okada, N. *et al.* A positive feedback between p53 and miR-34 miRNAs mediates tumor suppression. *Genes Dev.* **28**, 438–450 (2014).

Supplemental Material

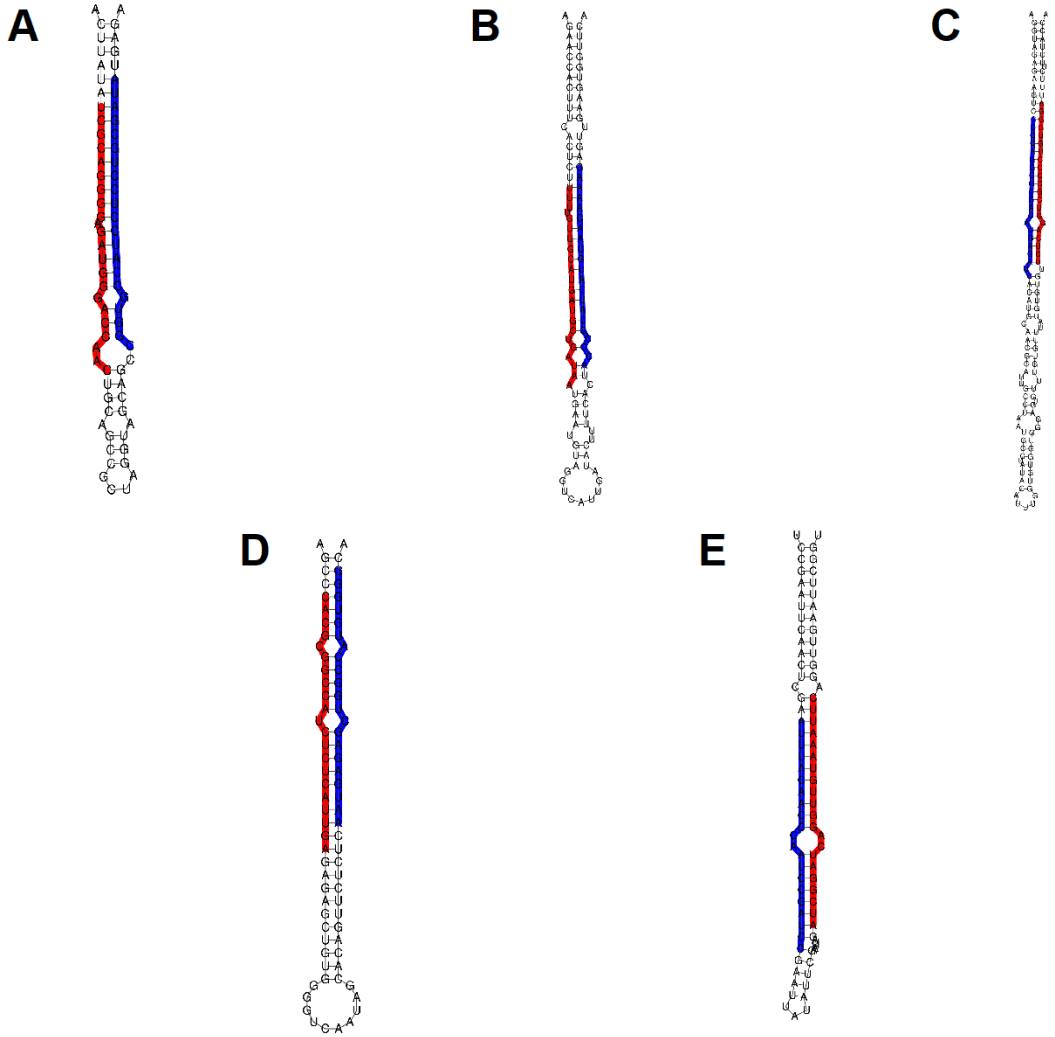

Supplemental Figure 1.1. Stem-loop precursor structures of novel miRNAs observed in sweet orange juice vesicles predicted from *Citrus clementina* reference genome. The mature miRNA sequences are highlighted in red and the miRNA star sequences are highlighted in blue (A) Ccl_n01; (B) Ccl_n02; (C) Ccl_n03; (D) Ccl_n04; (E) Ccl_n05

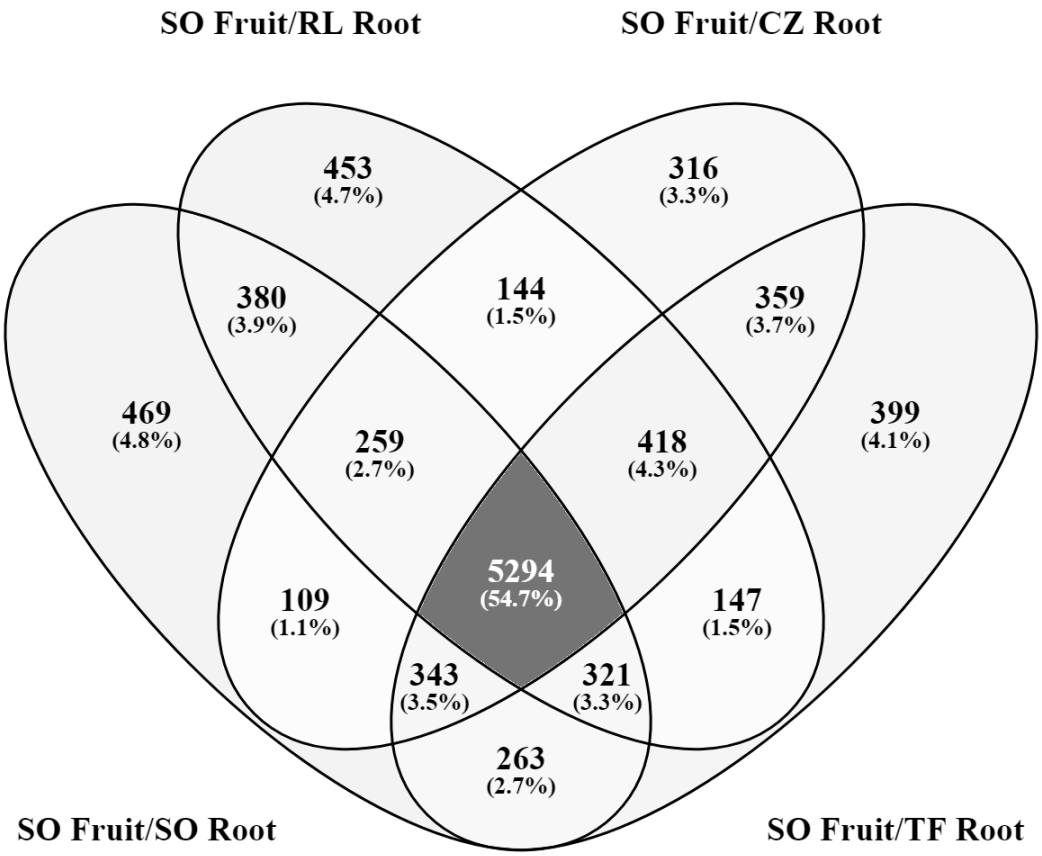

Supplemental Figure 1.2. Venn diagram of overlapping DEGs in fruit from trees grafted onto various rootstocks over the course of the growing season. Genes were compared at time point 2, 3, and 4 to time point 1 for each scion-rootstock combination.

Supplemental Table 1.1. The gene-specific real-time qPCR primers for miRNAs and their targets.

Name	Primer sequence (5’ -> 3’)	Gene ID
PIP2 F	GACTCCCATGTTCCTGTCTTG	Ciclev10012379m.g
PIP2 R	GTTGATGCCAGTTCCAGTGA	
EXP1 F	CTGTGTCTTACAGAAGGGTTCC	Ciclev10021897m.g
EXP1 R	GCCTCCGACGTTTGTGATTA	
ATPase F	TGTCTCAAGTTCCCTCTGTTATAC	Ciclev10018566m.g
ATPase R	TAAGTGCCCAGCCAAGTATC	
IAA16 F	GGTGATGTACCATGGGATATGTT	Ciclev10002290m.g
IAA16 R	AGCTTCTGTTCTTGCACTTCT	
Myb77 F	CCGGAACTTCAGGGTTTCAT	Ciclev10002239m.g
Myb77 R	GAACACCACCACACCCATTA	
SAUR78 F	GGCGACAATACTACCTGACTTC	Ciclev10026743m.g
SAUR78 R	CACAAGCAACCACAACTTCAC	
TBL23 F	GCATGCTCTCAACGGTAGAA	Ciclev10020137m.g
TBL23 R	GGGACCAAATAACTGACACAGA	
B-Fruct F	TGAGAGTATTGGTGGATCATTCG	Ciclev10019134m.g
B-Fruct R	CGGCTCCATAAATTGCCTTTG	
HAM3 F	GACAGTCTTCCCTTGTTCTCTG	Ciclev10019083m.g
HAM3 R	GGCACCTTTGCAACCAATTTA	
AHG1 F	GTGATCACAAGCCGGATAGAC	Ciclev10004981m.g
AHG1 R	CATGGCAAGAATGCCTTCAAC	
GAPDH F	CTGCAAAGGCTGTTGGAAAG	
GAPDH R	GGTCAACCACTGAGACATCAA	
Csi-miR845	CAAGTGGTATCAGAGCTAAGGAAA	

Ctr-miR319	TTGGACTGAAGGGAGCTCCCA	
Csi-miR833.1	CATTTATTGTTGATATGGGTCAAAAA	
Csi-miR390a	AAGCTCAGGAGGGATAGCGCC	
Csi-miR5671	CATGGTGGTGACGGGTGAC	
Ccl_n01	CGTTTTGTTGCATGATGCTGATAA	
Csi-miR1092.2b	TTCCACCAAAGCATTCATTTCC	
Csi-miR164a	TGGAGAAGCAGGGCACGTGCA	
Csi-miR1863	CAGAGTTTGTGGCTGTATCATTACTA	
Csi-miR1023	AGACTGAGAATTGAAGAGAGTGCA	
Universal miRNA reverse primer	mRQ 3' Primer (Takara Bio)	

*F and R denote forward and reverse primers, respectively

Supplemental Table 1.2. Differentially expressed genes in fruit of sweet orange grafted onto trifoliate orange compared to rough lemon rootstocks and potentially involved in fruit quality

Gene ID	Log_2 Fold Change at each timepoint				Best hit Arabidopsis locus	Arabidopsis gene name	Arabidopsis annotation
	TF1F-RL1F	TF2F-RL2F	TF3F-RL3F	TF4F-RL4F			
Ciclev10000098m.g	0.385	0.279	-1.350	-0.393	AT3G03050.1	ATCSLD3,CSLD3,KJK	cellulose synthase-like D3
Ciclev10000531m.g	-1.315	0.225	-0.294	-0.395	AT5G28540.1	BIP1	heat shock protein 70 (Hsp 70) family protein
Ciclev10000654m.g	-0.254	0.907	1.940	0.491	AT2G38470.1	ATWRKY33, WRKY33	WRKY DNA-binding protein 33
Ciclev10001389m.g	-0.361	1.032	0.011	0.255	AT1G65910.1	anac028,NAC028	NAC domain containing protein 28

Ciclev10001956m.g	-0.408	1.154	2.655	-0.208	AT1G01720.1	ANAC002,ATAF1	NAC (No Apical Meristem) domain transcriptional regulator superfamily protein
Ciclev10001976m.g	0.206	1.171	1.658	-0.462	AT1G01720.1	ANAC002,ATAF1	NAC (No Apical Meristem) domain transcriptional regulator superfamily protein
Ciclev10002239m.g	0.235	1.135	-5.152	-2.449	AT3G50060.1	MYB77	myb domain protein 77
Ciclev10002290m.g	-0.023	1.284	0.491	-0.580	AT3G04730.1	IAA16	indoleacetic acid-induced protein 16
Ciclev10002774m.g	-1.083	-0.407	-2.190	0.130	AT3G22930.1	CML11	calmodulin-like 11
Ciclev10003746m.g	-1.425	1.582	2.444	-0.223	AT4G37540.1	LBD39	LOB domain-containing protein 39
Ciclev10003847m.g	0.351	-0.436	1.181	-0.420	AT1G21360.1	GLTP2	glycolipid transfer protein 2
Ciclev10004281m.g	0.287	-1.046	0.969	-0.295	AT3G22400.1	LOX5	PLAT/LH2 domain-containing lipoxygenase family protein
Ciclev10004385m.g	-0.332	0.229	1.741	-0.055	AT3G23150.1	ETR2	Signal transduction histidine kinase, hybrid-type, ethylene sensor
Ciclev10004394m.g	-0.461	1.158	-0.356	0.181	AT4G24000.1	ATCSLG2,CSLG2	cellulose synthase like G2
Ciclev10005072m.g	0.186	-1.083	-0.211	0.766	AT1G02000.1	GAE2	UDP-D-glucuronate 4-epimerase 2
Ciclev10005102m.g	0.503	2.779	-3.080	1.035	AT1G16490.1	ATMYB58,MYB58	myb domain protein 58
Ciclev10005233m.g	0.192	0.170	1.233	-0.204	AT2G42280.1		basic helix-loop-helix (bHLH) DNA-binding superfamily protein
Ciclev10005341m.g	0.367	0.835	-1.109	-0.240	AT1G54330.1	ANAC020,NAC020	NAC domain containing protein 20

Ciclev10007428m.g	-0.405	1.523	0.471	-0.187	AT2G18700.1	ATTPS11,ATTPSB,TPS11	trehalose phosphatase/synthase 11
Ciclev10007653m.g	0.471	-1.066	0.258	-0.323	AT1G55850.1	ATCSLE1,CSLE1	cellulose synthase like E1
Ciclev10007787m.g	0.326	-0.904	2.210	-1.205	AT1G73590.1	ATPIN1,PIN1	Auxin efflux carrier family protein
Ciclev10008080m.g	0.753	-2.058	1.209	-0.253	AT5G56590.1		O-Glycosyl hydrolases family 17 protein
Ciclev10008176m.g	-0.135	0.266	-1.498	-0.487	AT5G55180.1		O-Glycosyl hydrolases family 17 protein
Ciclev10008616m.g	0.205	-1.039	0.163	0.052	AT5G55950.1		Nucleotide/sugar transporter family protein
Ciclev10008762m.g	0.673	0.279	4.736	-0.611	AT4G26530.2		Aldolase superfamily protein
Ciclev10008778m.g	-1.484	3.608	-4.857	0.069	AT4G25810.1	XTH23,XTR6	xyloglucan endotransglycosylase 6
Ciclev10008836m.g	0.204	0.440	1.842	0.501	AT4G31550.1	ATWRKY11,WRKY11	WRKY DNA-binding protein 11
Ciclev10008896m.g	0.177	-0.388	-1.154	-0.029	AT1G55860.1	UPL1	ubiquitin-protein ligase 1
Ciclev10009119m.g	-1.089	1.921	-5.725	-1.168	AT4G25810.1	XTH23,XTR6	xyloglucan endotransglycosylase 6
Ciclev10009245m.g	-2.665	2.881	-1.700	0.442	AT4G32280.1	IAA29	indole-3-acetic acid inducible 29
Ciclev10009361m.g	0.170	0.134	-1.252	-0.007	AT3G20310.1	ATERF-7,ATERF7,ERF7	ethylene response factor 7
Ciclev10010436m.g	-0.167	0.918	-1.814	0.537	AT1G10970.1	ATZIP4,ZIP4	zinc transporter 4 precursor
Ciclev10011214m.g	-0.048	0.026	1.009	-0.001	AT1G32640.1	ATMYC2,JAI1,JIN1,MYC2,RD22BP1,ZBF1	Basic helix-loop-helix (bHLH) DNA-binding family protein
Ciclev10011295m.g	0.172	-1.067	1.462	-0.503	AT2G05790.1		O-Glycosyl hydrolases family 17 protein

Ciclev10011474m.g	-0.818	0.674	0.469	1.996	AT5G40010.1	AATP1	AAA-ATPase 1
Ciclev10011556m.g	-0.513	1.323	1.961	-0.593	AT5G39660.2	CDF2	cycling DOF factor 2
Ciclev10011592m.g	0.318	0.323	-1.114	0.008	AT5G03150.1	JKD	C2H2-like zinc finger protein
Ciclev10011654m.g	0.171	-0.547	-0.608	-1.298	AT5G01930.1		Glycosyl hydrolase superfamily protein
Ciclev10011948m.g	0.427	-1.054	0.238	-0.475	AT3G01140.1	AtMYB106,MYB106,NOK	myb domain protein 106
Ciclev10012072m.g	1.946	-1.490	7.193	-0.799	AT1G21070.1		Nucleotide-sugar transporter family protein
Ciclev10012089m.g	0.061	0.700	-2.463	0.209	AT2G37630.1	AS1,ATMYB91,ATPHAN,MYB91	myb-like HTH transcriptional regulator family protein
Ciclev10012152m.g	0.517	-0.096	-1.125	0.265	AT3G28910.1	ATMYB30,MYB30	myb domain protein 30
Ciclev10012379m.g	0.146	0.626	-1.745	-0.374	AT2G37170.1	PIP2;2,PIP2B	plasma membrane intrinsic protein 2
Ciclev10012583m.g	0.138	-0.191	-1.081	0.061	AT2G38310.1	PYL4,RCAR10	PYR1-like 4
Ciclev10012620m.g	-0.469	0.384	1.501	-0.205	AT1G09950.1	RAS1	RESPONSE TO ABA AND SALT 1
Ciclev10012633m.g	0.322	0.181	-1.462	-0.552	AT5G60660.1	PIP2;4,PIP2F	plasma membrane intrinsic protein 2;4
Ciclev10013012m.g	0.229	1.166	-3.493	0.535	AT1G66400.1	CML23	calmodulin like 23
Ciclev10013453m.g	0.334	0.810	2.852	0.386	AT2G01060.1		myb-like HTH transcriptional regulator family protein
Ciclev10013705m.g	0.240	-1.454	-2.624	1.184	AT3G02550.1	LBD41	LOB domain-containing protein 41
Ciclev10013866m.g	0.027	1.024	-0.562	-0.002	AT3G02470.3	SAMDC	S-adenosylmethionine decarboxylase

Ciclev10014075m.g	0.087	-0.039	1.075	-0.249	AT4G18820.1		AAA-type ATPase family protein
Ciclev10014091m.g	-0.256	0.543	2.446	-0.138	AT3G63380.1		ATPase E1-E2 type family protein / haloacid dehalogenase-like hydrolase family protein
Ciclev10014240m.g	0.364	-0.461	-1.919	-0.109	AT5G12950.1		Putative glycosyl hydrolase of unknown function (DUF1680)
Ciclev10014586m.g	1.248	1.152	-0.836	0.158	AT2G32540.1	ATCSLB04,ATCSLB4,CSLB04	cellulose synthase-like B4
Ciclev10014962m.g	-0.070	1.059	0.396	0.060	AT1G50460.1	ATHKL1,HKL1	hexokinase-like 1
Ciclev10015210m.g	0.708	1.426	-1.341	3.409	AT1G61800.1	ATGPT2,GPT2	glucose-6-phosphate/phosphate translocator 2
Ciclev10015492m.g	0.395	-0.222	-0.147	1.143	AT5G35735.1		Auxin-responsive family protein
Ciclev10015554m.g	0.488	0.062	-1.072	-0.253	AT3G49190.1		O-acyltransferase (WSD1-like) family protein
Ciclev10015616m.g	0.628	-0.923	-3.377	-1.726	AT5G53390.1		O-acyltransferase (WSD1-like) family protein
Ciclev10015727m.g	0.732	-1.009	0.452	-0.981	AT5G54770.1	THI1,THI4,TZ	thiazole biosynthetic enzyme, chloroplast (ARA6) (THI1) (THI4)
Ciclev10016309m.g	0.274	1.416	-0.572	-0.100	AT2G01290.1	RPI2	ribose-5-phosphate isomerase 2
Ciclev10016351m.g	0.168	0.733	-1.486	-0.553	AT2G27080.1		Late embryogenesis abundant (LEA) hydroxyproline-rich glycoprotein family
Ciclev10016457m.g	-0.072	1.160	-0.280	-0.496	AT3G07880.1	SCN1	Immunoglobulin E-set superfamily protein
Ciclev10016668m.g	0.004	0.180	-1.174	-0.040	AT1G50640.1	ATERF3,ERF3	ethylene responsive element binding factor 3

Ciclev10016820m.g	0.503	-0.044	-2.741	-0.871	AT3G27810.1	ATMYB21,ATMYB3,MYB21	myb domain protein 21
Ciclev10016995m.g	0.691	0.185	-1.289	1.347	AT3G23240.1	ATERF1,ERF1	ethylene response factor 1
Ciclev10017856m.g	0.514	1.202	-1.688	0.337	AT2G43820.1	ATSAGT1,GT,SAGT1,SGT1,UGT74F2	UDP-glucosyltransferase 74F2
Ciclev10018566m.g	0.452	-0.718	1.127	0.295	AT1G68710.1		ATPase E1-E2 type family protein / haloacid dehalogenase-like hydrolase family protein
Ciclev10018826m.g	0.184	-2.099	-0.114	0.684	AT4G24790.1		AAA-type ATPase family protein
Ciclev10018842m.g	0.579	0.090	1.578	-0.300	AT1G23870.1	ATTPS9,TPS9	trehalose-phosphatase/synthase 9
Ciclev10018972m.g	0.066	-0.614	1.379	-0.206	AT3G04580.2	EIN4	Signal transduction histidine kinase, hybrid-type, ethylene sensor
Ciclev10019083m.g	-0.028	0.238	1.054	-0.440	AT4G00150.1	ATHAM3,HAM3	GRAS family transcription factor
Ciclev10019134m.g	0.245	0.312	-1.953	0.128	AT1G12240.1	ATBETAFRUCT4,VAC-INV	Glycosyl hydrolases family 32 protein
Ciclev10019301m.g	0.555	-1.537	0.313	-0.332	AT1G64390.1	AtGH9C2,GH9C2	glycosyl hydrolase 9C2
Ciclev10019393m.g	1.226	0.515	-3.151	0.328	AT2G47750.1	GH3.9	putative indole-3-acetic acid-amido synthetase GH3.9
Ciclev10019730m.g	-0.340	0.190	-1.101	0.053	AT1G32640.1	ATMYC2,JAI1,JIN1,MYC2,RD22BP1,ZBF1	Basic helix-loop-helix (bHLH) DNA-binding family protein
Ciclev10019872m.g	-0.551	1.108	1.708	-0.356	AT5G39660.2	CDF2	cycling DOF factor 2
Ciclev10019977m.g	-0.108	0.068	1.249	-0.519	AT2G45120.1		C2H2-like zinc finger protein
Ciclev10019997m.g	-1.482	0.841	-1.380	-0.472	AT5G56350.1		Pyruvate kinase family protein

Ciclev10020144m.g	0.270	-1.979	0.155	0.697	AT4G01680.1	AtMYB55,MYB55	myb domain protein 55
Ciclev10020187m.g	-0.001	-1.078	-0.412	0.582	AT4G00110.1	GAE3	UDP-D-glucuronate 4-epimerase 3
Ciclev10020360m.g	0.695	-1.564	4.470	4.198	AT3G61950.1		basic helix-loop-helix (bHLH) DNA-binding superfamily protein
Ciclev10020376m.g	-5.872	1.005	-1.095	-0.184	AT5G66460.1		Glycosyl hydrolase superfamily protein
Ciclev10020681m.g	-0.551	1.812	2.375	-0.180	AT1G05805.1		basic helix-loop-helix (bHLH) DNA-binding superfamily protein
Ciclev10020725m.g	-0.048	1.436	1.060	-0.448	AT3G61850.4	DAG1	Dof-type zinc finger DNA-binding family protein
Ciclev10021399m.g	-0.726	0.544	4.070	-0.235	AT3G47870.1	LBD27,SCP	LOB domain-containing protein 27
Ciclev10021622m.g	-0.498	1.075	4.560	-0.604	AT3G23240.1	ATERF1,ERF1	ethylene response factor 1
Ciclev10021652m.g	-1.788	0.706	3.046	-0.029	AT4G17500.1	ATERF-1,ERF-1	ethylene responsive element binding factor 1
Ciclev10021887m.g	1.050	-1.406	0.494	-0.868	AT2G03090.1	ATEXP15,ATEXPA15,ATHEXP ALPHA 1.3,EXP15,EXPA15	expansin A15
Ciclev10021897m.g	0.527	-0.134	-1.434	0.375	AT1G69530.2	AT-EXP1,ATEXP1,ATEXPA1,ATHEXP ALPHA 1.2,EXP1,EXPA1	expansin A1
Ciclev10021992m.g	-1.056	0.474	-1.783	0.926	AT2G45420.1	LBD18	LOB domain-containing protein 18
Ciclev10022068m.g	0.335	-2.575	-4.019	3.164	AT3G02550.1	LBD41	LOB domain-containing protein 41
Ciclev10022290m.g	0.511	-0.443	1.437	-0.400	AT4G01410.1		Late embryogenesis abundant (LEA)

							hydroxyproline-rich glycoprotein family
Ciclev10022400m.g	0.658	-1.586	0.108	0.302	AT4G02980.1	ABP,ABP1	endoplasmic reticulum auxin binding protein 1
Ciclev10022560m.g	-0.588	1.380	-0.008	0.458	AT3G60690.1		SAUR-like auxin-responsive protein family
Ciclev10022579m.g	-0.543	2.089	1.168	-0.566	AT4G29900.1	ACA10,ATACA10,CIF1	autoinhibited Ca(2+)-ATPase 10
Ciclev10023484m.g	0.516	1.190	-2.625	2.869	AT2G46150.1		Late embryogenesis abundant (LEA) hydroxyproline-rich glycoprotein family
Ciclev10024136m.g	-0.078	0.435	2.375	1.001	AT1G74310.1	ATHSP101,HOT1,HSP101	heat shock protein 101
Ciclev10024438m.g	-4.264	0.502	2.795	-1.191	AT4G00080.1	UNE11	Plant invertase/pectin methylesterase inhibitor superfamily protein
Ciclev10024546m.g	0.054	1.573	1.992	-0.623	AT5G48890.1		C2H2-like zinc finger protein
Ciclev10024879m.g	0.274	-0.039	1.145	0.210	AT1G17260.1	AHA10	autoinhibited H(+)-ATPase isoform 10
Ciclev10025169m.g	-0.082	-0.381	1.556	-0.606	AT5G66770.1		GRAS family transcription factor
Ciclev10025211m.g	0.330	1.387	-0.667	-0.302	AT2G14960.1	GH3.1	Auxin-responsive GH3 family protein
Ciclev10025492m.g	0.561	-0.389	1.254	-0.217	AT4G36250.1	ALDH3F1	aldehyde dehydrogenase 3F1
Ciclev10025631m.g	0.252	0.813	-1.293	-0.414	AT5G66460.1		Glycosyl hydrolase superfamily protein
Ciclev10025741m.g	0.311	0.101	-1.581	0.155	AT2G17500.4		Auxin efflux carrier family protein
Ciclev10025754m.g	0.068	-0.216	2.432	-1.670	AT2G23060.1		Acyl-CoA N-acyltransferases (NAT) superfamily protein

Ciclev10025887m.g	0.062	-0.033	-0.175	-1.428	AT5G43060.1		Granulin repeat cysteine protease family protein
Ciclev10026374m.g	0.001	1.145	-0.124	-0.734	AT3G49940.1	LBD38	LOB domain-containing protein 38
Ciclev10026510m.g	-0.238	0.525	-1.839	-0.110	AT3G50770.1	CML41	calmodulin-like 41
Ciclev10026552m.g	-0.556	-2.379	-0.705	-0.241	AT1G15380.2		Lactoylglutathione lyase / glyoxalase I family protein
Ciclev10026743m.g	0.715	-1.434	-2.984	2.428	AT1G72430.1		SAUR-like auxin-responsive protein family
Ciclev10027413m.g	0.083	1.259	0.251	-0.780	AT3G13840.1		GRAS family transcription factor
Ciclev10028058m.g	-0.045	3.014	-2.390	0.598	AT2G14960.1	GH3.1	Auxin-responsive GH3 family protein
Ciclev10028113m.g	0.499	-0.550	-3.272	0.368	AT4G19170.1	CCD4,NCED4	nine-cis-epoxycarotenoid dioxygenase 4
Ciclev10028164m.g	0.705	-2.169	0.553	0.765	AT5G22740.1	ATCSLA02,ATCSLA2,CSLA02,CSLA2	cellulose synthase-like A02
Ciclev10028389m.g	-0.111	1.253	2.531	-0.989	AT5G58940.1	CRCK1	calmodulin-binding receptor-like cytoplasmic kinase 1
Ciclev10028618m.g	-0.600	1.127	-0.343	0.060	AT5G22290.1	anac089,NAC089	NAC domain containing protein 89
Ciclev10028633m.g	-0.490	1.087	2.028	-0.526	AT4G34850.1	LAP5	Chalcone and stilbene synthase family protein
Ciclev10028715m.g	-0.327	0.938	1.332	-0.793	AT5G28650.1	ATWRKY74, WRKY74	WRKY DNA-binding protein 74
Ciclev10029019m.g	0.290	0.320	-1.003	0.669	AT3G46130.4	ATMYB48,ATMYB48-1,ATMYB48-2,ATMYB48-3,MYB48	myb domain protein 48
Ciclev10029274m.g	-1.065	1.335	2.801	-0.778	AT3G49940.1	LBD38	LOB domain-containing protein 38

Ciclev10029451m.g	-0.085	-1.667	0.338	1.338	AT2G16060.1	AHB1,ARATH GLB1,ATGLB1,GLB1,HB1,NSHB1	hemoglobin 1
Ciclev10029507m.g	-0.454	0.897	1.846	-0.375	AT5G53300.4	UBC10	ubiquitin-conjugating enzyme 10
Ciclev10029597m.g	-0.505	-2.858	6.080	0.008	AT5G01075.1		Glycosyl hydrolase family 35 protein
Ciclev10029653m.g	0.791	-0.484	-4.712	1.925	AT4G38840.1		SAUR-like auxin-responsive protein family
Ciclev10030185m.g	-0.158	1.107	0.062	0.072	AT3G13040.2		myb-like HTH transcriptional regulator family protein
Ciclev10030384m.g	0.394	-0.166	-3.762	0.507	AT4G19170.1	CCD4,NCED4	nine-cis-epoxycarotenoid dioxygenase 4
Ciclev10030787m.g	-0.251	0.072	1.213	-0.471	AT1G07530.1	ATGRAS2,GRAS2,SCL14	SCARECROW-like 14
Ciclev10031003m.g	0.291	0.127	-1.461	0.012	AT4G19170.1	CCD4,NCED4	nine-cis-epoxycarotenoid dioxygenase 4
Ciclev10031010m.g	0.796	-1.506	0.175	-0.535	AT5G05730.1	AMT1,ASA1,JDL1,TRP5,WEI2	anthranilate synthase alpha subunit 1
Ciclev10031433m.g	-0.553	2.043	2.848	-1.062	AT5G39660.1	CDF2	cycling DOF factor 2
Ciclev10031652m.g	0.153	-1.251	-0.379	-0.129	AT5G17630.1		Nucleotide/sugar transporter family protein
Ciclev10031938m.g	-1.300	0.856	2.255	-0.065	AT5G50260.1		Cysteine proteinases superfamily protein
Ciclev10032304m.g	-1.819	2.755	2.861	-0.853	AT1G69490.1	ANAC029,ATNAP,NAP	NAC-like, activated by AP3/PI
Ciclev10032547m.g	0.091	1.103	-1.853	0.279	AT5G13180.1	ANAC083,NAC083,VNI2	NAC domain containing protein 83
Ciclev10033363m.g	-2.088	2.358	1.349	-0.204	AT5G50760.1		SAUR-like auxin-responsive protein family

A.

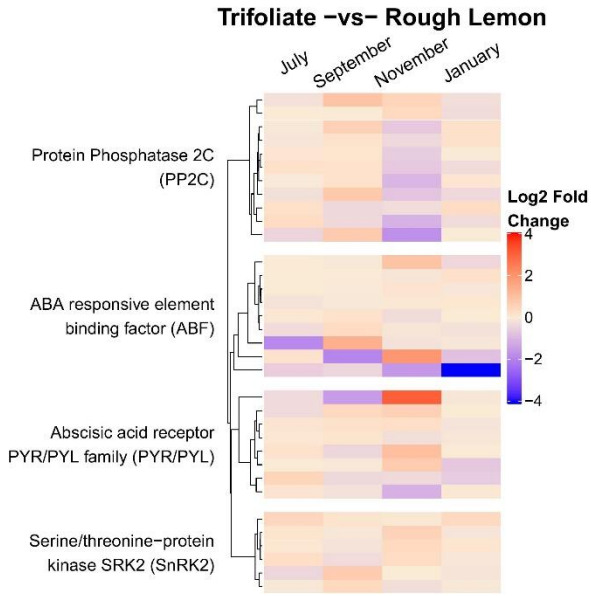

B.

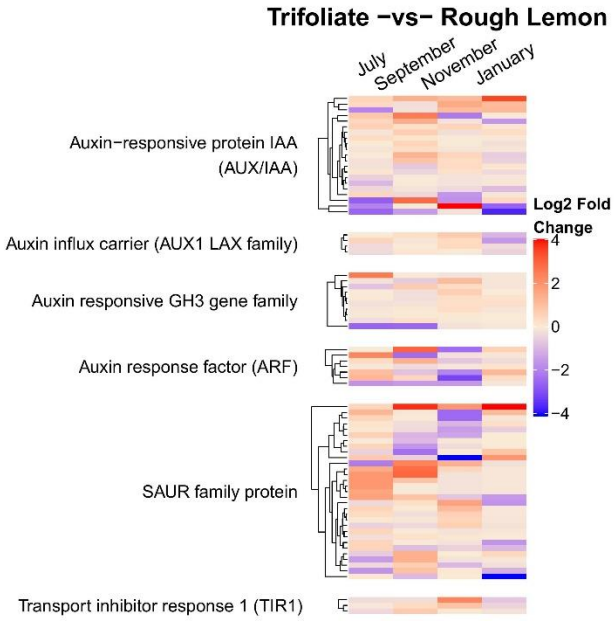

Supplemental Figure 1.3 Heatmaps of regulatory genes in select hormone-signaling pathways in fruit tissue. Hierarchical clustering of all citrus genes in the (A) ABA-signaling and (B) auxin-signaling pathways observed between fruit grown on trees grafted to trifoliate orange vs rough lemon rootstocks at each time point (1, 2, 3, and 4). Genes were first separated by gene family and subsequently clustered by expression levels.

Chapter 2. Computational Identification and Target Analysis of Novel and Conserved miRNAs by Illumina Sequencing in Root Tissues of Grafted Citrus Trees

Abstract

Citrus is one of the most economically important crops in the world. All commercial citrus is propagated by grafting. Citrus rootstocks have well-known effects on tree size, fruit size, and various fruit quality factors. Despite the economic and horticultural value of citrus rootstocks, there is a serious lack of transcriptomic data available for the genotypes typically used as root systems, especially in relation to fruit quality. Therefore, in the present study, transcriptomic data from four diverse citrus genotypes at four time points throughout fruit development was produced. Transcriptomic data about the roots in this study can aid in selective breeding and biotechnology for improved fruit quality in citrus.

In this study, differentially expressed genes (DEGs) and differentially expressed miRNAs (DEMs) were identified between the citrus genotypes. Functional analysis revealed that the ‘GO’ terms ‘cell wall organization or biogenesis’ and ‘defense response’ were significantly enriched. Additionally, KEGG pathway analysis revealed that genes for nitrogen metabolism, plant-pathogen interaction, starch and sucrose metabolism, and plant hormone signal transduction were enriched between rootstocks. It was found that many of the genes DE between genotypes had roles in controlling root system architecture and the roots ability to adapt to various biotic and abiotic stressors.

Furthermore, miRNA-mRNA interaction pairs were identified to understand potential regulatory mechanisms of these genes.

Introduction

Citrus is now grown in more than 140 countries in tropical, subtropical and Mediterranean regions. It is one of the most economically important crops in the world. Citrus are rarely grown from seed and virtually all commercial citrus is propagated by grafting. This reduces the juvenile phase, allowing for the trees to produce fruit many years earlier than would trees grown from seed[1]. Due to the large variation in growing conditions and climate in the regions where citrus is grown, different citrus rootstocks are required to improve yield and fruit quality in numerous diverse climates, as well as resist various pests and diseases[2]. Rootstocks impart certain traits to the scion and the effects of rootstocks can be large. The most significant impacts are on growth, vigor and yield, tree nutrition, stress resistance, and fruit quality[3–6]. The rootstock effects on various aspects of tree growth and fruit development are well documented, but the molecular mechanisms underlying most of these differences are unknown.

Previous studies have shown changes in the transcriptome of various rootstock genotypes, especially in response to biotic and abiotic stressors. These types of changes have been seen in Arabidopsis, corn, mulberry, tomato, and poplar[7–11]. In citrus, gene expression profiling has been used to understand rootstock effects and responses to biotic and abiotic factors[12–14]. In another study, expression studies of

leaves from mandarin grafted onto various rootstocks were analyzed in order to explain rootstock effects on the growth of scions[15].

There is extremely limited tissue-specific transcriptome knowledge in citrus, especially for root tissue. A small number of studies have evaluated trifoliate, trifoliate hybrid, and mandarin root transcriptomes in response to citrus diseases, but these studies each assessed only one genotype[16–18]. Only recently has an RNA-seq based approach been used to establish a reference transcriptome for citrus and of the 28 samples used in the study, only two were obtained from roots[19]. The root samples collected for this study were sour orange and trifoliate genotypes, but samples were grouped by organ to perform differential expression and subsequent analyses. To our knowledge, there are no comparative studies of citrus root transcriptomes between genotypes.

In plants, the root system is critical for plant growth and development. It serves the functions of anchorage, nutrient and water uptake, and is the main boundary between the plant and its soil environment. Root growth relies on a specific set of signals that involves hormone signaling, availability of nutrients and carbon supply[20]. There is a large degree of genotypic variation in crop plant root systems that can influence the plants growth and production including root length, root density, root angle, lateral root number, and root:shoot ratio. These parameters can impact the plant's size, tolerance to biotic and abiotic stressors, and ability to uptake water and nutrients[21]. For this reason, grafting, a process which connects the roots of one plant to the scion of another, has been widely using in plant breeding programs in order to improve vigor, alter plant architecture, enhance tolerance to disease and abiotic stress, and contribute to the

quality of crops[3-6]. In citrus, rootstocks are bred for a variety of traits that are imparted to scions, such as tree size, yield, tolerance to salt, cold, and drought, tolerance to various pests and diseases, and improved fruit quality[22]. Many studies in citrus have been conducted to assess the impacts of genetically differing rootstocks on these traits[3,23–31]. However, the study of molecular mechanisms behind root attributes lags far behind above ground tissues in plants, especially in perennial crops. Understanding the genetics of how root systems develop, and the regulatory controls of these processes will help optimize the improvement of yield and quality in citrus.

Root system length, growth, and architecture control the ability of plants to respond to various stress conditions. The development of the root system and its architecture is determined by genetic factors interacting with numerous environmental factors[32]. Plants must adapt to their environment by controlling their physiological reactions and morphogenesis. This can create complex root system architectures. For example, different root types can produce lateral roots that significantly extend the elaborate root system and allow the plant to search the soil for water and nutrient-rich areas. The increase in lateral root formation allows plants to more easily uptake these essential molecules in order to survive in unfavorable conditions[33–35]. Rootstock genotypes exhibiting higher abilities to adapt to stress and create more extensive root systems improve nutritional status and water uptake, which can increase marketable yield. A clear example of this was seen in grafted mini-watermelon and tomato plants[36,37].

Studies in Arabidopsis, rice, and corn have identified several genes that influence root development and root system architecture (RSA)[38–40]. In citrus, transcriptomic studies

have been performed to understand the effect of rootstocks on growth and in response to cold, nutrient deficiency, and fungal inoculation[12–15,41]. Besides these studies, little effort has been invested into studying the effects of citrus rootstocks at the molecular level, especially genotype-specific effects and their relation to fruit quality.

Plants have evolved to cope with a constantly changing environment, modifying the root system architecture in response to nutrient availability and soil microorganisms. This flexibility requires fine tuning of gene expression. Among the molecules that control root development, small RNAs (sRNAs) play a vital role in regulating genes at the post-transcriptional level in plants. The most well-studied class of sRNAs are microRNAs (miRNAs), which are approximately 21 nucleotides in length and are produced from non-coding transcripts. Mature miRNAs have been shown to negatively regulate gene expression at the post-transcriptional level by specific binding and subsequent cleavage of their target mRNAs, or by the repression of target translation[42–45]. Increasing evidence demonstrates that plant miRNAs play critical roles in almost all biological and metabolic processes[46]. A review of miRNAs in roots indicated that they participate in root development, the modulation of root architecture, and root biotic interactions[47]. This review focuses on numerous studies using Arabidopsis and legume plants as models. In citrus, miRNAs profiling has revealed their involvement in adaptation to nutrient deficiency, drought and salinity stress, and pathogen infection[48–51]. However, no information, to date, is available about the role of miRNAs underlying differences in fruit quality observed between citrus rootstocks.

In the present study, trees grafted onto four rootstocks were chosen from a rootstock trial at the University of California, Riverside to assess for various fruit quality traits; Argentina sweet orange, Schaub rough lemon, Carrizo citrange, and Rich 16-6 trifoliate orange. Generally speaking, rough lemon rootstocks produce the highest yield and fruit size, but this fruit is often of lower quality (lower acidity and lower levels of total soluble solids). Trifoliate orange rootstock, when well adapted, produces high quality fruit, with high yield on smaller trees. Carrizo citrange rootstocks produce intermediate yield with good fruit quality. Sweet orange rootstocks produce good quality fruit but are very susceptible to various citrus diseases, and therefore are rarely used as rootstocks for commercial trees. An RNA-seq approach was used to assess differences in gene expression between rootstocks that produce fruit with varying quality traits with the aim of identifying genes that could potentially play a role in improvement of fruit quality. Moreover, miRNA expression profiles were obtained for each of the rootstocks to identify potential regulatory mechanisms associated with their target genes.

Materials and Methods

Plant materials

The citrus cultivar, ‘Washington’ navel sweet orange (*Citrus sinensis* (L.) Osbeck) scion was previously grafted onto the following rootstocks: Argentina sweet orange (*Citrus sinensis* (L.) Osbeck), Schaub rough lemon (*Citrus jambhiri* Lush), Carrizo citrange trifoliate hybrid (*Citrus sinensis* 'Washington' navel sweet orange X *Poncirus trifoliata*), and Rich 16-6 trifoliate (*Poncirus trifoliata* (L.) Raf.). The grafted trees were part of a

rootstock trial conducted at the Citrus Research Center and Agricultural Experiment Station (CRC-AES) at the University of California, Riverside (UCR) that included 28 rootstocks. Trees were planted in 2011 in a randomized block design with ten replications. Trees were planted on berms, irrigated with minisprinklers according to soil moisture sensors, and treated with fertilizers and pesticides according to standard commercial practices. Plastic mulch was used to cover the berms to suppress weeds and retain soil moisture. Trees were grown in a fine sandy loam and surface soil pH was 7.3 at the time of planting. It is important to note that no trees with Huanglongbing have been identified at UCR.

For sequencing, roots from two biological replicate trees were harvested at four time points throughout the 2014-2015 growing season (July, September, November, and January). Young, newly growing fibrous root tissue was collected from the first 6 inches of soil along the outer edge of the canopy. Samples from all sides of the tree were bulked, rinsed twice with distilled water, immediately frozen on dry ice in the field, and kept at -80°C for RNA extraction.

RNA extraction, library construction, and sequencing

The root samples from two biological replicates of each of the four genotypes at the four collection time points were subjected to RNA-seq (32 samples total). Samples were ground in liquid nitrogen and total RNA was extracted from ~200mg tissue using the ZR Plant RNA MiniPrep™ kit (Zymo Research) per manufacturer's instructions. An Agilent Bioanalyzer (Agilent Technologies) was used to confirm the integrity of the total RNA.

The RNA with a RIN (RNA Integrity Number) value greater than seven qualified for RNA-seq.

For messenger RNA-seq, sequencing libraries were created using TruSeq Stranded mRNA Library Preparation Kit (Illumina) according to the manufacturer's protocol. For small RNA-seq, sequencing libraries were created using TruSeq Small RNA Library Preparation Kit (Illumina) according to the manufacturer's protocol. Each library was prepared for multiplexing with a unique indexed primer. Quantification of all libraries was performed with Nanodrop and Qubit fluorometer. The library size distribution and quality were measured with an Agilent Bioanalyzer. Multiplexed libraries were sequenced in a single lane on an Illumina NextSeq 500 instrument at the University of California, Riverside Genomics Core facility. An average of 11 samples were sequenced per lane.

Illumina sequence analysis

The data analysis was carried out using the RNA-seq workflow module of the systemPipeR package available on Bioconductor[52]. RNA-seq reads were demultiplexed and preprocessed by quality filtering and trimming of adaptors. Quality reports were created with the FastQC function. *Citrus clementina v 1.0* genome assembly and annotations were downloaded from JGI's portal (https://phytozome.jgi.doe.gov/pz/portal.html). Sequencing reads were then mapped against the *Citrus clementina v 1.0* reference genome using the Bowtie2 alignment suite[53] for small RNAs and HISAT2 alignment suite[54] for messenger RNAs. Messenger RNA raw reads were counted in a strand-specific manner. Known miRNA gene

coordinates, required for counting, were acquired by downloading all known plant miRNAs from the plant miRNA database (PMRD)[55], aligning these sequences to the *Citrus clementina v 1.0* reference genome using Bowtie2 with perfect alignment, and extracting the alignment coordinates. Small RNA raw reads were then counted at the known miRNA locations using the summarizeOverlaps function from systemPipeR. Sample-wise correlation analysis was performed using rlog transformed expression values generated by the DESeq2 package[56].

Identification of novel miRNAs

Sequences that aligned to the *Citrus clementina* reference genome but did not match any know plant miRNAs were used to predict novel miRNAs. Novel miRNAs were predicted using three miRNA prediction tools (Shortstack[57], miRA[58], and miR-PREFeR[59]). These three programs assess the expression patterns, Dicer cleavage site, and secondary structure of miRNA precursors to predict novel miRNAs from small RNA-seq data. *Citrus clementina* reference genome was input as the reference for determining flanking sequences to predict secondary structures of the miRNA precursors. ShortStack was run with default settings with the exception of the following changes: --dicermin 20; --dicermax 24; --foldsize 400. miRA was run with default settings with the exception of the following changes: cluster_gap_size = 100; min_precursor_length= 0; max_precursor_length= 400; max_pvalue = 0.05; max_duplex_length = 26. miR-PREFeR was run with default settings with the exception of the following changes: PRECURSOR_LEN = 400; READS_DEPTH_CUTOFF = 30; NUM_OF_CORE = 10; MIN_MATURE_LEN = 20; MAX_MATURE_LEN = 24. To avoid

false positive results, only miRNAs that were predicted by all three programs were considered to be “real” novel miRNAs and were included in downstream analyses.

In addition to predicting novel miRNAs using the *Citrus clementina* reference genome, custom *Poncirus trifoliata* and *Citrus jambhiri* ‘pseudo’ reference genomes were created in order to identify any species-specific novel miRNAs that may have been overlooked due to differences in sequence between these species. To make the custom ‘pseudo’ reference genomes, SNP variant data corresponding to the Flying Dragon trifoliate and Rough lemon variety was previously generated at the University of California, Riverside using whole-genome sequencing data deposited in NCBI’s Sequence Read Archive (SRA)[60] (data publicly available at SRA Study: SRP095606; accession numbers SRX2442485 and SRX2442476, respectively). Flying Dragon trifoliate orange was chosen because it is a member of the “small-flower” group and is genetically nearly identical to Rich 16-6[61]. These variants, in Variant Call Format (VCF), were subsequently used to build a consensus sequence using the BCFtools consensus tool (https://github.com/samtools/bcftools), which replaces the reference base(s) at a site of variation with the base(s) supplied by the VCF file. Novel miRNAs were then predicted in the same manner described above, except using the newly made *Poncirus trifoliata* or *Citrus jambhiri* ‘pseudo’ reference genome as input.

Differential expression analysis of miRNAs and mRNAs

Normalization, fold-change calculations, and statistical analysis of differentially expressed genes (DEGs) and differentially expressed miRNAs (DEMs) were performed

using the DESeq2 package. The adjusted p-value (aka false discovery rate (FDR)), was calculated by the DESeq2 package using the Benjamini-Hochberg procedure. DEGs and DEMs were considered as those with a fold change $\geq$ 2 and FDR of $\leq$ 0.05 for comparisons between two genotypes at a single time point. Protein-coding genes with an average of 5 reads per kilobase of transcript per million mapped reads (RPKM) and miRNAs with an average of 5 reads per million (RPM) were included in downstream analyses. Dendrograms, heatmaps, and Venn diagrams were created using R packages DESeq2, ComplexHeatmap[62], and ggplot2[63] and InteractiVenn[64]. Heatmaps displaying gene expression represent normalized expression values (RPKM), with red representing increased expression and blue representing decreased expression.

GO and KEGG pathway analysis

Gene Ontology (GO) functional annotation enrichment analysis was conducted using the GO Term Enrichment Tool in PlantRegMap[65] (http://plantregmap.cbi.pku.edu.cn/go.php) using *Citrus clementina* genome annotation IDs as input. Pathway analysis was performed using the Gene-list Enrichment Tool in KOBAS 3.0[66] (http://kobas.cbi.pku.edu.cn/anno_iden.php) using *Citrus clementina* Entrez Gene IDs as input. GO terms and KEGG pathways with p value $\leq$ 0.05 were considered significantly enriched.

Target gene prediction of identified differentially expressed miRNAs and correlation analysis with mRNA seq data

Targets genes of each differentially expressed miRNAs were predicted by the psRNATarget program (https://plantgrn.noble.org/psRNATarget/analysis)[67] default parameters. An in-house R script was then used to compare the predicted targets with the list of DEGs identified in our samples. The script also identified combinations of DEMs and DEGs based on the expected negative correlation between fold changes of miRNAs and their predicted targets.

Quantitative RT-PCR validation of differentially expressed genes and miRNAs

Several combinations of miRNAs and target DEGs found to be negatively correlated were quantified by real-time PCR (qRT-PCR). qRT-PCR was conducted to detect relative expression of these selected miRNAs and target mRNAs. Total RNA (including sRNAs) from each sample was first polyadenylated and reverse transcribed to cDNA using Mir-X miRNA First-Strand Synthesis and SYBR qRT-PCR Kit (Takara Bio Inc) according to the manufacturer's protocol. The 10-µl cDNA reaction was diluted one to ten to a final volume of 100 µl. cDNA was amplified on a BioRad CFX-96 real time system (Bio-Rad). The gene-specific primers were designed using IDT PrimerQuest software[68] and are listed in Supplemental Table 2.1**.** Reference gene expression stability across genotype and developmental stage was calculated by NormFinder and Bestkeeper software[69,70].

For miRNA qPCR, *snoR14* served as a reference gene. Reactions of 15-µl were prepared containing 1.5 µL cDNA, 7.5 µL 2x TB Green Advantage qPCR premix (Takara Bio), 0.3 µL each primer (0.1 mM) and 5.4 µL molecular grade water. PCR cycling conditions were as follows: 95 °C for 5 min, 40 cycles of 95 °C for 10 s, and 60 °C for 25 s. For mRNA qPCR, *EF1A* served as a reference gene. Reactions of 10-µl reactions were prepared containing 1 µL cDNA, 5 µL SSO Advanced Universal SYBR Green Supermix (Bio-Rad), 0.2 µL each primer (0.1 mM) and 3.6 µL molecular grade water. PCR cycling conditions were as follows: 95°C for 5 min, 40 cycles of 95°C for 20 s, and 60°C for 40 s. A melting curve analysis beginning at 65°C and increasing by increments of 0.5°C every 5 seconds to 90°C was added at the end of each PCR to evaluated the specificity of the amplified product. For each sample two biological replicates were used and all reactions were performed in triplicate for technical replication. No template controls (NTC) were run in duplicate for each primer pair. The relative expression levels of miRNAs and the predicted target genes was calculated using the Pfaffl method in order to correct for PCR efficiencies[71]. Statistical significance was determined using Student's t-test with two independent biological replicates, each representing an average of three technical replicates.

Results

Global mRNA expression profiling in citrus roots during fruit development

In order to profile the expression of mRNAs in differing rootstocks, total RNA was extracted from root tissue of Argentina sweet orange (SO), Schaub rough lemon (RL), Carrizo citrange trifoliate hybrid (CZ), and Rich 16-6 trifoliate orange (TF) collected at four time points throughout the 2014-2015 growing season. Young root tissue was collected in July (Time 1), September (Time 2), November (Time 3), and January (Time 4) (Figure 2.1). These timepoints were chosen because they correlated with the phases of citrus growth[72]. Time 1 was collected during cell division (phase I), time 2 was collected during early cell enlargement (phase II), time 3 was collected during late cell enlargement (phase II), and time 4 was collected during maturation and ripening (phase III).

Poly(A)-enriched fractions (mRNA) were used to construct libraries for Illumina sequencing. The sequencing statistics displayed in Table 2.1 are an average of the libraries sequenced for each genotype. After adapter removal and quality filtering, there was an average of 54,567,244; 65,048,264; 55,138,129; and 57,999,302 clean mRNA reads in libraries of from each rootstock genotype (SO, CZ, RL, and TF, respectively). Of the clean mRNA reads, 44,866,886 (82.82%) in SO, 52,275,821 (81.65%) in CZ, 45,667,152 (83.10%) in RL, and 46,057,869 (80.32%) in TF were mappable and could be aligned to the *Citrus clementina v 1.0* reference genome using HISAT2. On average,

73.40% of clean reads could be aligned to annotated genes. Of the 24,533 annotated genes in the clementine gene models, 22,829 (96.12%) were detected by sequencing in these root libraries. A hierarchical clustering tree of the samples reflected an age and genotype-specific structure, as mRNA samples mostly organized into clades based on time of collection, and secondarily by genotype (Figure 2.2).

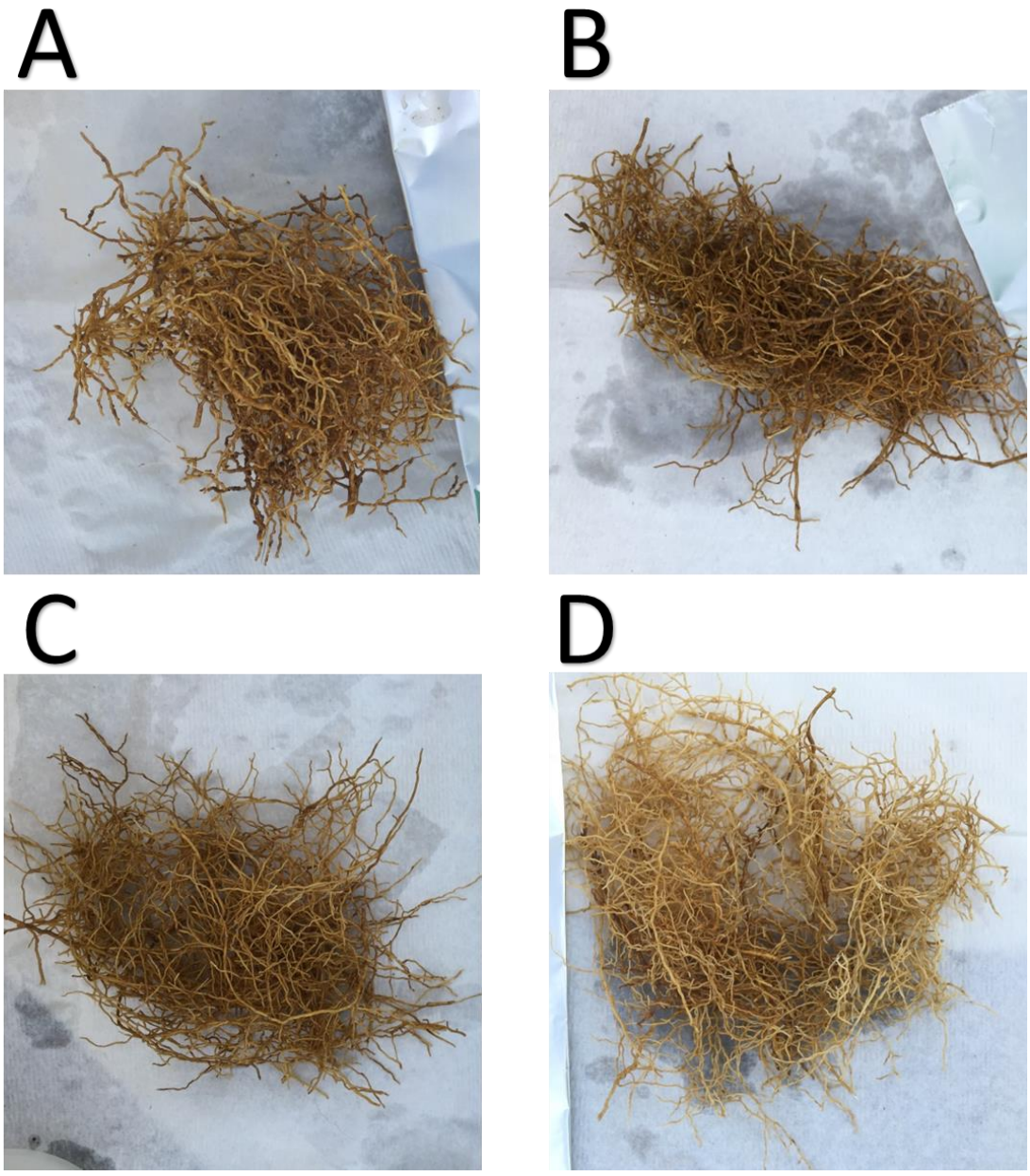

Figure 2.1. Young, fibrous roots of various rootstocks. Roots collected from (A) Argentine sweet orange, (B) Schaub rough lemon, (C) Carrizo citrange and (D) Rich 16-6 trifoliate orange rootstock in July 2014.

Table 2.1 Summary statistics of the small RNA and mRNA sequencing results for four citrus rootstock varieties

	Category	Sweet Orange Rootstock	Carrizo Rootstock	Rough Lemon Rootstock	Rich 16-6 Trifoliate Rootstock
Small RNA sequencing	Number clean reads	14,344,972	14,272,703	12,553,033	15,489,479
	Percent reads aligned to genome (%)	63.46	64.71	65.63	64.83
	Percent reads aligned to known miRNAs (%)	10.60	10.80	10.99	10.33
mRNA sequencing	Number clean reads	54,567,244	64,048,264	55,138,130	57,999,302
	Percent reads aligned to genome (%)	82.82	81.65	83.09	80.32
	Percent reads aligned to transcripts (%)	73.66	73.99	74.56	73.40

A.

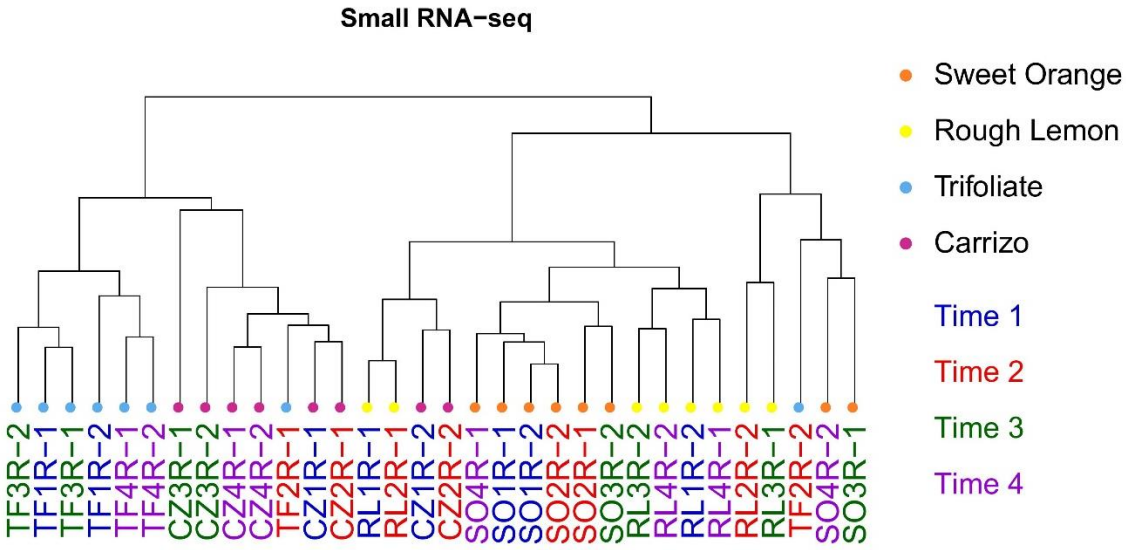

B.

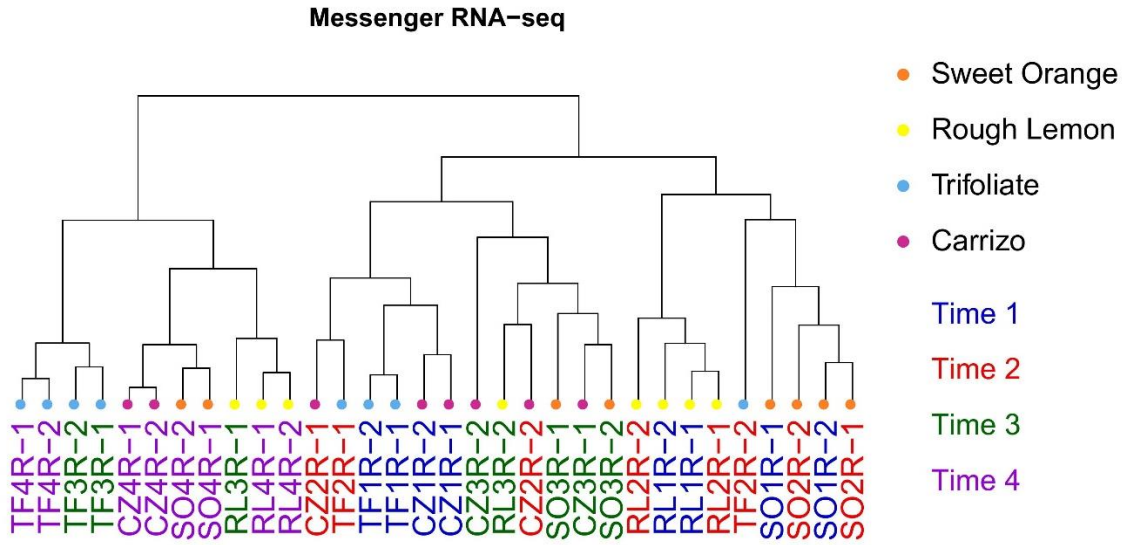

Figure 2.2. Hierarchical clustering of samples. Clustering of samples based on small RNA expression (A) or mRNA expression (B) represented by a dendrogram. Distance between samples is measured as 1 - Spearman's correlation coefficient. SO = sweet orange rootstock; CZ = Carrizo rootstock; RL = rough lemon rootstock; TF = trifoliate rootstock; R = root sample. Numbers directly after rootstock indicate time point of collection, while numbers after dash indicate biological replicates.

Differential expression analysis of genes in different rootstocks

In this study, RNA-sequencing produced reads that aligned to 21,964, 21,754, 21,622, and 21,500 citrus genes in samples of sweet orange, Carrizo citrange, rough lemon, and trifoliate orange rootstocks, respectively. With criterium of at least 2-fold difference and a p-value less than 0.05 ($|\log2FC| \geq 1$, $p < 0.05$), a total of 11,368 differentially expressed genes (DEGs) were identified between genotypes in at least one time point. There were 4,182 genes DE between rough lemon and sweet orange rootstocks, 2,932 DEGs between Carrizo citrange and sweet orange, 6,810 DEGs between trifoliate orange and sweet orange, 4,177 DEGs between rough lemon and Carrizo citrange, 4,401 DEGs between trifoliate orange and Carrizo citrange, and 7,729 DEGs between trifoliate and rough lemon (Figure 2.3). Of these, 306 DEGs overlapped in all 6 comparisons. Many of the DEGs were specific to the pairwise comparison between trifoliate orange and rough lemon rootstock (924 DEGs). The largest phenotypic differences in fruit quality traits are generally seen when comparing fruit grown on trifoliate to fruit grown on rough lemon rootstocks (Chapter 1). DEGs belonging to this comparison are likely to play a role in the phenotypic changes seen when fruit are grown on trifoliate orange versus rough lemon rootstock. Due to the large number of DEGs observed between these rootstocks, in combination with the phenotypic observations in the fruit grown on these rootstocks (Chapter 1), this comparison was focused on for the remainder of this study.

A.

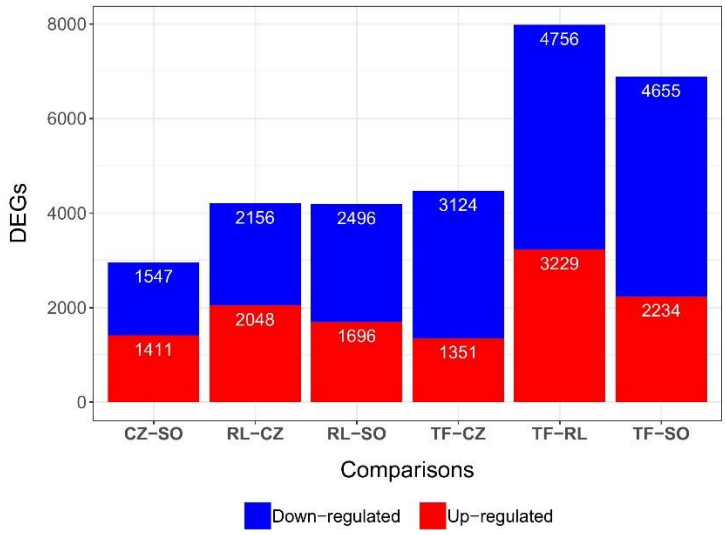

B.

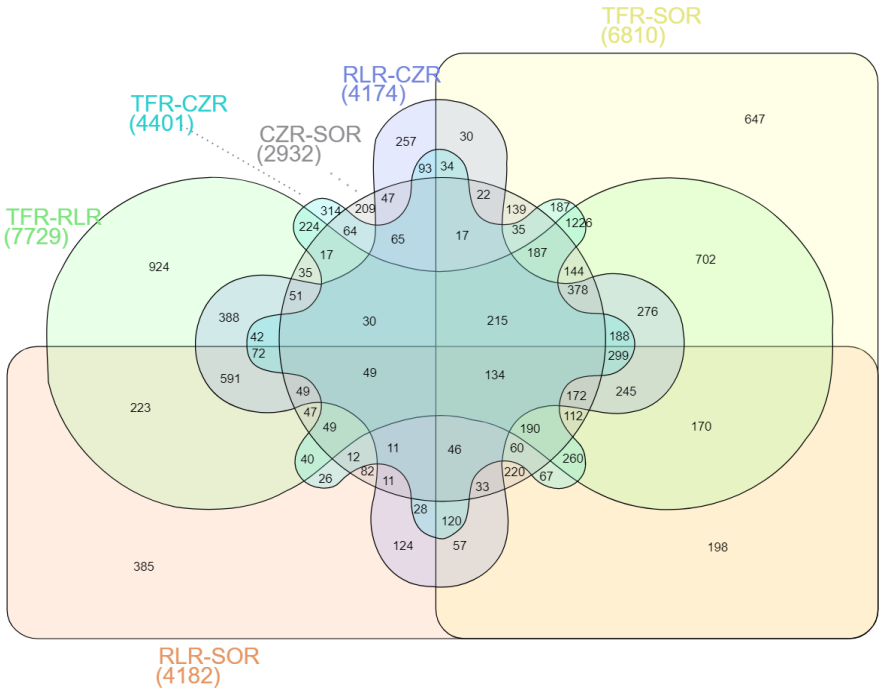

Figure 2.3. Differential gene expression analysis of citrus genes in various rootstocks. (A) The number of differentially expressed genes (DEGs) for all pairwise comparisons (P <0.05); red, DEGs with up-regulated expression; blue, DEGs with down-regulated expression. (B) Venn diagram of overlapping DEGs among various pairwise comparisons.

Transcriptional changes of citrus genes with possible roles in fruit quality

Among the identified DEGs, there were many genes that could play potential roles in fruit quality. Over 300 citrus genes were DE in this study that function in pathways known to be related to improved fruit quality (Figure 2.4, Supplemental Table 2.2). Of these, 20, 27, 68, and 120 DEGs identified had functions in nitrogen metabolism, transporters, starch and sucrose metabolism, and hormone-signaling pathways, respectively (Figure 2.5).

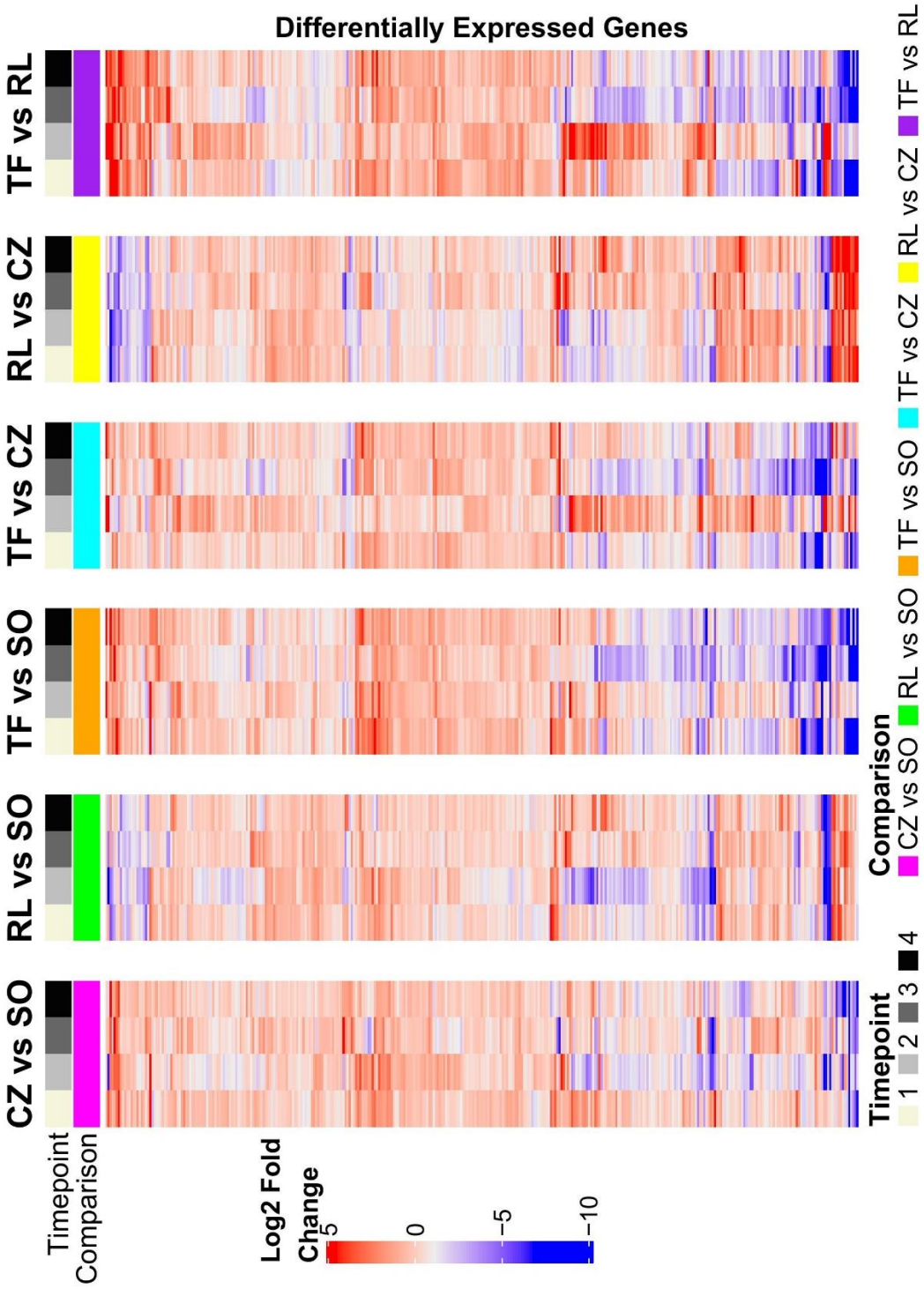

Figure 2.4. Heatmaps of all differentially expressed genes (DEGs) between different genotype comparisons at each time point (1, 2, 3, and 4).

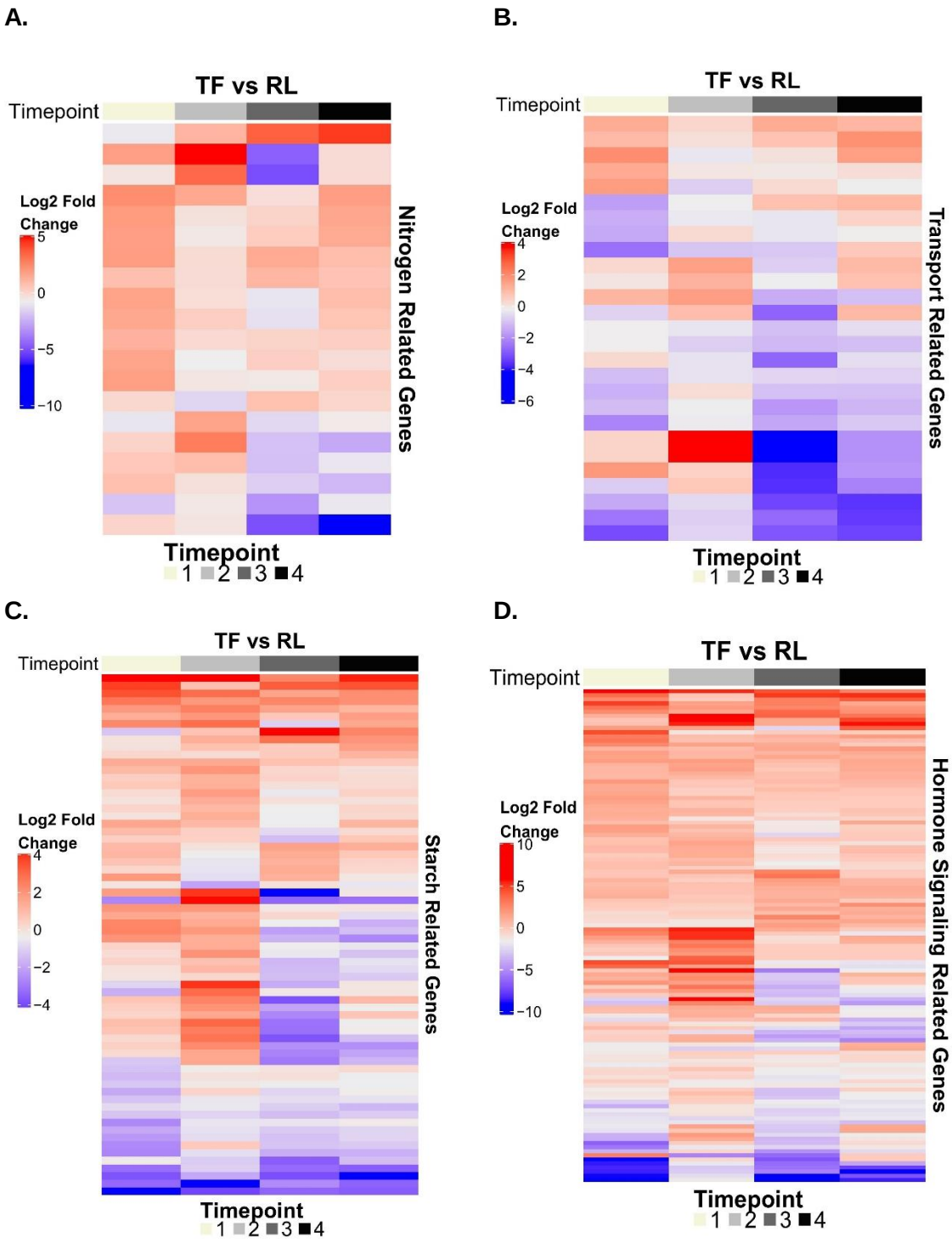

Figure 2.5. Heatmaps of differentially expressed genes (DEGs) with potential roles relating to fruit quality between trifoliate orange and rough lemon rootstocks at each time point (1, 2, 3, and 4). (A) Nitrogen metabolism genes (n=20). (B) Transport-related genes (n=27). (C) Starch metabolism genes (n=68). (D) Hormone signaling-related genes (n=120).

Functional classification of DEGs

Gene Ontology (GO) and pathway-enrichment analyses were conducted to explore the functions of genes that were DE between trifoliate orange and rough lemon rootstock varieties. GO categorization showed that the biological process GO terms ‘cell wall organization or biogenesis’ and ‘defense response’ and several carbohydrate metabolism processes were significantly enriched (p-value < 0.05) (Figure 2.6). KEGG pathway analysis revealed that genes for nitrogen metabolism, plant-pathogen interaction, starch and sucrose metabolism, and plant-hormone signal transduction were significantly enriched (p-value < 0.05) when comparing trifoliate to rough lemon rootstocks (Figure 2.7). Many genes involved in various hormone-signaling pathways were DE, including genes in the auxin-, cytokinin-, gibberellin-, abscisic acid-, brassinosteroid-, jasmonic acid-, and salicylic acid-response pathways (Supplemental Figure 2.3). Several genes related to cell division and the cell cycle were up-regulated in trifoliate rootstock compared to rough lemon. Additionally, there were many DE transporter genes, including nitrate transporters that were up-regulated (Figure 2.8).

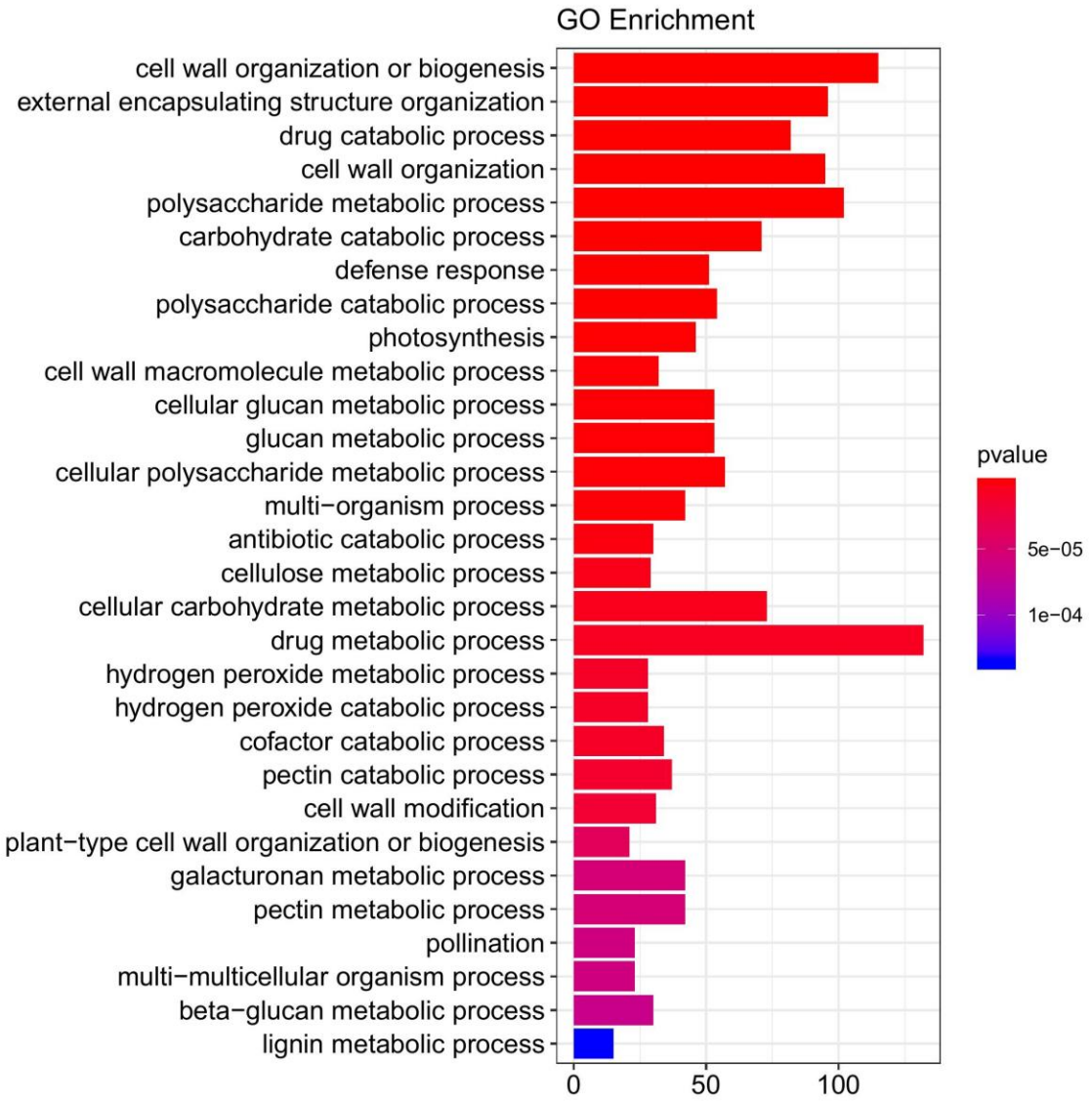

Figure 2.6. Gene ontology analysis of differentially expressed genes in trifoliate orange compared to rough lemon rootstock.

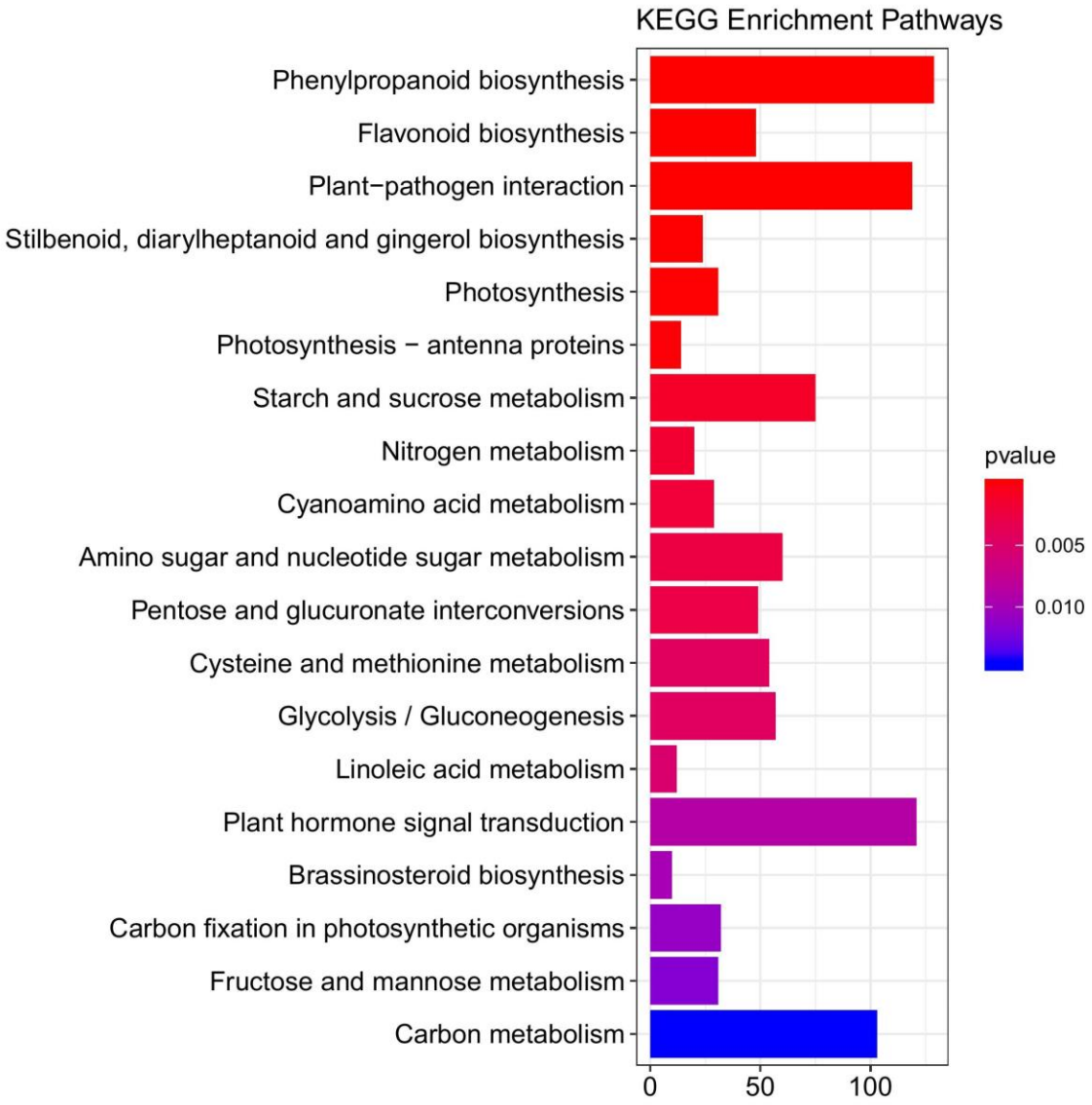

Figure 2.7. KEGG pathway enrichment of differentially expressed genes in trifoliate orange compared to rough lemon rootstock.

A.

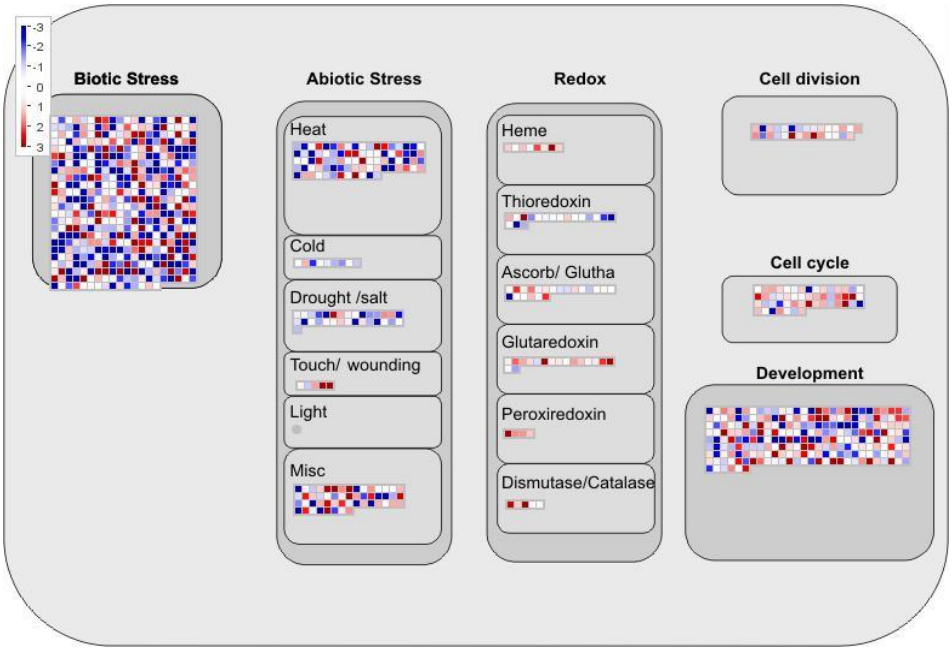

B.

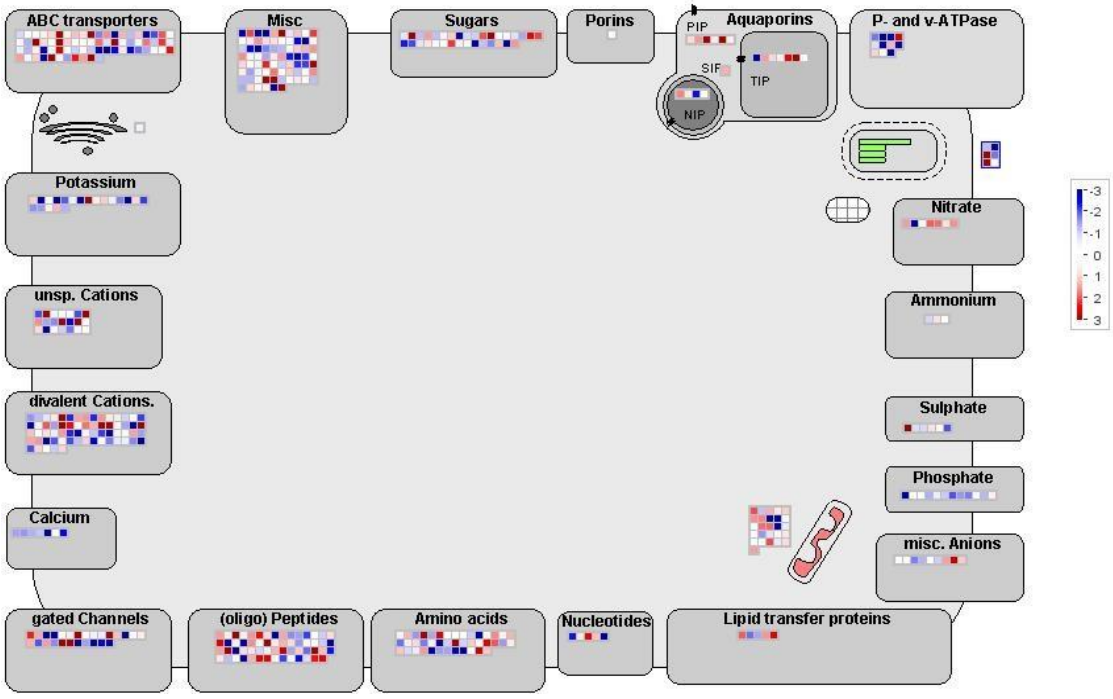

Figure 2.8. Relative expression levels of DEGs involved in (A) cellular responses and (B) transport. Genes that are up-regulated in trifoliate orange rootstock compared to rough lemon rootstock are represented in red and down-regulated genes are represented in blue. The map is from MapMan Application Software.

Deep sequencing results of sRNA libraries prepared from roots of various citrus rootstocks

sRNA fractions that were size selected were used to construct libraries for Illumina sequencing. Sequencing statistics in Table 2.1 are an average of the libraries sequenced for each genotype. After 3' adaptor trimming, quality filtering, and removal of reads shorter than 18 nt and longer than 30 nt, there was an average of 14,344,972; 14,272,703; 12,553,033; and 15,489,479 clean sRNA reads in libraries from each of the four rootstock genotypes (SO, CZ, RL, and TF, respectively) (Table 2.2). Of the clean small RNA reads, 9,232,697 (63.47%) in SO, 9,214175 (64.72%) in CZ, 8,184,291 (65.64%) in RL, and 10,018,179 (64.83%) in TF were mappable and could be aligned to the *Citrus clementina v 1.0* reference genome, most of which were between 21 and 24 nt in length. For reads 18-30 nt, all libraries showed similar size distributions, with most reads belonging to the 21 nt class, followed by the reads of 24 nt, which is consistent with previous reports in Chinese yew[73] and pine[74] (Figure 2.9).

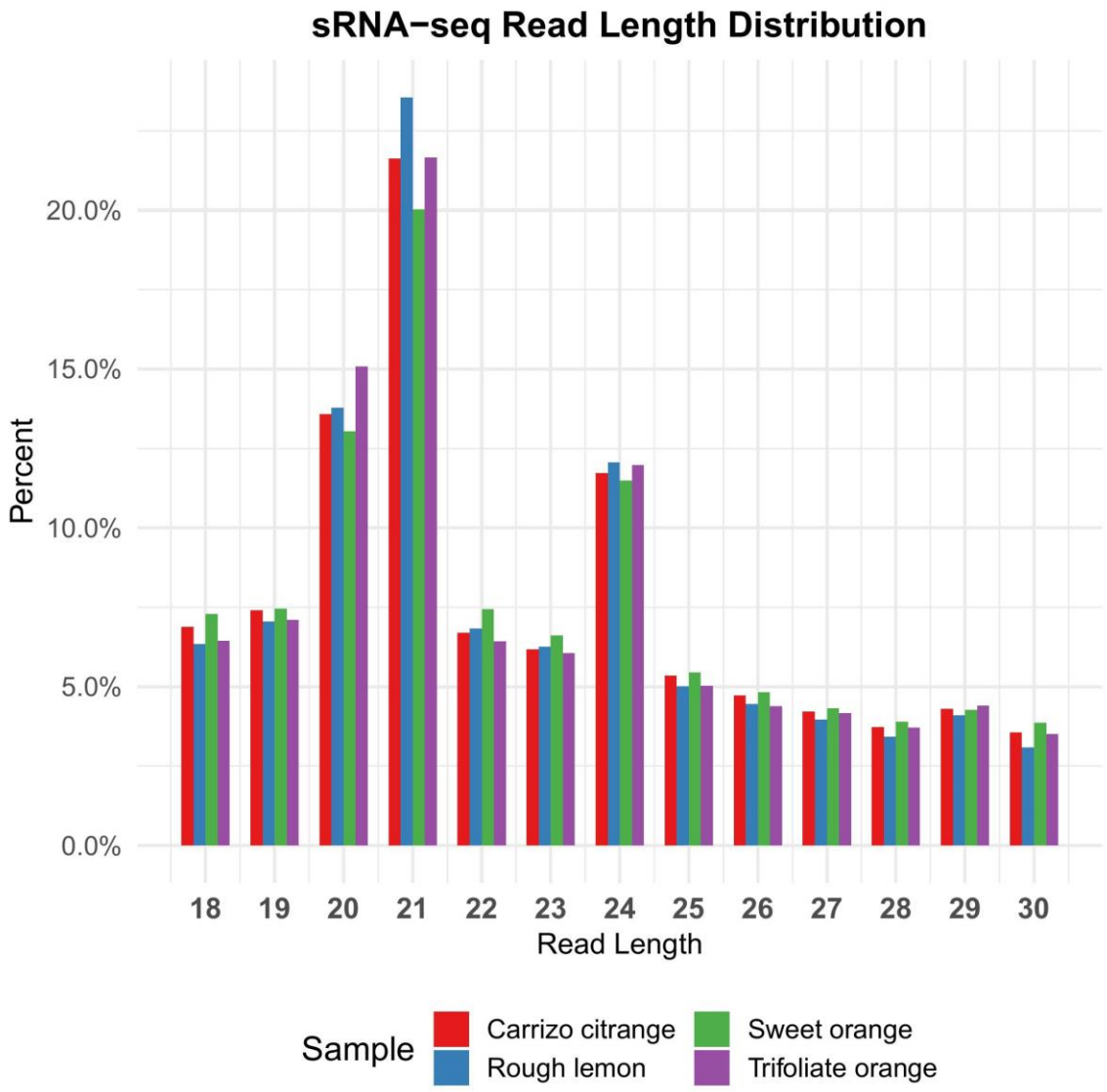

Figure 2.9. Read length (nt) distribution of sRNA libraries of various rootstocks.

Detection of known and novel miRNAs in citrus rootstocks

Using the Bowtie2 aligner, a total of 669 known conserved plant miRNAs could be mapped to the *Citrus clementina v 1.0* reference genome. Of these, 603 were retrieved in this study by deep sequencing of the root samples. Additionally, putative novel miRNAs were investigated by Shortstack, miRA, and miR-PREFeR software. These programs combine the position and frequency of mature sRNAs with the secondary fold-back structure of miRNA precursor molecules in order to provide probable miRNAs that may be specifically found in citrus. A 'pseudo' reference genome for *Poncirus trifoliata* and *Citrus jambhiri* was used as input for these software programs. The reference genomes were made for the purposes of this project by applying knowledge of SNP information from whole genome sequencing of these genotypes to the *Citrus clementina* reference genome (see Materials and Methods section for details). By applying this method, 12 potential novel miRNAs not homologous to those of any other plant species were predicted (nine from trifoliate orange and three from rough lemon) (Table 2.2, Supplemental Figure 2.1).

Table 2.2. Novel miRNA candidates detected in *Poncirus trifoliata* and *Citrus jambhiri* reference genome

Novel miRNA*	Mature Sequence (5' -> 3')	Scaffold	Start position	End position
FDT_n01	GCUCACUGCUCUUUCUGUCAGC	1	1106500	1106584
FDT_n02	ACCGGCGCUGCACUCGAUCAUG	2	32635171	32635281
FDT_n03	UUCUCUUAUCUUUUAUCUGUGC	1	20939724	20939849
FDT_n04	ACCUGGCAACUUUGGGCAUCC	5	2217337	2217519
FDT_n05	UUGAAAGUAAUAAGGAUUAUU	3	45812481	45812600
FDT_n06	UGUUUUGGGUGAAACGGGUGUU	6	18932958	18933103
FDT_n07	CAUGUGCCCUAGCUCUCCAGC	7	7639775	7639856
FDT_n08	UCAUUCGCGCUCUCAUCAUU	1	27929982	27930113
FDT_n09	UUCUAAACUCUCUCCCUCAUGG	2	11647304	11647434
JAM_n01	GUGCUCUCUACCAUUGUCAUA	2	25521807	25521904
JAM_n02	ACUCUCCCUCAAGGGCUUCUGG	3	1030866	1030958
JAM_n03	CUUUCAGCAGCCUCCGGCGUC	6	18400394	18400500

*Note: FDT (Flying Dragon Trifoliate) and JAM indicate novel miRNA was detected when *Poncirus trifoliata* or *Citrus jambhiri* reference genomes were used as input in novel miRNA detection software, respectively

Differential expression analysis of miRNAs and target prediction of miRNAs

Levels of expression of known and novel miRNAs were compared between pairs of rootstocks at each of the four time points throughout fruit development. With a criteria of

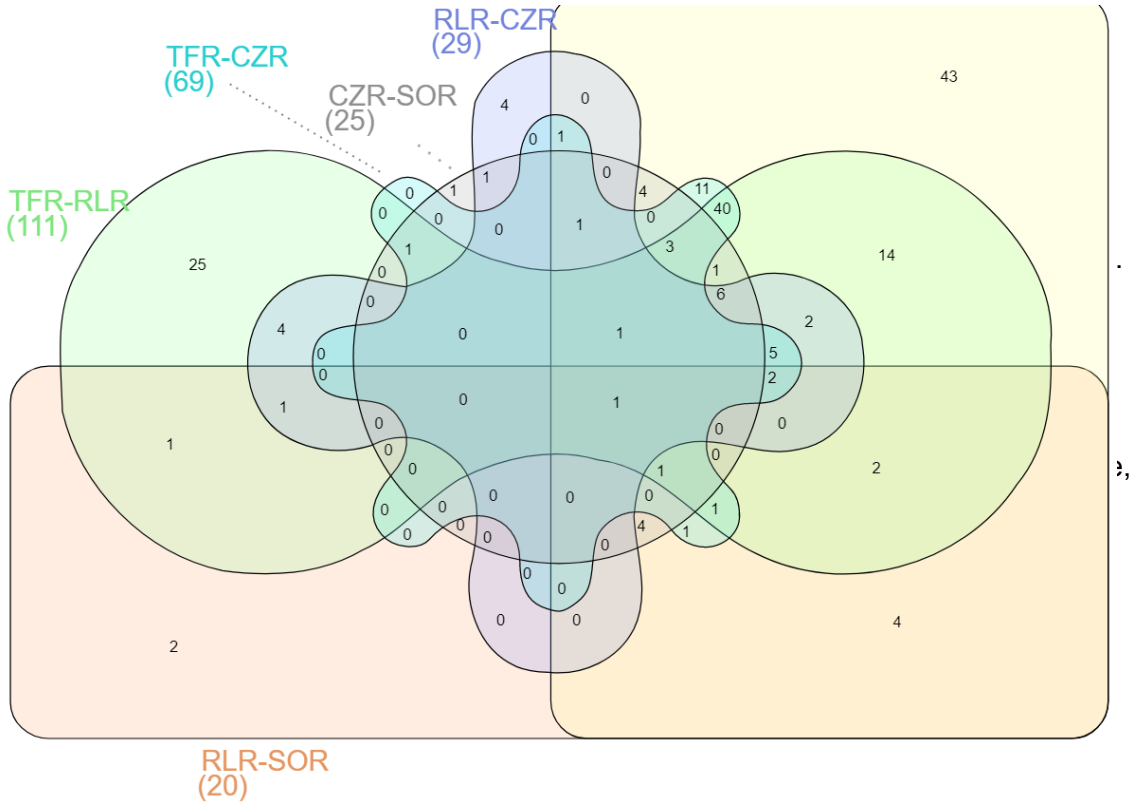

Figure 2.10).

For this study, the psRNATarget website (https://plantgrn.noble.org/psRNATarget/analysis) was used to predict potential target mRNAs of the DEMs. This approach accepts a list of DEMs identified through deep sequencing and predicts targets from the *Citrus clementina 182 v1.0* transcript fasta file (data found at https://phytozome.jgi.doe.gov/pz/portal.html) according to the criteria described by Meyers et al.[75]. There were over 5,000 potential mRNA targets of the DEMs identified by the program.

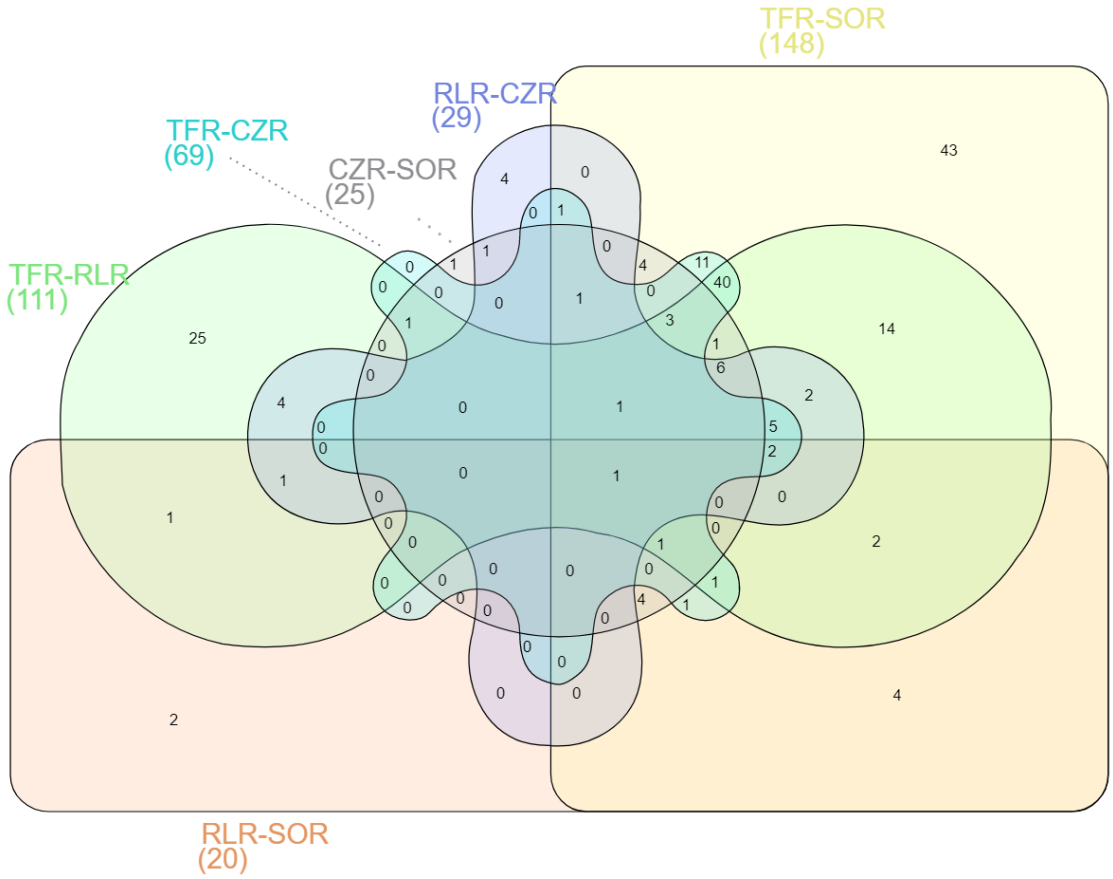

Figure 2.10. Differential miRNA expression analysis of citrus rootstocks. Venn diagram of overlapping DEMs among various pairwise comparisons.

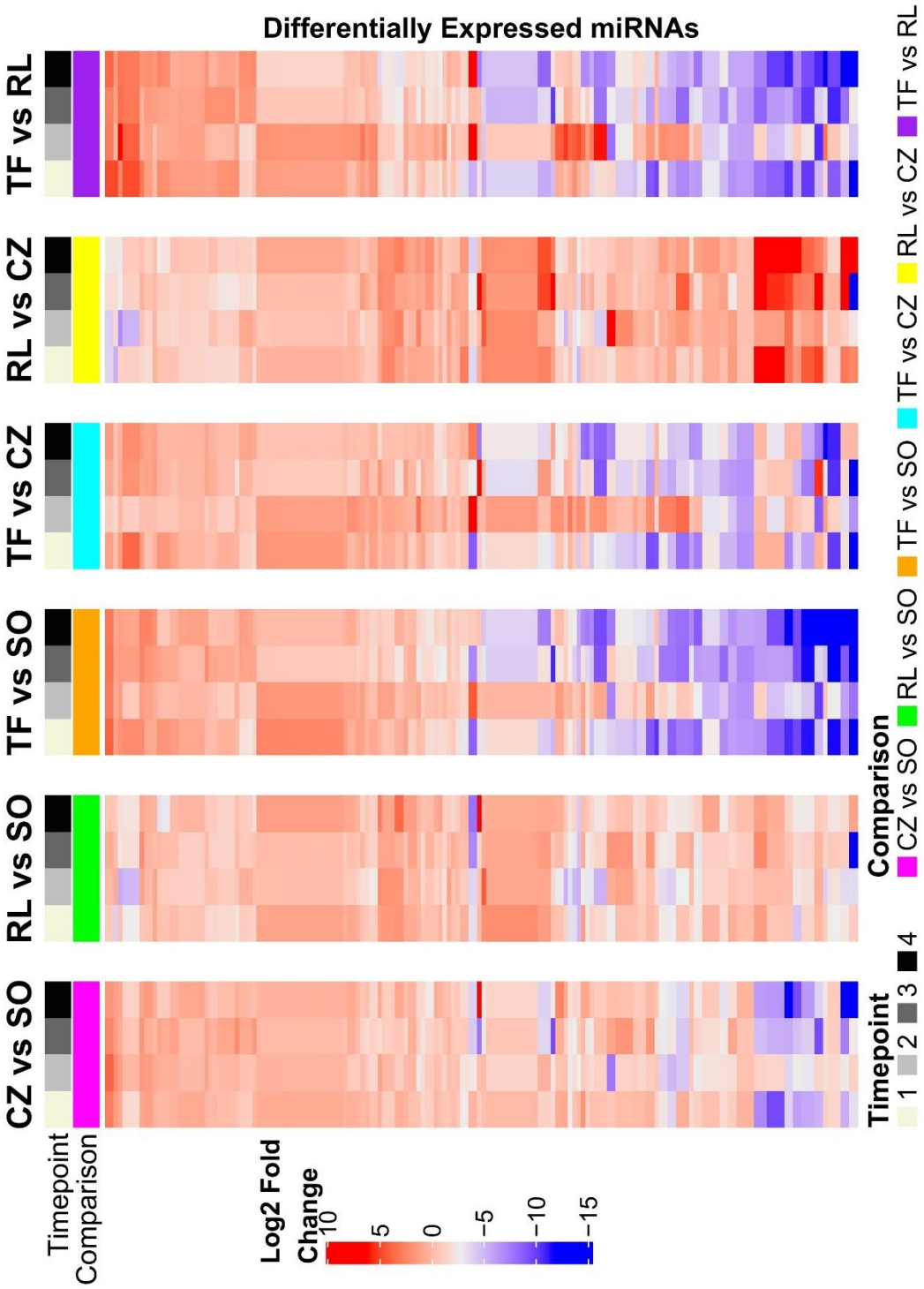

Figure 2.11. Heatmaps of all differentially expressed miRNAs (DEGs) between different genotype comparisons at each time point (1, 2, 3, and 4).

miRNA–mRNA interaction

To further understand the potential genetic influence of rootstocks on fruit quality, we focused on the expression changes of miRNAs and their target genes. miRNAs are post-transcriptional regulators that cause down-regulation of target genes[42]. Therefore, if a target gene is down-regulated by a miRNA, a negative correlation between miRNA expression and the target mRNA expression is expected.

The RNA-seq data was then analyzed with an in-house R-script in order to select for DEGs that overlapped with mRNAs that were predicted to be targets of the DEMs. miRNA-mRNA interaction pairs were then selected that displayed the expected negative correlation in gene expression. After removal of genes that did not have any functional annotation, there were 465 combinations of miRNA-mRNA pairs that showed reciprocal expression patterns. Comparing these genes with enriched GO terms and KEGG pathways led to several candidate miRNA-mRNA interactions that could be causing changes in fruit quality when differentially expressed between rootstocks. These genes included transporters, hormone signal-transduction genes, membrane trafficking genes, and carbohydrate metabolism genes.

Validation of the sequencing data by quantitative qRT-PCR

Based on the interaction pairs identified and their relevance to fruit quality, nine pairs of miRNAs and target mRNAs were selected for validation via qRT-PCR analysis (Table 2.3). The miRNA-mRNA interaction analysis indicated that multiple miRNAs can target the same gene. For example, three miRNAs (Csi-miR3465, Csi-miR391a.3, and Csi-miR394b) each exhibited negative correlations with two different target mRNAs, both of

which were chosen for validation (Table 2.3). Samples collected at time points one and four (July and January, respectively) were selected for validation to compare differences in expression levels of genes in trifoliate orange compared to rough lemon rootstocks at the beginning and end of fruit development. For qRT-PCR, two biological replicates and three technical replicates were performed to accurately quantify expression of each gene.

Of the nine miRNA-mRNA interaction pairs chosen for validation, five miRNAs were up-regulated at both timepoints, while their target genes were down-regulated and four miRNAs were down-regulated at both timepoints, while their target genes were up-regulated (Figure 2.12). The correlation between the relative expression level detected by qRT-PCR and by RNA-sequencing was calculated. Pearson correlation values were highly significant with $r = 0.83$, which strongly supported the sequencing data (Figure 2.13). However, two miRNA-mRNA pairs did not have the expected fold changes between time points. For example, Csi-miR394b is more up-regulated in trifoliate vs rough lemon rootstock (shows an increase in fold change) from July (Time 1) to January (Time 4). This should correlate with the target mRNA (*SAG101*) being more down-regulated in trifoliate vs rough lemon rootstock from July to January, but instead, we see the target become less down-regulated (an increase in the target mRNA expression) from July to January. Only this pair and FDT_n01 - SWEETIE show this inconsistency. The results for the remaining seven pairs were consistent with their expected changes in expression levels. According to the qRT-PCR experiment, four of the miRNAs had decreased expression levels between July and January, while two miRNAs increased in expression from the beginning to the end of fruit development.

Table 2.3. Deep sequencing and qRT-PCR relative expression of selected miRNAs and their predicted target genes.

sRNA	Predicted target gene (*C. clementina* locus name)	Arabidopsis Homology	Arabidopsis gene name and description	RNA-seq				qRT-PCR				RNA-seq - qPCR Correlation	sRNA-mRNA Correlation
				Fold change of sRNA		Fold change of target gene		Fold change of sRNA		Fold change of target gene			
				Time 1	Time 4	Time 1	Time 4	Time 1	Time 4	Time 1	Time 4		
Csi-miR3465	Ciclev10001581m.g	AT5G65420.1	CYCD4;1 - CYCLIN D4;1	-3.076 *	-2.337 *	1.046	0.327	-0.186	-0.376 *	0.333	0.546 *	0.885	-0.609
Csi-miR3465	Ciclev10007952m.g	AT5G25510.1	PP2A - Protein phosphatase 2A regulatory B subunit family protein	-3.076 *	-2.337 *	0.559 *	1.354 *	-0.186	-0.376 *	0.104 *	1.226 *	0.826	-0.206
Csi-miR391a.3	Ciclev10001649m.g	AT1G32170.1	XTR4, XTH30 - xyloglucan endotransglucosylase/hydrolase 30	-3.740 *	-4.384 *	1.262 *	1.234 *	-2.271 *	-2.455 *	0.515 *	1.354 *	0.983	-0.508
Csi-miR391a.3	Ciclev10004368m.g	AT2G44900.1	ARABIDILLO-1	-3.740 *	-4.384 *	2.019 *	1.293 *	-2.271 *	-2.455 *	0.695 *	1.633 *	0.962	-0.402
Csi-miR394b	Ciclev10011372m.g	AT5G14930.2	SAG101 - senescence-associated gene 101	1.295 *	2.077 *	-1.045 *	-0.282	1.249 *	2.048 *	-1.847 *	-0.304 *	0.988	0.915
Csi-miR394b	Ciclev10023463m.g	AT1G63440.1	HMA5 - heavy metal atpase 5	1.295 *	2.077 *	-1.435 *	-1.527 *	1.249 *	2.048 *	-1.551 *	-1.586	1	-0.526
Csi-miR390a-3p	Ciclev10031846m.g	AT1G68840.2	EDF2,RAP2.8,RAV2, TEM2 - related to ABI3/VP1 2	1.367 *	0.391	-1.724 *	-0.271	1.423 *	0.986 *	-1.870 *	-0.289	0.981	-0.864
Csi-miR2928	Ciclev10032182m.g	AT2G38750.1	ANNAT4 - annexin 4	4.788 *	3.034 *	-2.789 *	-2.485 *	1.289 *	0.938 *	-3.316 *	-3.113 *	0.992	0.672
FDT_n01	Ciclev10011943m.g	AT1G67140.3	SWEETIE - HEAT repeat-containing protein	0.017	1.640 *	-0.225	-0.51	0.502 *	1.023 *	-0.713 *	-0.603 *	0.858	-0.42

Both fold change of sRNAs and target genes are the ratio of the expression levels in trifoliate rootstock compared to rough lemon rootstock. The value for fold change in qRT-PCR experiments is an average of two biological replicates with three technical replicates; * indicates a significant difference at $P < 0.05$

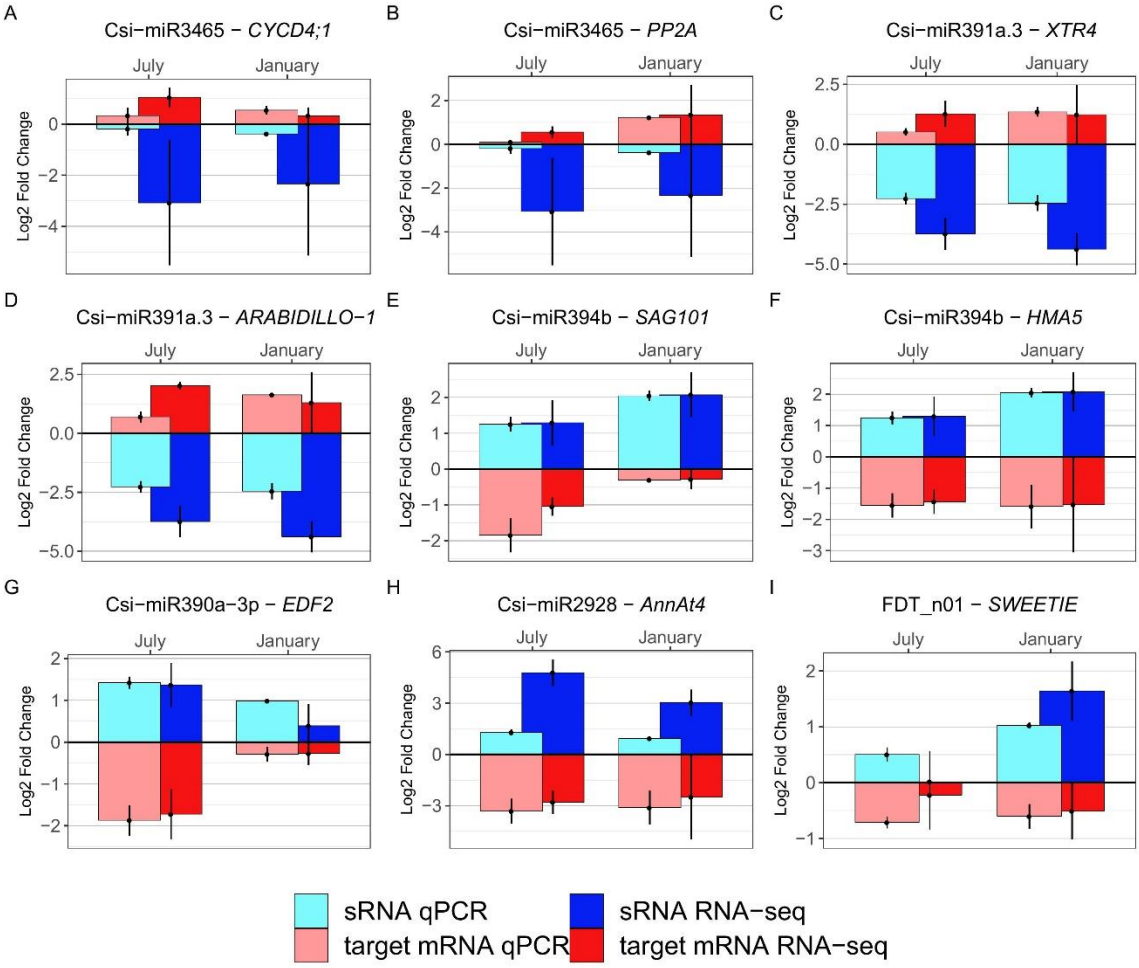

Figure 2.12. qRT-PCR validation of differential expression patterns of genes and miRNAs in trifoliate orange and rough lemon rootstocks.
Relative expression levels of trifoliate compared to rough lemon rootstocks is shown. qPCR log2 fold changes are represented by light blue and pink for miRNA and mRNA expression, respectively. The corresponding RNA-seq data is represented by dark blue and red for miRNA-mRNA pair. EF1A and snoR14 were used as the endogenous controls for mRNA and miRNA, respectively. The error bars indicate standard error of the means of two biological replicates and three technical replicates. (A) Csi-miR3465 - *CYCD4;1* (CyclinD4;1); (B) Csi-miR3465 - *PP2A*, (Protein phosphatase 2A regulatory B subunit family protein); (C) Csi-miR391a.3 - *XTR4*, (xyloglucan endotransglucosylase/hydrolase 30); (D) Csi-miR391a.3 - *ARABIDILLO-1*; (E) Csi-miR394b - *SAG101*, (Senescence-Associated Gene 101); (F) Csi-miR394b - *HMA5,* (Heavy Metal ATPase 5); (G) Csi-miR390a-3p - *EDF2*, (Early Response DNA Binding Factor 2); (H) Csi-miR2928 - *AnnAt4*, (Annexin 4); (I) FDT_n01 - *SWEETIE*, (HEAT repeat-containing protein).

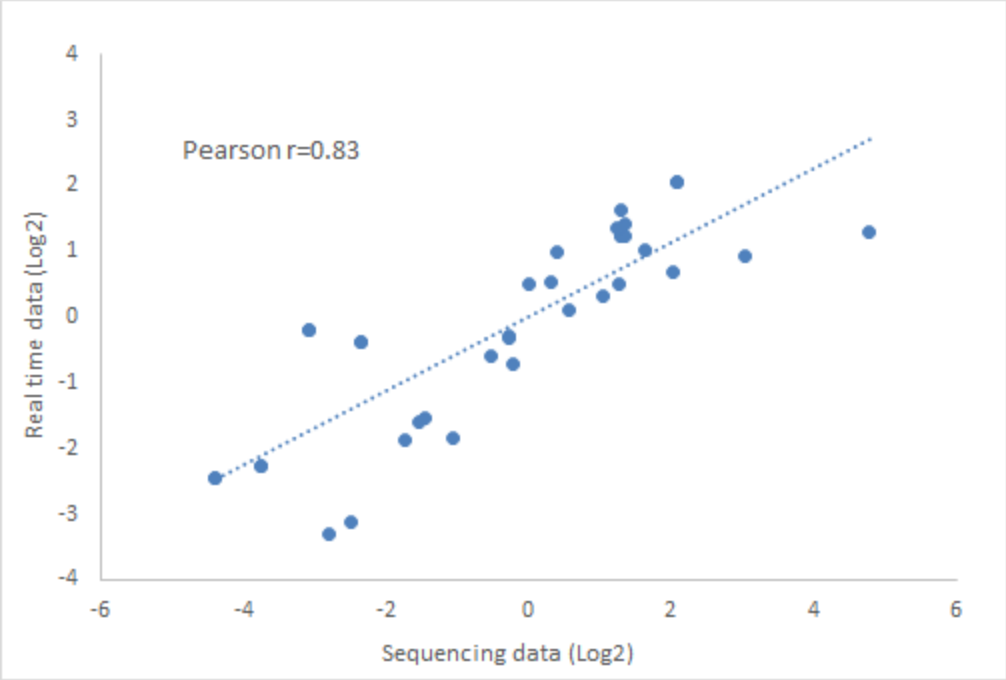

Figure 2.13. Correlation of gene expression ratios between sequencing data and quantitative RT-PCR data. Pearson correlation scatter plot of comparisons of ratios measured by sequencing and quantitative RT-PCR in mRNAs and miRNAs. 15 genes, including 9 mRNAs and 6 miRNAs, were subjected to quantitative real-time PCR analysis. RNA-seq data (fold changes in gene expression) were plotted against qRT-PCR data (fold-changes in gene expression). Both the x and y-axes are shown in log2 scale. r indicates the Pearson correlation coefficient.

Discussion

The objective of this study was to investigate transcriptome changes between various citrus rootstocks with the goal of identifying genes potentially influencing fruit quality. For this study, four rootstocks were chosen from a citrus rootstock trial with Washington navel orange scion in Riverside, California; Argentina sweet orange, Schaub rough lemon, Carrizo citrange, and Rich 16-6 trifoliate orange. Previously mentioned reports of rootstock effects on fruit quality indicate that while rough lemon rootstock increases overall growth, yield, and fruit size, fruit is often lacking in sugar and acid levels (Chapter

1). The quality of fruit grown on trifoliate is much higher, as well as having the added benefits of imparting dwarfing, cold hardiness, and tolerance to certain pests and diseases[16,75]. Presently, there is very little molecular-level understanding of the differences seen among citrus rootstocks. In the present study, an integrated miRNA and mRNA high throughput sequencing analysis was performed on genetically diverse rootstocks in order to further our understanding of rootstock effects on fruit quality. Additionally, an innovative approach to predict uncharacterized, potential novel miRNAs was performed, involving the use of a newly made, 'pseudo' reference genome for citrus genotypes that have limited genetic information available.

The differentially expressed miRNAs and mRNAs identified in different rootstocks during fruit development

In this study, RNA-seq technology was used to investigate miRNome and transcriptome differences between various rootstocks and explore miRNA-target mRNA interaction pairs that may play a role in the quality of fruit produced. Young root samples from four genetically diverse rootstocks at four time points throughout fruit development were sequenced. Many genes were identified as differentially expressed over the course of the season, which suggests a transcriptional reprogramming of the root system during the summer, fall, and early winter seasons (all timepoints collected). Only about 15% of these genes (1,613 genes) were shared between all genotypes. The largest group of genes with genotype-specific expression patterns was found in trifoliate roots (20.5%) (Supplemental Figure 2.2). This is not surprising considering trifoliate is the most genetically distinct of the three rootstocks. Based on the genetic divergence of trifoliate

and the large phenotypic differences between fruit produced on trees with trifoliate vs rough lemon rootstock, the remainder of this study focused on DEGs identified between these genotypes during fruit development.

A total 4,182 genes were significantly DE between RL and SO, 2,932 between CZ and SO, 6,810 between TF and SO, 4,174 between RL and CZ, 4,401 between TF and CZ, and 7,729 between TF and RL rootstocks. Most of the differentially expressed genes are observed in comparisons involving trifoliate rootstocks, especially compared to rough lemon and sweet orange. This, again, is not very surprising based on the phylogenetic relationships of these varieties[76]. A total of 20 miRNAs were significantly DE between RL and SO, 25 between CZ and SO, 148 between TF and SO, 29 between RL and CZ, 69 between TF and CZ, and 111 between TF and RL rootstocks. These included 10 potential novel miRNAs. Similarly to the DEGs, the highest numbers of DEMs were identified in comparisons including trifoliate rootstock. It is interesting that although Carrizo is an F1 hybrid of trifoliate orange, mRNA and miRNA expression in Carrizo roots is more similar to that of rough lemon and sweet orange than to that seen in trifoliate orange.

Among the differentially expressed genes were several genes with functions that could possibly lead to changes in fruit quality traits, such as those relating to nitrogen metabolism, starch and sucrose metabolism, hormone signaling pathway-related genes, and transporters. GO Term enrichment analysis identified defense response, cell wall organization or biosynthesis, and many other cell wall related processes. KEGG pathway analysis displayed nitrogen metabolism, plant-pathogen interaction, and starch

and sucrose metabolism, and plant hormone signal transduction pathways to be significantly enriched. Several cell division and the cell cycle-related genes, as well as transporter genes were DE in trifoliate compared to rough lemon rootstock. Genes involved in these pathways were chosen to validate the RNA-seq data by qRT-PCR at the first and fourth time points to assess potential biologically significant genes at the beginning and end of the growing season.

Genes impacting root system architecture (RSA) in citrus rootstocks

Plants must adapt to their environment to survive and be productive. Plants rely heavily on environmental cues and have different adaptive characteristics in order to overcome various stressors. In root systems, an increase in lateral root formation allows plants to more easily uptake water and essential nutrients in order to survive in unfavorable conditions[33–35]. Variations in RSA are genotype dependent. In the present study, the transcriptomes of genetically diverse root systems were compared in order to identify genes that may influence RSA, and therefore, impact overall growth and fruit quality traits.

Citrus rootstocks are characterized as vigorous if they have an extensive root system with an abundance of fibrous roots. Less vigorous rootstocks have much shallower root systems with the majority of their fibrous roots clustered near the surface[77]. Several genes were identified in this study that could contribute to root system architecture, a majority of which were associated with changes to size or abundance of lateral roots. The first stage in lateral root development is characterized by an auxin gradient that promotes cell cycle activation and asymmetric cell division[78,79]. Cell cycle reactivation

and control is imperative for lateral root initiation and is induced by the accumulation of high auxin levels that induce the upregulation of cell cycle genes, such as cyclins and cyclin-dependent kinases[80–82]. In Arabidopsis, a D-type cyclin, *CYCD4;1*, was found to be required for normal lateral root density. *CYCD4;1* mutants have a reduced lateral root density[83]. *CYCD4;1* was found to be DE in the present study. This gene was up-regulated in trifoliate roots compared to rough lemon roots (Table 2.3, Figure 2.12A). If this gene plays a similar role in citrus as Arabidopsis, it could cause an increase in root density in trifoliate root systems.

Another gene in that is known to regulate cell differentiation and proliferation is *ARABIDILLO-1*. Mutations in *ARABIDILLO-1* formed fewer lateral roots, while overexpression lines produced more lateral roots than wild-type seedlings[84,85]. It was suggested that this F-box protein in Arabidopsis promotes lateral root development by degrading some positive regulator of the gibberellin (GA)-signaling pathway through selective protein degradation of ubiquitin/26S. GA negatively affects lateral root formation by inhibiting lateral root primordium initiation[86]. *ARABIDILLO-1* was also up-regulated in trifoliate rootstocks, suggesting that it could cause trifoliate rootstock to produce more lateral roots than rough lemon rootstock using a similar mechanism to that seen in Arabidopsis (Table 2.3, Figure 2.12D).

A third gene in citrus found to be involved in lateral root development encodes a protein phosphatase 2A regulatory B subunit family protein (PP2AB). PP2A is one of the most important Serine/Threonine (Ser/Thr) protein phosphatases. It regulates many cellular processes, such as transcription, translation, the cell cycle, metabolism, and apoptosis[87].

PP2A positively regulates salt stress response by modulating polar auxin transport. In Arabidopsis, this salt-induced auxin redistribution leads to increased lateral root development[88]. An overexpression line of a wheat *PP2AB* gene displayed a similar phenotype of increased lateral roots, especially when treated with salt[89]. PP2A is a positive regulator of lateral root development under osmotic stress, and the increased expression of this gene in trifoliate roots could be serving a similar function in this rootstock (Table 2.3, Figure 2.12B).

Shallow, yet dense fibrous root systems have been observed in trifoliate rootstocks[90]. Neves et al.[91] reported that trifoliate and citrange had larger root systems than rough lemon. Furthermore, about 55% of trifoliate roots was recorded within the top 12 inches of the soil, where samples were collected from, while only about 30% of rough lemon roots were found near the surface. Trifoliate roots also had higher growth rate, root length density, and root length per unit root dry mass (specific root length; SRL) than rough lemon[92]. Taken together, the above-mentioned genes could offer insights into the molecular mechanism underlying the differences in root system architecture between these rootstocks.

A delicate balance exists when it comes to heavy metal homeostasis in plants. For example, copper (Cu) is an essential micronutrient required for a great number of physiological processes at optimal concentrations yet can become toxic at elevated levels. Plants have developed sophisticated homeostasis networks to regulate intracellular levels of Cu, controlling the uptake, distribution, and accumulation of this metal ion[93]. Cu distribution takes place via a family of P-type transporters in Arabidopsis.

The *Heavy Metal P-type ATPase* (*HMA5*) gene plays a role in Cu detoxification in Arabidopsis roots. *hma5* mutants are hypersensitive to Cu and while *hma5* primary roots have reduced length, these plants began to grow more lateral roots than the wild type plants[94]. This gene was down-regulated in trifoliate rootstocks compared to rough lemon rootstocks (Table 2.3, Figure 2.12F). This expression pattern would be observed if there were a Cu deficiency in the soil where these samples were collected. A similar downregulation of Cu ATPase was observed in cucumber roots upon Cu deficiency[95]. This suggests that a shortage of Cu potentially enhances the growth of lateral roots in trifoliate, while rough lemon rootstock is not as responsive to the deficiency. This would be in agreement with the increased lateral root phenotypes described above. Cu levels recorded at planting of this rootstock trial were just above optimal levels (1.1 PPM at 8-16" soil depth; optimal level is >1.0 PPM). It is plausible that trifoliate roots could be better adapted to a potential deficiency of Cu in subsequent years. Further testing of nutrient levels in the plant and soil will need to be performed to confirm these hypotheses.

An interesting gene was identified as DE that could potentially contribute to the dwarfing phenotype sometimes seen when trifoliate is used as a rootstock. SWEETIE, identified in Arabidopsis, is a sugar transporter that controls sugar flux and modulates many important processes[96]. A mutation in this gene causes modified carbohydrate metabolism that leads to a dwarfed phenotype[97]. *SWEETIE* was down-regulated in trifoliate roots compared to rough lemon (Table 2.3, Figure 2.12I). While this dwarfed phenotype was observed in roots and shoots in Arabidopsis, it is conceivable that the

molecular mechanism of dwarfing in grafted citrus plants could involve the movement of sugars from the rootstock to the scion via the transporter encoded by SWEETIE. This would be consistent with previous studies reporting that the graft union can cause differences in carbohydrate transport, resulting in dwarfing[28,98–100]. In the University of California, Riverside rootstock trial sampled, trees on rough lemon were 28.7.% larger than trees on Rich 16-6 trifoliate orange, potentially due to differing abilities of the rootstocks to transport carbohydrates.

Differential expression of biotic and abiotic stress responsive genes

Plants, being immobile, endure a variety of environmental stresses over the course of their lifetime. Therefore, they have acquired specific and sensitive ways to sense and react to each type of stress[101]. For example, abiotic stress can trigger the production of ABA, which leads to the activation of the expression of an assortment of stress-responsive genes[102]. Cold stress can lead to water-deficit conditions in plant cells, which induces changes in cytosolic calcium (Ca^{2+}) levels[103,104]. Ca^{2+}, acting as a messenger, is able to activate signaling pathways and induce a variety of plant growth, development and stress responses[105]. Annexin is a Ca^{2+}-binding protein that senses Ca^{2+} and transmits the signal to downstream signaling components of the ABA and abiotic signaling pathway, regulating stress response in plants[106]. In Arabidopsis, a mutation in *AnnAt4* displayed tolerance to dehydration, while *AnnAt4* overexpressing transgenic plants were more sensitive to this stress. *AnnAt4*, was down-regulated in trifoliate roots, suggesting that it may play a role in the ability of this rootstock to respond to cold stress-induced dehydration (Table 2.3, Figure 2.12H).

Cell wall architecture is important in plant resistance to abiotic stress. Cell wall-related proteins are thought to play a central role in modulating cell wall elasticity, which facilitates cell enlargement and expansion. These proteins include xyloglucan endo-β-transglucosylases/hydrolases (XET/XTHs), endo-1,4-β-D-glucanase (EGase), and expansins (EXPs)[107,108]. Most cases of abiotic stress are associated with an increase in XTH proteins, which helps maintain cell wall plasticity in response to stress[109]. The overexpression of *XET-related (XTR)* genes in Arabidopsis has been associated with improved freezing tolerance[110]. Similar results of increased *XET* expression in response to cold were also seen in rice and poplar[111,112]. In the present study, there was increased in *XTR4/XTH30* in trifoliate compared to rough lemon roots (Table 2.3, Figure 2.12C). It is conceivable that this gene is having a similar effect in trifoliate roots, enhancing tolerance of this rootstock to cold stress.

Additionally, *Senescence-Associated Gene 101 (SAG101)* was DE in this study and has a role in response to both abiotic and biotic stress. In Arabidopsis, SAG101 interacts with an *Enhanced Disease Susceptibility 1 (EDS1)* to facilitate plant-defense signaling[113]. These genes are also involved in the regulation of freezing tolerance in Arabidopsis[114]. Transgenic plants with mutated versions of *SAG101* had altered lipid composition, resulting in enhanced cold tolerance compared to wild-type plants. *SAG101* was down-regulated in trifoliate roots compared to rough lemon, suggesting that it could contribute to trifoliate roots increased freezing tolerance (Table 2.3, Figure 2.12C).

The Arabidopsis Ethylene Response DNA Binding Factor/Related to ABI3/VP1 (EDF/RAV) subfamily is a group of plant-specific B3 transcription factors. In Arabidopsis, expression of *EDF2/RAV2* was repressed by ABA and overexpression of this gene negatively regulated plant growth and development[115]. Similar results were displayed while overexpressing the soybean homolog *GmRAV*[116]. *GmRAV-OX* lines exhibited slower plant growth rate (dwarfing), reduced root elongation, delayed flowering time, and reduced photosynthetic rate. Additionally, RAV2 was found to influence plant defense response in Arabidopsis[117], specifically it was required by viral suppressors of silencing. Decreased expression of this gene restored the silencing defense mechanism of the plant, allowing the plant to defend itself against plant viruses. *EDF2/RAV2* was down-regulated in trifoliate roots compared to rough lemon, suggesting the trifoliate rootstock has increased plant defense mechanisms, as well as increased growth and development (Table 2.3, Figure 2.12G). Trifoliate rootstock confers better tolerance to several diseases than rough lemon, including Citrus tristeza virus, Phytophthora root rot, and citrus nematodes[118–123]. This gene could be a good candidate for further studies of plant defense and the relation to subsequent signaling pathways induced by pathogens.

Role of miRNAs in rootstock-scion interactions

Small RNA-seq reads that did not match to any known plant miRNA were used in prediction tools that combine the expression patterns, Dicer cleavage site, and secondary structure of miRNA precursor molecules to more accurately predict novel miRNAs. Several studies have predicted miRNAs using the *Citrus clementina* and *Citrus sinensis* reference genomes for prediction of miRNA precursor molecules[124–128]. Using recently available SNP variant calls from whole genome sequencing information of

Poncirus trifoliata and *Citrus jambhiri*, we created 'pseudo' reference genomes for these varieties. These were created by building a consensus sequence based off the *Citrus clementina* reference genome and replacing any of the newly acquired SNP variant data for each respective genotype. By utilizing this method, nine novel miRNAs were discovered using the trifoliate pseudo-reference genome and three were discovered using the rough lemon pseudo-reference genome. The increased number of novel miRNAs in trifoliate is likely due to the fact that it is more divergent from clementine than rough lemon, resulting in more polymorphisms that were only detected in the trifoliate pseudo-reference genome.

Typically, an increase in miRNA expression will lead to the downregulation of its mRNA target, while a decrease in miRNA activity will lead to upregulation of its target. In plants, miRNAs generally regulate target gene expression through cleavage, and subsequent degradation of the target mRNA[42,129]. An integrated analysis of miRNA and mRNA expression profiles can help identify miRNA-mRNA interaction pairs involved in regulating specific biological processes. By using this approach, we identified several important regulatory miRNAs potentially involved in control of root system architecture and response to abiotic and biotic stressors. Interestingly, some of these miRNAs had multiple mRNA targets, suggesting there is a complicated regulatory network in citrus rootstocks and some miRNAs may control multiple aspects of root growth.

Three of the miRNAs chosen for validation were predicted to target two separate mRNAs. Csi-miR3465 targeted *CYCD4;1* and *PP2A*; Csi-miR391a.3 targeted *XTR4* and

ARABIDILLO-1; and Csi-miR394b targeted *SAG101* and *HMA5*. All six miRNA genes and the nine mRNAs they targeted were detected by qRT-PCR. Pearson correlation coefficient value between the relative expression level detected by qRT-PCR and by RNA-sequencing was highly significant with r = 0.83. Of the nine interaction pairs, seven followed expected fold changes between timepoints (for example a miRNA showing an increase in fold change from July (Time 1) to January (Time 4) should correlate with a decreased fold change in the target gene). Therefore, it is likely that these eight target mRNAs are being regulated to some extent by their respective miRNA. Only two pairs (Csi-miR394b – SAG101 and FDTn01 – SWEETIE) do not follow the expected inverse relationship between timepoints, which has also been observed in previous reports[50,130]. There have also been reports of target genes having a negative or positive feedback regulation on their respective miRNA, which could be another explanation for the inconsistent correlations seen in this study[131,132].

According to these results, we speculate that miRNAs could regulate the expression of diverse genes and that altered expression of miRNAs could play a crucial role in genotype-specific improvement of grafted citrus. The discovery of miRNAs involved in control of root system architecture and response to stress enable further studies of genotype effects on fruit quality. Evaluations of these miRNAs could identify markers for breeding of improved rootstocks in the future.

Conclusion

To the best of our knowledge, this study is the first comparative study to simultaneously characterize the transcriptome and miRNome of diverse citrus rootstocks. A large number of mRNAs and miRNAs were expressed in citrus roots and are annotated as involved in a range of biological process and pathways. The majority of the differences seen between genotypes give rise to potential changes in root system architecture, most likely as a result of the varying extent to which they can respond to abiotic and biotic stress. Taken together, trifoliate rootstock appears to be more adapted to stressors and can respond more appropriately than rough lemon.

Although the gene-to-phenotype relationship of these genes could not be assessed in this study, this lays the groundwork for functional analyses in the future that should provide insights into the molecular mechanisms underlying improved fruit quality of citrus grafts. The set of miRNA and gene expression patterns obtained from this study provides a sizeable list of candidate genes for functional analysis, along with a better overview of the mechanisms of complex metabolic and regulatory systems of grafted citrus. Functional experiments aiming at understanding which gene(s) play key roles in rootstock effects on fruit quality can be designed based of this study. These genes or miRNAs may be useful for developing improved rootstock varieties in citrus breeding.

References

1. Wareing, P. F. Problems of juvenility and flowering in trees. *Journal of the Linnean Society of London, Botany* **56**, 282–289 (1959).

2. Bitters, W. P. Citrus rootstocks: their characters and reactions (an unpublished manuscript) ca. 1986. 236 (1986).

3. Martínez-Cuenca, M.-R., Primo-Capella, A. & Forner-Giner, M. A. Influence of rootstock on citrus tree growth: effects on photosynthesis and carbohydrate distribution, plant size, yield, fruit quality, and dwarfing genotypes. *Plant Growth* (2016). doi:10.5772/64825

4. Simpson, C. R. *et al.* Growth response of grafted and ungrafted citrus trees to saline irrigation. *Scientia Horticulturae* **169**, 199–205 (2014).

5. Castle, W. S. Rootstock as a fruit quality factor in citrus and deciduous tree crops. *New Zealand Journal of Crop and Horticultural Science* **23**, 383–394 (1995).

6. Zhang, X., Breksa, A. P., Mishchuk, D. O. & Slupsky, C. M. Elevation, rootstock, and soil depth affect the nutritional quality of mandarin oranges. *J. Agric. Food Chem.* **59**, 2672–2679 (2011).

7. Checker, V. G., Saeed, B. & Khurana, P. Analysis of expressed sequence tags from mulberry (Morus indica) roots and implications for comparative transcriptomics and marker identification. *Tree Genetics & Genomes* **8**, 1437–1450 (2012).

8. Cohen, D. *et al.* Comparative transcriptomics of drought responses in Populus: a meta-analysis of genome-wide expression profiling in mature leaves and root apices across two genotypes. *BMC Genomics* **11**, 630 (2010).

9. Jansen, L. *et al.* Comparative transcriptomics as a tool for the identification of root branching genes in maize. *Plant Biotechnology Journal* **11**, 1092–1102 (2013).

10. Ntatsi, G. *et al.* Rootstock sub-optimal temperature tolerance determines transcriptomic responses after long-term root cooling in rootstocks and scions of grafted tomato plants. *Front. Plant Sci.* **8**, (2017).

11. Weber, M., Harada, E., Vess, C., Roepenack-Lahaye, E. v & Clemens, S. Comparative microarray analysis of Arabidopsis thaliana and Arabidopsis halleri roots identifies nicotianamine synthase, a ZIP transporter and other genes as potential metal hyperaccumulation factors. *The Plant Journal* **37**, 269–281 (2004).

12. Gao, X., Zhao, S., Xu, Q.-L. & Xiao, J.-X. Transcriptome responses of grafted Citrus sinensis plants to inoculation with the arbuscular mycorrhizal fungus Glomus versiforme. *Trees* **30**, 1073–1082 (2016).

13. Huang, Y., Si, Y. & Dane, F. Impact of grafting on cold responsive gene expression in Satsuma mandarin (Citrus unshiu). *Euphytica* **177**, 25–32 (2011).

14. Liu, X. *et al.* Transcriptome changes associated with boron deficiency in leaves of two citrus scion-rootstock combinations. *Front. Plant Sci.* **8**, (2017).

15. Liu, X.-Y., Li, J., Liu, M.-M., Yao, Q. & Chen, J.-Z. Transcriptome profiling to understand the effect of citrus rootstocks on the growth of 'Shatangju' mandarin. *PLOS ONE* **12**, e0169897 (2017).

16. An, J. *et al.* Comparative transcriptome analysis of Poncirus trifoliata identifies a core set of genes involved in arbuscular mycorrhizal symbiosis. *J Exp Bot* **69**, 5255–5264 (2018).

17. Zhang, Y., Barthe, G., Grosser, J. W. & Wang, N. Transcriptome analysis of root response to citrus blight based on the newly assembled Swingle citrumelo draft genome. *BMC Genomics* **17**, 485 (2016).

18. Zhong, Y. *et al.* Comparative transcriptome and iTRAQ proteome analyses of citrus root responses to Candidatus liberibacter asiaticus infection. *PLOS ONE* **10**, e0126973 (2015).

19. Terol, J., Tadeo, F., Ventimilla, D. & Talon, M. An RNA-Seq-based reference transcriptome for Citrus. *Plant Biotechnology Journal* **14**, 938–950 (2016).

20. Hodge, A., Berta, G., Doussan, C., Merchan, F. & Crespi, M. Plant root growth, architecture and function. *Plant Soil* **321**, 153–187 (2009).

21. O'Toole, J. C. & Bland, W. L. Genotypic variation in crop plant root systems. in *Advances in Agronomy* (ed. Brady, N. C.) **41**, 91–145 (Academic Press, 1987).

22. Castle, W. S. A career perspective on citrus rootstocks, their development, and commercialization. *HortScience* **45**, 11–15 (2010).

23. Al-Jaleel, A. & Zekri, M. Effects of rootstocks on yield and fruit quality of 'Parent Washington Navel' trees. *Proceedings of the Florida State Horticultural Society* **116**, 270–275 (2003).

24. Cantuarias-Avilés, T., Mourão Filho, F. de A. A., Stuchi, E. S., Silva, S. R. da & Espinoza-Núñez, E. Tree performance and fruit yield and quality of 'Okitsu' Satsuma mandarin grafted on 12 rootstocks. *Scientia Horticulturae* **123**, 318–322 (2010).

25. Continella, A. *et al.* Influence of different rootstocks on yield precocity and fruit quality of 'Tarocco Scirè' pigmented sweet orange. *Scientia Horticulturae* **230**, 62–67 (2018).

26. Legua, P., Bellver, R., Forner, J. & Forner-Giner, M. A. Plant growth, yield and fruit quality of 'Lane Late' navel orange on four citrus rootstocks. *Spanish Journal of Agricultural Research* **9**, 271–279 (2011).

27. Louzada, E. S. *et al.* Eight new somatic hybrid citrus rootstocks with potential for improved disease resistance. *HortScience* **27**, 1033–1036 (1992).

28. Martínez-Alcántara, B. *et al.* Relationship between hydraulic conductance and citrus dwarfing by the Flying Dragon rootstock (Poncirus trifoliata L. Raft var. monstruosa). *Trees* **27**, 629–638 (2013).

29. Roose, M. L., Cole, D. A., Atkin, D. & Kupper, R. S. Yield and tree size of four citrus cultivars on 21 rootstocks in California. *Journal of the American Society for Horticultural Science* (1989).

30. Rouse, R. E. Citrus fruit quality and yield of six Valencia clones on 16 rootstocks in the Immokalee foundation grove. *Proceedings of the Florida State Horticultural Society* **113**, 112–114 (2000).

31. Zekri, M. & Parsons, L. R. Salinity tolerance of citrus rootstocks: effects of salt on root and leaf mineral concentrations. *Plant Soil* **147**, 171–181 (1992).

32. Lynch, J. Root architecture and plant productivity. *Plant Physiol.* **109**, 7–13 (1995).

33. Lavenus, J. *et al.* Lateral root development in Arabidopsis: fifty shades of auxin. *Trends in Plant Science* **18**, 450–458 (2013).

34. Malamy, J. E. Intrinsic and environmental response pathways that regulate root system architecture. *Plant, Cell & Environment* **28**, 67–77 (2005).

35. Malamy, J. E. & Ryan, K. S. Environmental regulation of lateral root initiation in Arabidopsis. *Plant Physiology* **127**, 899–909 (2001).

36. Flores, F. B. *et al.* The effectiveness of grafting to improve tomato fruit quality. *Scientia Horticulturae* **125**, 211–217 (2010).

37. Rouphael, Y., Cardarelli, M., Colla, G. & Rea, E. Yield, mineral composition, water relations, and water use efficiency of grafted mini-watermelon plants under deficit irrigation. *HortScience* **43**, 730–736 (2008).

38. Hochholdinger, F., Park, W. J., Sauer, M. & Woll, K. From weeds to crops: genetic analysis of root development in cereals. *Trends in Plant Science* **9**, 42–48 (2004).

39. Inukai, Y. *et al.* Crown rootless1, which is essential for crown root formation in rice, Is a target of an AUXIN RESPONSE FACTOR in auxin signaling. *The Plant Cell* **17**, 1387–1396 (2005).

40. Okushima, Y., Fukaki, H., Onoda, M., Theologis, A. & Tasaka, M. ARF7 and ARF19 regulate lateral root formation via direct activation of LBD/ASL genes in Arabidopsis. *The Plant Cell* **19**, 118–130 (2007).

41. Licciardello, C. *et al.* A transcriptomic analysis of sensitive and tolerant citrus rootstocks under natural iron deficiency conditions. *Journal of the American Society for Horticultural Science* **138**, 487–498 (2013).

42. Bartel, D. P. MicroRNAs: genomics, biogenesis, mechanism, and function. *Cell* **116**, 281–297 (2004).

43. Brousse, C. *et al.* A non-canonical plant microRNA target site. *Nucleic Acids Res.* **42**, 5270–5279 (2014).

44. Reinhart, B. J., Weinstein, E. G., Rhoades, M. W., Bartel, B. & Bartel, D. P. MicroRNAs in plants. *Genes Dev.* **16**, 1616–1626 (2002).

45. Voinnet, O. Origin, biogenesis, and activity of plant microRNAs. *Cell* **136**, 669–687 (2009).

46. Sun, G. MicroRNAs and their diverse functions in plants. *Plant Mol Biol* **80**, 17–36 (2012).

47. Couzigou, J.-M. & Combier, J.-P. Plant microRNAs: key regulators of root architecture and biotic interactions. *New Phytologist* **212**, 22–35 (2016).

48. Huang, J.-H. *et al.* Illumina microRNA profiles reveal the involvement of miR397a in Citrus adaptation to long-term boron toxicity via modulating secondary cell-wall biosynthesis. *Scientific Reports* **6**, (2016).

49. Wu, J., Fu, L. & Yi, H. Genome-wide identification of the transcription factors involved in citrus fruit ripening from the transcriptomes of a late-ripening sweet orange mutant and its wild type. *PLOS ONE* **11**, e0154330 (2016).

50. Xie, R. *et al.* Combined analysis of mRNA and miRNA identifies dehydration and salinity responsive key molecular players in citrus roots. *Scientific Reports* **7**, (2017).

51. Zhong, Y. *et al.* Comparison of micro RNA (miRNA) profiles and some miRNA target gene expression levels in roots of non-infected and Huanglongbing-infected tangerine (Citrus reticulata Blanco cv.'Sanhu') trees. *Journal of Citrus Pathology* **1**, (2014).

52. Backman, T. W. H. & Girke, T. systemPipeR: NGS workflow and report generation environment. *BMC Bioinformatics* **17**, 388 (2016).

53. Langmead, B. & Salzberg, S. L. Fast gapped-read alignment with Bowtie 2. *Nature Methods* **9**, 357–359 (2012).

54. Kim, D., Langmead, B. & Salzberg, S. L. HISAT: a fast spliced aligner with low memory requirements. *Nature Methods* **12**, 357–360 (2015).

55. Zhang, Z. *et al.* PMRD: plant microRNA database. *Nucleic Acids Res* **38**, D806–D813 (2010).

56. Love, M. I., Huber, W. & Anders, S. Moderated estimation of fold change and dispersion for RNA-seq data with DESeq2. *Genome Biol* **15**, (2014).

57. Axtell, M. J. ShortStack: comprehensive annotation and quantification of small RNA genes. *RNA* **19**, 740–751 (2013).

58. Evers, M., Huttner, M., Dueck, A., Meister, G. & Engelmann, J. C. miRA: adaptable novel miRNA identification in plants using small RNA sequencing data. *BMC Bioinformatics* **16**, 370 (2015).

59. Lei, J. & Sun, Y. miR-PREFeR: an accurate, fast and easy-to-use plant miRNA prediction tool using small RNA-Seq data. *Bioinformatics* **30**, 2837–2839 (2014).

60. Leinonen, R., Sugawara, H. & Shumway, M. The Sequence Read Archive. *Nucleic Acids Res* **39**, D19–D21 (2011).

61. Fang, D. Q., Roose, M. L., Krueger, R. R. & Federici, C. T. Fingerprinting trifoliate orange germ plasm accessions with isozymes, RFLPs, and inter-simple sequence repeat markers. *Theor Appl Genet* **95**, 211–219 (1997).

62. Gu, Z., Eils, R. & Schlesner, M. Complex heatmaps reveal patterns and correlations in multidimensional genomic data. *Bioinformatics* **32**, 2847–2849 (2016).

63. Wickham, H. ggplot2. *Wiley Interdisciplinary Reviews: Computational Statistics* **3**, 180–185 (2011).

64. Heberle, H., Meirelles, G. V., da Silva, F. R., Telles, G. P. & Minghim, R. InteractiVenn: a web-based tool for the analysis of sets through Venn diagrams. *BMC Bioinformatics* **16**, (2015).

65. Jin, J. *et al.* PlantTFDB 4.0: toward a central hub for transcription factors and regulatory interactions in plants. *Nucleic Acids Res* **45**, D1040–D1045 (2017).

66. Xie, C. *et al.* KOBAS 2.0: a web server for annotation and identification of enriched pathways and diseases. *Nucleic Acids Res* **39**, W316–W322 (2011).

67. Dai, X., Zhuang, Z. & Zhao, P. X. psRNATarget: a plant small RNA target analysis server (2017 release). *Nucleic Acids Res* **46**, W49–W54 (2018).

68. Owczarzy, R. *et al.* IDT SciTools: a suite for analysis and design of nucleic acid oligomers. *Nucleic Acids Research* **36**, W163–W169 (2008).

69. Andersen, C. L., Jensen, J. L. & Ørntoft, T. F. Normalization of real-time quantitative reverse transcription-PCR data: a model-based variance estimation approach to identify genes suited for normalization, applied to bladder and colon cancer data sets. *Cancer Res* **64**, 5245–5250 (2004).

70. Pfaffl, M. W., Tichopad, A., Prgomet, C. & Neuvians, T. P. Determination of stable housekeeping genes, differentially regulated target genes and sample integrity: BestKeeper – Excel-based tool using pair-wise correlations. *Biotechnology Letters* **26**, 509–515 (2004).

71. Pfaffl, M. W. A new mathematical model for relative quantification in real-time RT–PCR. *Nucleic Acids Res* **29**, e45–e45 (2001).

72. Tadeo, F. R. *et al.* Molecular Physiology of development and quality of citrus. in *Advances in Botanical Research* **47**, 147–223 (Academic Press, 2008).

73. Qiu, D. *et al.* High throughput sequencing technology reveals that the taxoid elicitor methyl jasmonate regulates microRNA expression in Chinese yew (Taxus chinensis). *Gene* **436**, 37–44 (2009).

74. Morin, R. D. *et al.* Comparative analysis of the small RNA transcriptomes of Pinus contorta and Oryza sativa. *Genome Res.* **18**, 571–584 (2008).

75. Meyers, B. C. *et al.* Criteria for annotation of plant microRNAs. *The Plant Cell* **20**, 3186–3190 (2008).

76. Ferguson, J. J. & Chaparro, J. Dwarfing and freeze hardiness potential of trifoliate *orange rootstocks*. (University of Florida Cooperative Extension Service, Institute of Food and Agricultural Sciences, EDIS, 2004).

77. Wu, G. A. *et al.* Genomics of the origin and evolution of Citrus. *Nature* **554**, 311–316 (2018).

78. Castle, W. S. Citrus root systems: their structure, function, growth, and relationship to tree performance. *Proceedings of the International Society of Citriculture 1978.* 62–69 (1980).

79. De Smet, I. *et al.* Auxin-dependent regulation of lateral root positioning in the basal meristem of Arabidopsis. *Development* **134**, 681–690 (2007).

80. Malamy, J. E. & Benfey, P. N. Down and out in Arabidopsis: the formation of lateral roots. *Trends in Plant Science* **2**, 390–396 (1997).

81. Boniotti, M. B. & Gutierrez, C. A cell-cycle-regulated kinase activity phosphorylates plant retinoblastoma protein and contains, in Arabidopsis, a CDKA/cyclin D complex. *The Plant Journal* **28**, 341–350 (2001).

82. Meijer, M. & Murray, J. A. H. The role and regulation of D-type cyclins in the plant cell cycle. *Plant Mol Biol* **43**, 621–633 (2000).

83. Soni, R., Carmichael, J. P., Shah, Z. H. & Murray, J. A. A family of cyclin D homologs from plants differentially controlled by growth regulators and containing the conserved retinoblastoma protein interaction motif. *The Plant Cell* **7**, 85–103 (1995).

84. Nieuwland, J. *et al.* The D-type cyclin CYCD4;1 modulates lateral root density in Arabidopsis by affecting the basal meristem region. *PNAS* **106**, 22528–22533 (2009).

85. Coates, J. C., Laplaze, L. & Haseloff, J. Armadillo-related proteins promote lateral root development in Arabidopsis. *PNAS* **103**, 1621–1626 (2006).

86. Mu, C. *et al.* F-box protein Arabidillo-1 promotes lateral root development by depressing the functioning of GA3 in Arabidopsis. *J. Plant Biol.* **53**, 374–380 (2010).

87. Gou, J. *et al.* Gibberellins regulate lateral root formation in Populus through interactions with auxin and other Hormones. *Plant Cell* **22**, 623–639 (2010).

88. Chávez-Avilés, M. N., Andrade-Pérez, C. L. & Reyes de la Cruz, H. PP2A mediates lateral root development under NaCl-induced osmotic stress throughout auxin redistribution in Arabidopsis thaliana. *Plant Soil* **368**, 591–602 (2013).

89. Liu, D., Li, A., Mao, X. & Jing, R. Cloning and characterization of TaPP2AbB-α, a member of the PP2A regulatory subunit in wheat. *PLoS One* **9**, (2014).

90. Jackson, L. E. *Ecology in Agriculture*. (Academic Press, 1997).

91. Neves, C. S. V. J. *et al.* Root distribution of rootstocks for 'Tahiti' lime. *Scientia Agricola* **61**, 94–99 (2004).

92. Eissenstat, D. M. On the relationship between specific root length and the rate of root proliferation: a field study using citrus rootstocks. *New Phytologist* **118**, 63–68 (1991).

93. Burkhead, J. L., Reynolds, K. A. G., Abdel-Ghany, S. E., Cohu, C. M. & Pilon, M. Copper homeostasis. *New Phytologist* **182**, 799–816 (2009).

94. Andrés-Colás, N. *et al.* The Arabidopsis heavy metal P-type ATPase HMA5 interacts with metallochaperones and functions in copper detoxification of roots. *The Plant Journal* **45**, 225–236 (2006).

95. Migocka, M., Posyniak, E., Maciaszczyk-Dziubinska, E., Papierniak, A. & Kosieradzaka, A. Functional and biochemical characterization of cucumber genes encoding two copper ATPases CsHMA5.1 and CsHMA5.2. *Journal of Biological Chemistry* **290**, 15717–15729 (2015).

96. Veyres, N., Aono, M., Sangwan-Norreel, B. S. & Sangwan, R. S. Has Arabidopsis SWEETIE protein a role in sugar flux and utilization? *Plant Signal Behav* **3**, 722–725 (2008).

97. Veyres, N. *et al.* The Arabidopsis sweetie mutant is affected in carbohydrate metabolism and defective in the control of growth, development and senescence. *The Plant Journal* **55**, 665–686 (2008).

98. Gaudillère, J.-P., Moing, A. & Carbonne, F. Vigour and non-structural carbohydrates in young prune trees. *Scientia Horticulturae* **51**, 197–211 (1992).

99. Kubota, N., Kohno, A. & Shimamura, K. Translocation and distribution of 13C-photosynthates in 'Sanyo Suimitsu' peach trees as affected by different rootstocks. *J. Japan. Soc. Hort. Sci.* **59**, 319–324 (1990).

100. Olmstead, M. A., Lang, N. S. & Lang, G. A. Carbohydrate profiles in the graft union of young sweet cherry trees grown on dwarfing and vigorous rootstocks. *Scientia Horticulturae* **124**, 78–82 (2010).

101. Mahajan, S. & Tuteja, N. Cold, salinity and drought stresses: An overview. *Archives of Biochemistry and Biophysics* **444**, 139–158 (2005).

102. Xiong, L., Lee, H., Ishitani, M. & Zhu, J.-K. Regulation of osmotic stress-responsive gene expression by the LOS6/ABA1 locus in Arabidopsis. *J. Biol. Chem.* **277**, 8588–8596 (2002).

103. Knight, H., Brandt, S. & Knight, M. R. A history of stress alters drought calcium signalling pathways in Arabidopsis. *The Plant Journal* **16**, 681–687 (1998).

104. Yadav, S. K. Cold stress tolerance mechanisms in plants. A review. *Agronomy for Sustainable Development* **30**, (2010).

105. Sánchez-Barrena, M. J., Martínez-Ripoll, M., Zhu, J.-K. & Albert, A. The structure of the Arabidopsis thaliana SOS3: molecular mechanism of sensing calcium for salt stress response. *Journal of Molecular Biology* **345**, 1253–1264 (2005).

106. Mortimer, J. C. *et al.* Annexins: multifunctional components of growth and adaptation. *J Exp Bot* **59**, 533–544 (2008).

107. Eklöf, J. M. & Brumer, H. The XTH gene family: an update on enzyme structure, function, and phylogeny in xyloglucan remodeling. *Plant Physiology* **153**, 456–466 (2010).

108. Sampedro, J. & Cosgrove, D. J. The expansin superfamily. *Genome Biology* **6**, 242 (2005).

109. Le Gall, H. *et al.* Cell wall metabolism in response to abiotic stress. *Plants* **4**, 112–166 (2015).

110. Shi, H. *et al.* AtHAP5A modulates freezing stress resistance in Arabidopsis through binding to CCAAT motif of AtXTH21. *New Phytologist* **203**, 554–567 (2014).

111. Dong, J., Jiang, Y., Chen, R., Xu, Z. & Gao, X. Isolation of a novel xyloglucan endotransglucosylase (OsXET9) gene from rice and analysis of the response of this gene to abiotic stresses. *African Journal of Biotechnology* **10**, 17424-17434–17434 (2011).

112. Ko, J.-H., Prassinos, C., Keathley, D., Han, K.-H. & Li, C. Novel aspects of transcriptional regulation in the winter survival and maintenance mechanism of poplar. *Tree Physiol* **31**, 208–225 (2011).

113. Feys, B. J. *et al.* Arabidopsis senescence-associated gene 101 stabilizes and signals within an enhanced disease susceptibility 1 complex in plant innate immunity. *The Plant Cell* **17**, 2601–2613 (2005).

114. Chen, Q.-F. *et al.* Disruption of the Arabidopsis defense regulator Genes SAG101, EDS1, and PAD4 confers enhanced freezing tolerance. *Mol Plant* **8**, 1536–1549 (2015).

115. Fu, M., Kang, H. K., Son, S.-H., Kim, S.-K. & Nam, K. H. A subset of Arabidopsis RAV transcription factors modulates drought and salt stress responses independent of ABA. *Plant Cell Physiol* **55**, 1892–1904 (2014).

116. Zhao, L., Luo, Q., Yang, C., Han, Y. & Li, W. A RAV-like transcription factor controls photosynthesis and senescence in soybean. *Planta* **227**, 1389–1399 (2008).

117. Endres, M. W. *et al.* Two plant viral suppressors of silencing require the ethylene-inducible host transcription factor RAV2 to block RNA silencing. *PLoS Pathog* **6**, (2010).

118. Deng, Z., Xiao, S., Huang, S. & Gmitter Jr., F. G. Development and characterization of SCAR markers linked to the citrus tristeza virus resistance gene from Poncirus trifoliata. *Genome* **40**, 697–704 (1997).

119. Inserra, R. N., Duncan, L. W., O'Bannon, J. H. & Fuller, S. A. Citrus nematode biotypes and resistant citrus rootstocks in Florida. *University of Florida Cooperative Extension Service, Institute of Food and Agriculture Sciences, EDIS* 5 (1994).

120. Rao, N. N. R. & Prasad, M. B. N. V. Evaluation of strains of Poncirus trifoliata and trifoliate orange hybrids for resistance to Phytophthora root rot. *Scientia Horticulturae* **20**, 85–90 (1983).

121. Rai, M. Refinement of the Citrus tristeza virus resistance gene (Ctv) positional map in Poncirus trifoliata and generation of transgenic grapefruit (Citrus paradisi) plant lines with candidate resistance genes in this region. *Plant Mol. Biol.* **61**, 399–414 (2006).

122. Tuzcu, O. Resistance of citrus rootstocks to *Phytophthora citrophthora* during winter dormancy. *Plant Disease* **68**, 502 (1984).

123. Verdejo-Lucas, S., Sorribas, F. J., Forner, J. B. & Alcaide, A. Screening hybrid citrus rootstocks for resistance to Tylenchulus semipenetrans Cobb. *HortScience* **32**, 1116–1119 (1997).

124. Guo, R. *et al.* Identification of novel and conserved miRNAs in leaves of in vitro grown Citrus reticulata “Lugan” plantlets by Solexa sequencing. *Front Plant Sci* **6**, (2016).

125. Liang, W.-W. *et al.* MicroRNA-mediated responses to long-term magnesium-deficiency in Citrus sinensis roots revealed by Illumina sequencing. *BMC Genomics* **18**, (2017).

126. Song, C. *et al.* Computational identification of citrus microRNAs and target analysis in citrus expressed sequence tags. *Plant Biol (Stuttg)* **12**, 927–934 (2010).

127. Sun, L.-M. *et al.* Identification and comparative profiling of miRNAs in an early flowering mutant of trifoliate orange and its wild type by genome-wide deep sequencing. *PLOS ONE* **7**, e43760 (2012).

128. Zhang, J.-Z. *et al.* Identification of miRNAs and their target genes using deep sequencing and degradome analysis in trifoliate orange [Poncirus trifoliate (L.) Raf]. *Mol Biotechnol* **51**, 44–57 (2012).

129. Rhoades, M. W. *et al.* Prediction of plant microRNA targets. *Cell* **110**, 513–520 (2002).

130. Zheng, C. *et al.* Integrated RNA-Seq and sRNA-seq analysis identifies chilling and freezing responsive key molecular players and pathways in tea plant (Camellia sinensis). *PLOS ONE* **10**, e0125031 (2015).

131. Cho, J.-H., Dimri, M. & Dimri, G. P. MicroRNA-31 is a transcriptional target of histone deacetylase inhibitors and a regulator of cellular senescence. *J. Biol. Chem.* **290**, 10555–10567 (2015).

132. Okada, N. *et al.* A positive feedback between p53 and miR-34 miRNAs mediates tumor suppression. *Genes Dev.* **28**, 438–450 (2014).

Supplemental Material

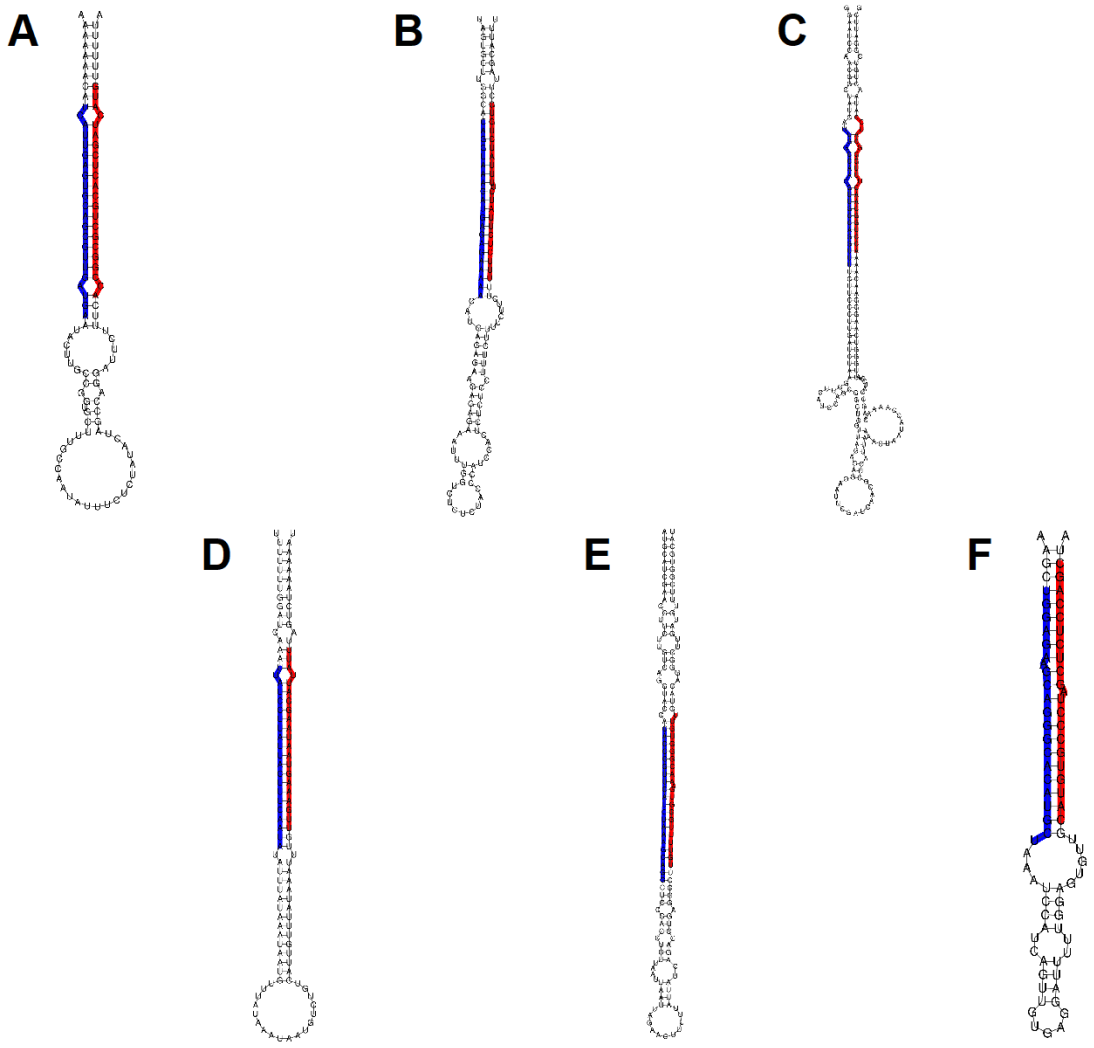

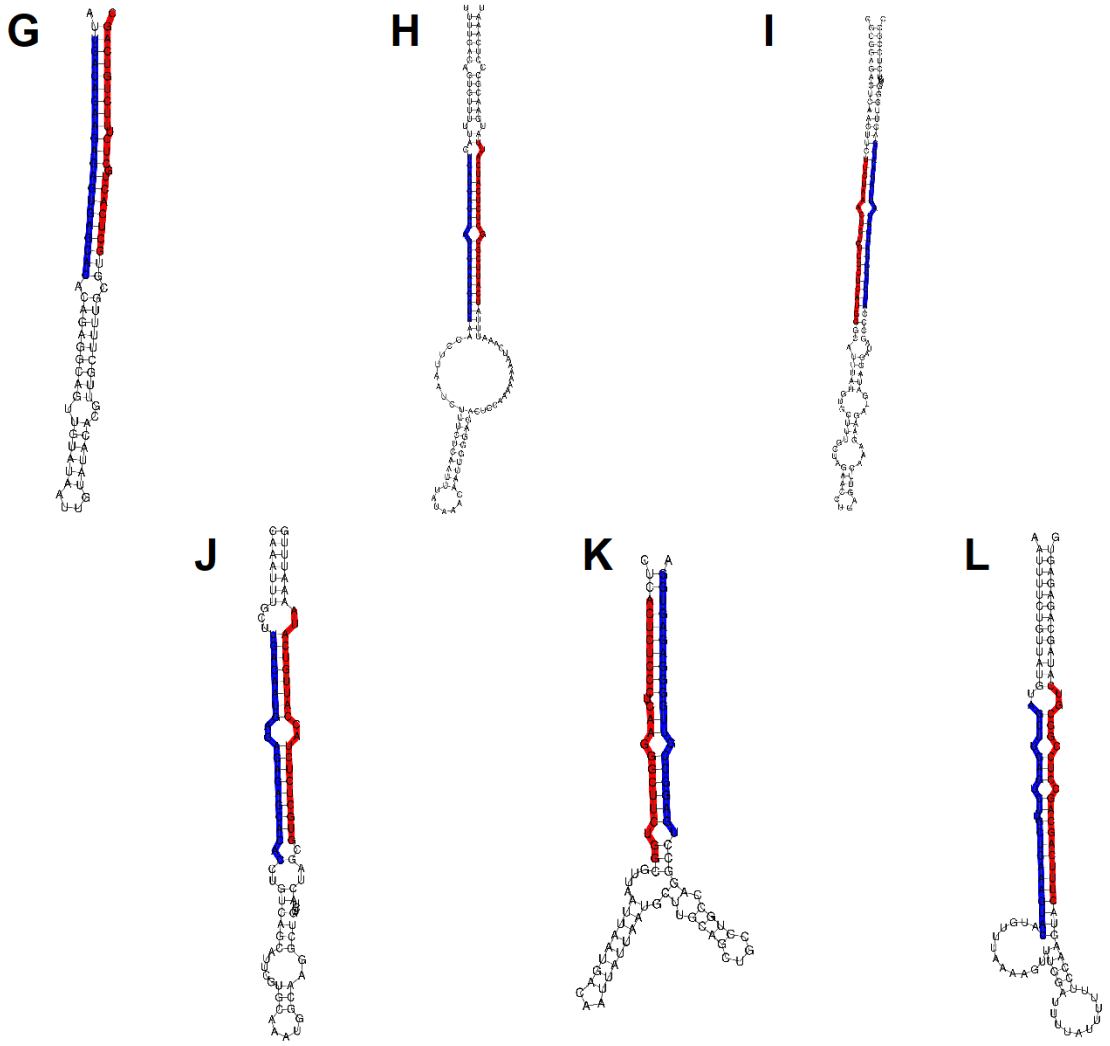

Supplemental Figure 2.1. Stem-loop precursor structures of novel miRNAs observed in citrus rootstocks predicted from Poncirus trifoliata (FDT) and Citrus jambhiri (JAM) 'pseudo' reference genomes. The mature miRNA sequences are highlighted in red and the miRNA star sequences are highlighted in blue (A) FDT_n01; (B) FDT_n02; (C) FDT_n03; (D) FDT_n04; (E) FDT_n05; (F) FDT_n06; (G) FDT_n07; (H) FDT_n08; (I) FDT_n09; (J) JAM_n01; (K) JAM_n02; (L) JAM_n03

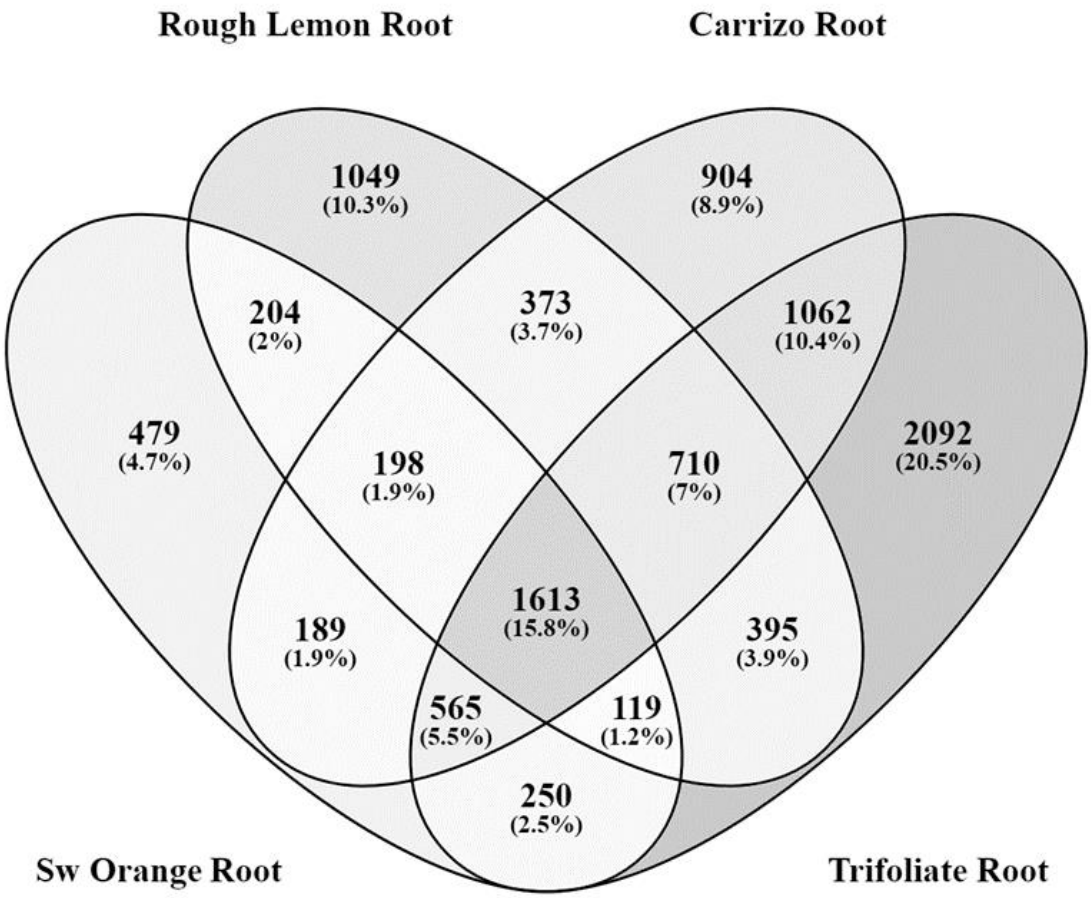

Supplemental Figure 2.2. Venn diagram of overlapping DEGs in various rootstocks over the course of the growing season. Genes were compared at time point 2, 3, and 4 to time point 1 for each rootstock and unique genes were used as one dataset in the diagram.

Supplemental Table 2.1. The gene-specific real-time qPCR primers for miRNAs and their targets

Name	Primer sequence (5’ -> 3’)	Gene ID
EDF2 F	TTGGAGGTTTAGGTACTCCTACT	Ciclev10031846m.g
EDF2 R	GTCACCGGCTTTCAAATTCTTC	
XTR4 F	GTACAATCACGGGTTCTTTAGCG	Ciclev10001649m.g
XTR4 R	GGAACACGTCTCCATTTGATGTATAG	
ADIL F	AGGTGTGCAGGCACTTATTC	Ciclev10004368m.g
ADIL R	CAATGTCCTCCATTCTCCCATC	
ANNAT4 F	TCATATTTCAGCCGGGTATTGG	Ciclev10004368m.g
ANNAT4 R	GTCGTCACTGATCGCTCTTATG	
SWEETIE F	AGGCACAGGTTCAACCAAA	Ciclev10011943m.g
SWEETIE R	TGCTCTAGTGAACGGCAAAG	
HMA5 F	GCAAGCGAAGTTGGAATTGAA	Ciclev10023463m.g
HMA5 R	CGGTATATCCTGAAGCCTGTAAC	
PP2A F	CCATTACCAGGTGGCTGAA	Ciclev10007952m.g
PP2A R	GCTGGGAAGACAAGAGGAATAA	
CYCD4 F	CTATTGGCTGTGGCATGTTTG	Ciclev10001581m.g
CYCD4 R	CTTCGATTGTCCCACCTGTAG	
SAG101 F	GTGAAGCGTCTCATGTCTACC	Ciclev10011372m.g
SAG101 R	ACCGCTTTGCTGTCTTCTATTA	
EF1A F	GCAATCGCCACACACTTAGA	Ciclev10007529m.g
EF1A R	TATGGCACTTTGCTTTGCAG	
Csi-miR3465	CATCTGTAGATCTAACCAGGCAAA	
Csi-miR391a.3	TTGTCGCCGGAGAGATAGCACC	
Csi-miR394	TTGGCATTCTGTCCACCTCC	

Csi-miR390a	CGCTATCCATCCTGAGTTTCA	
Csi-miR2928	CAATGAAGACGACTGTTTTGAAA	
FDT_n01	GCTCACTGCTCTTTCTGTCAGC	
Universal miRNA reverse primer	mRQ 3' Primer (Takara Bio)	

*F and R denote forward and reverse primers, respectively

Supplemental Table 2.2. Differentially expressed genes in trifoliate orange compared to rough lemon rootstocks that are potentially involved in fruit quality

Gene ID	Log_2 Fold Change at each timepoint				Best hit Arabidopsis locus	Arabidopsis gene name	Arabidopsis annotation
	TF1R-RL1R	TF2R-RL2R	TF3R-RL3R	TF4R-RL4R			
Ciclev10000220m.g	1.695	-0.197	-0.987	0.866	AT1G77760.1	GNR1,NIA1,NR1	nitrate reductase 1
Ciclev10000510m.g	-0.983	-0.042	-0.740	-1.556	AT4G37870.1	PCK1,PEPCK	phosphoenolpyruvate carboxykinase 1
Ciclev10000595m.g	0.238	2.438	0.299	-0.061	AT1G76550.1		Phosphofructokinase family protein
Ciclev10000603m.g	0.484	1.286	0.376	0.137	AT4G24620.1	PGI,PGI1	phosphoglucose isomerase 1
Ciclev10000722m.g	-0.033	1.375	0.021	-0.009	AT5G42740.1		Sugar isomerase (SIS) family protein
Ciclev10000848m.g	-8.685	-2.583	-7.302	-7.714	AT2G40890.1	CYP98A3	cytochrome P450, family 98, subfamily A, polypeptide 3
Ciclev10000939m.g	3.485	2.957	1.588	2.150	AT1G47840.1	HXK3	hexokinase 3
Ciclev10000949m.g	-1.406	-0.518	-0.951	-0.983	AT1G44170.1	ALDH3H1,ALDH4	aldehyde dehydrogenase 3H1

Ciclev10000981m.g	-0.655	0.894	-2.694	0.990	AT5G49630.1	AAP6	amino acid permease 6
Ciclev10001084m.g	0.831	-0.128	1.086	0.649	AT1G34430.1	EMB3003	2-oxoacid dehydrogenases acyltransferase family protein
Ciclev10001399m.g	0.284	0.018	2.250	1.176	AT1G22440.1		Zinc-binding alcohol dehydrogenase family protein
Ciclev10001405m.g	-2.220	2.417	-4.287	-1.379	AT5G13930.1	ATCHS,CHS,TT4	Chalcone and stilbene synthase family protein
Ciclev10001413m.g	4.211	7.476	-0.109	1.044	AT5G13930.1	ATCHS,CHS,TT4	Chalcone and stilbene synthase family protein
Ciclev10001416m.g	0.928	2.518	-2.724	0.131	AT4G34160.1	CYCD3,CYCD3;1	CYCLIN D3;1
Ciclev10001500m.g	1.572	5.177	-1.114	-0.639	AT1G77120.1	ADH,ADH1,ATADH,ATADH1	alcohol dehydrogenase 1
Ciclev10001708m.g	1.227	0.197	2.221	2.174	AT1G22170.1		Phosphoglycerate mutase family protein
Ciclev10001740m.g	-0.006	-0.257	0.706	2.354	AT5G42750.1	BKI1	BRI1 kinase inhibitor 1
Ciclev10001754m.g	0.563	0.302	1.444	0.922	AT1G78290.2	SNRK2-8,SNRK2.8,SRK2C	Protein kinase superfamily protein
Ciclev10001873m.g	-0.971	1.647	-1.323	-0.601	AT4G33580.1	ATBCA5,BCA5	beta carbonic anhydrase 5
Ciclev10001905m.g	4.580	8.300	-5.839	1.704	AT5G13930.1	ATCHS,CHS,TT4	Chalcone and stilbene synthase family protein
Ciclev10002029m.g	-1.285	-1.168	1.753	0.693	AT5G44080.1		Basic-leucine zipper (bZIP) transcription factor family protein
Ciclev10002068m.g	-1.666	0.414	0.227	0.689	AT4G09460.1	AtMYB6,MYB6	myb domain protein 6
Ciclev10002312m.g	0.663	1.284	-1.064	0.424	AT3G57040.1	ARR9,ATRR4	response regulator 9

Ciclev10002415m.g	-5.060	-4.194	-3.921	-2.928	AT5G48930.1	HCT	hydroxycinnamoyl-CoA shikimate/quinate hydroxycinnamoyl transferase
Ciclev10002417m.g	0.414	-0.194	-1.058	-0.687	AT4G24210.1	SLY1	F-box family protein
Ciclev10002569m.g	-0.215	0.988	-4.356	-3.650	AT5G43700.1	ATAUX2-11,IAA4	AUX/IAA transcriptional regulator family protein
Ciclev10002731m.g	1.009	-0.012	0.521	0.339	AT1G75390.1	AtbZIP44,bZIP44	basic leucine-zipper 44
Ciclev10003120m.g	0.794	0.242	1.129	1.299	AT1G49720.1	ABF1	abscisic acid responsive element-binding factor 1
Ciclev10003150m.g	2.100	1.635	-3.118	0.090	AT1G75590.1		SAUR-like auxin-responsive protein family
Ciclev10003227m.g	-0.893	1.109	3.562	4.378	AT1G08080.1	ACA7,ATACA7	alpha carbonic anhydrase 7
Ciclev10003291m.g	-9.593	-0.957	-9.171	-3.088	AT3G55440.1	ATCTIMC,CYTOTPI,TPI	triosephosphate isomerase
Ciclev10003317m.g	-3.654	-0.454	-4.791	-2.245	AT1G59750.1	ARF1	auxin response factor 1
Ciclev10003634m.g	-9.008	-1.342	-9.391	-8.361	AT1G10470.1	ARR4,ATRR1,IBC7,MEE7	response regulator 4
Ciclev10004010m.g	3.794	0.872	3.263	3.463	AT3G18080.1	BGLU44	B-S glucosidase 44
Ciclev10004052m.g	-0.051	6.795	-0.963	-5.152	AT1G77120.1	ADH,ADH1,ATADH,ATADH1	alcohol dehydrogenase 1
Ciclev10004140m.g	-3.334	-0.568	-2.222	-2.631	AT1G32750.1	GTD1,HAC13,HAF01,HAF1,TAF1	HAC13 protein (HAC13)
Ciclev10004221m.g	-3.742	-1.894	-3.854	-5.804	AT1G04920.1	ATSPS3F,SPS3F	sucrose phosphate synthase 3F
Ciclev10004341m.g	-5.043	-4.048	-3.374	-3.545	AT5G49190.1	ATSUS2,SSA,SUS2	sucrose synthase 2

Ciclev10004385m.g	0.867	1.533	0.352	1.250	AT3G23150.1	ETR2	Signal transduction histidine kinase, hybrid-type, ethylene sensor
Ciclev10004407m.g	-0.701	2.839	-1.669	0.116	AT3G49160.1		pyruvate kinase family protein
Ciclev10004465m.g	0.339	1.493	-2.637	0.718	AT1G12240.1	ATBETAFRUCT4,VAC-INV	Glycosyl hydrolases family 32 protein
Ciclev10004728m.g	-1.344	-0.284	-0.333	0.432	AT3G47420.1	ATPS3,PS3	phosphate starvation-induced gene 3
Ciclev10004777m.g	0.728	0.532	1.068	0.957	AT5G06160.1	ATO	splicing factor-related
Ciclev10004786m.g	0.417	3.849	-4.099	-1.898	AT1G16390.1	3-Oct,ATOCT3	organic cation/carnitine transporter 3
Ciclev10004795m.g	-1.368	-0.142	-2.889	-1.485	AT2G41370.1	BOP2	Ankyrin repeat family protein / BTB/POZ domain-containing protein
Ciclev10004817m.g	2.016	1.349	-1.640	-2.643	AT1G23210.1	AtGH9B6,GH9B6	glycosyl hydrolase 9B6
Ciclev10004965m.g	1.566	0.075	1.238	0.882	AT2G36530.1	ENO2,LOS2	Enolase
Ciclev10005058m.g	0.779	0.551	1.095	0.775	AT1G54340.1	ICDH	isocitrate dehydrogenase
Ciclev10005101m.g	0.429	1.600	0.439	0.189	AT1G79550.2	PGK	phosphoglycerate kinase
Ciclev10005133m.g	-3.052	-0.860	-2.488	-3.588	AT5G13930.1	ATCHS,CHS,TT4	Chalcone and stilbene synthase family protein
Ciclev10005200m.g	-3.802	-1.064	-1.860	-1.701	AT4G26080.1	ABI1,AtABI1	Protein phosphatase 2C family protein
Ciclev10005308m.g	0.373	1.395	-0.308	-0.557	AT5G51830.1		pfkB-like carbohydrate kinase family protein
Ciclev10005318m.g	0.041	1.149	-0.201	0.839	AT1G06330.1		Heavy metal transport/detoxification superfamily protein

Ciclev10005747m.g	-8.784	-2.154	-9.052	-6.829	AT4G16110.1	ARR2,RR2	response regulator 2
Ciclev10005789m.g	-0.178	-1.139	-1.229	-2.807	AT4G14550.1	IAA14,SLR	indole-3-acetic acid inducible 14
Ciclev10006534m.g	0.960	-0.199	1.816	0.900	AT1G50420.1	SCL-3,SCL3	scarecrow-like 3
Ciclev10006768m.g	-2.655	-0.740	-1.787	-1.708	AT1G35910.1		Haloacid dehalogenase-like hydrolase (HAD) superfamily protein
Ciclev10006823m.g	2.224	0.690	2.017	1.560	AT3G26040.1		HXXXD-type acyl-transferase family protein
Ciclev10006902m.g	0.113	-1.569	1.815	1.165	AT3G22830.1	AT-HSFA6B,HSFA6B	heat shock transcription factor A6B
Ciclev10006943m.g	0.289	-0.599	1.426	0.225	AT1G78090.1	ATTPPB,TPPB	trehalose-6-phosphate phosphatase
Ciclev10006986m.g	-1.102	-1.498	-0.753	-0.821	AT1G24430.1		HXXXD-type acyl-transferase family protein
Ciclev10007069m.g	1.365	-0.558	0.214	1.241	AT4G13620.1		Integrase-type DNA-binding superfamily protein
Ciclev10007312m.g	-2.238	-0.742	-1.352	-0.917	AT5G20280.1	ATSPS1F,SPS1F	sucrose phosphate synthase 1F
Ciclev10007338m.g	0.606	1.088	0.172	0.716	AT2G05710.1	ACO3	aconitase 3
Ciclev10007367m.g	-0.154	-0.338	-1.017	-0.462	AT2G24520.1	AHA5,HA5	H(+)-ATPase 5
Ciclev10007368m.g	1.332	0.040	-0.043	0.201	AT4G30190.1	AHA2,HA2,PMA2	H(+)-ATPase 2
Ciclev10007401m.g	-1.516	-0.002	0.048	-0.429	AT3G20440.2	BE1,EMB2729	Alpha amylase family protein
Ciclev10007428m.g	-2.605	-0.575	-0.569	-0.248	AT2G18700.1	ATTPS11,ATTPSB,TPS11	trehalose phosphatase/synthase 11

Ciclev10007708m.g	1.076	0.918	-0.207	0.328	AT2G25490.1	EBF1,FBL6	EIN3-binding F box protein 1
Ciclev10007739m.g	-0.128	1.202	-0.798	0.077	AT2G25490.1	EBF1,FBL6	EIN3-binding F box protein 1
Ciclev10007746m.g	-0.180	-0.393	1.358	1.043	AT5G54510.1	DFL1,GH3.6	Auxin-responsive GH3 family protein
Ciclev10007805m.g	3.011	2.443	-0.600	0.043	AT5G56200.1		C2H2 type zinc finger transcription factor family
Ciclev10007886m.g	0.948	2.595	-0.078	0.361	AT4G26270.1	PFK3	phosphofructokinase 3
Ciclev10007893m.g	1.305	0.371	1.298	1.077	AT4G32650.3	ATKC1,AtLKT 1,KAT3,KC1	potassium channel in Arabidopsis thaliana 3
Ciclev10008010m.g	-0.060	0.264	-1.399	-1.164	AT3G18080.1	BGLU44	B-S glucosidase 44
Ciclev10008012m.g	0.492	0.402	-1.419	0.683	AT5G54570.1	BGLU41	beta glucosidase 41
Ciclev10008037m.g	-0.154	-0.741	-1.146	-1.025	AT4G02050.1	STP7	sugar transporter protein 7
Ciclev10008091m.g	2.286	2.079	2.992	3.811	AT2G24270.4	ALDH11A3	aldehyde dehydrogenase 11A3
Ciclev10008125m.g	0.841	1.503	-2.234	-0.970	AT2G30490.1	ATC4H,C4H, CYP73A5,RE F3	cinnamate-4-hydroxylase
Ciclev10008181m.g	1.669	3.571	-0.361	-0.418	AT4G26270.1	PFK3	phosphofructokinase 3
Ciclev10008310m.g	-0.364	-0.671	-1.336	-1.177	AT5G54630.1		zinc finger protein-related
Ciclev10008366m.g	1.085	-0.062	1.628	1.446	AT5G57660.1	ATCOL5,COL 5	CONSTANS-like 5
Ciclev10008921m.g	0.189	-0.468	1.397	0.070	AT5G56110.1	AtMYB103,AT MYB80,MS18 8,MYB103	myb domain protein 103
Ciclev10008935m.g	-5.630	-1.787	-2.396	-1.235	AT4G32280.1	IAA29	indole-3-acetic acid inducible 29

Ciclev10008965m.g	1.237	0.999	1.511	1.515	AT5G57330.1		Galactose mutarotase-like superfamily protein
Ciclev10009118m.g	-9.045	-0.587	-6.841	-0.124	AT4G25810.1	XTH23,XTR6	xyloglucan endotransglycosylase 6
Ciclev10009158m.g	1.977	0.083	0.590	0.783	AT3G16500.1	IAA26,PAP1	phytochrome-associated protein 1
Ciclev10009172m.g	-1.945	-2.402	-1.963	-1.736	AT4G30270.1	MERI-5,MERI5B,SEN4,XTH24	xyloglucan endotransglucosylase/hydrolase 24
Ciclev10009186m.g	-1.294	0.206	-0.988	-1.012	AT1G67940.1	ATNAP3,AtSTAR1,NAP3	non-intrinsic ABC protein 3
Ciclev10009245m.g	-0.770	-0.054	0.548	1.305	AT1G04250.1	AXR3,IAA17	AUX/IAA transcriptional regulator family protein
Ciclev10010262m.g	2.535	-0.072	2.880	4.160	AT2G26040.1	PYL2,RCAR14	PYR1-like 2
Ciclev10010302m.g	-0.392	-2.133	-3.509	-3.272	AT2G24400.1		SAUR-like auxin-responsive protein family
Ciclev10010343m.g	1.929	2.500	1.616	1.136	AT3G43190.1	ATSUS4,SUS4	sucrose synthase 4
Ciclev10010410m.g	1.751	5.272	-0.892	1.302	AT3G04730.1	IAA16	indoleacetic acid-induced protein 16
Ciclev10010503m.g	0.315	-0.404	-2.670	-0.480	AT1G53270.1		ABC-2 type transporter family protein
Ciclev10010531m.g	-0.780	-1.191	1.260	1.478	AT4G25810.1	XTH23,XTR6	xyloglucan endotransglycosylase 6
Ciclev10010857m.g	-3.005	-1.233	-1.654	-2.259	AT5G48930.1	HCT	hydroxycinnamoyl-CoA shikimate/quinate hydroxycinnamoyl transferase
Ciclev10010858m.g	-1.653	-1.060	-1.535	1.054	AT4G25810.1	XTH23,XTR6	xyloglucan endotransglycosylase 6

Ciclev10010859m.g	-2.184	-0.986	-2.534	-1.863	AT5G57560.1	TCH4,XTH22	Xyloglucan endotransglucosylase /hydrolase family protein
Ciclev10010975m.g	-1.911	-0.668	-1.174	-0.911	AT3G29320.1		Glycosyl transferase, family 35
Ciclev10011060m.g	1.010	0.164	0.798	1.879	AT3G53720.1	ATCHX20,CHX20	cation/H+ exchanger 20
Ciclev10011062m.g	0.947	3.049	-3.084	-0.343	AT1G73370.1	ATSUS6,SUS6	sucrose synthase 6
Ciclev10011317m.g	1.347	4.285	-0.574	0.156	AT4G33070.1		Thiamine pyrophosphate dependent pyruvate decarboxylase family protein
Ciclev10011402m.g	0.600	1.428	0.366	0.514	AT3G08590.2		Phosphoglycerate mutase, 2,3-bisphosphoglycerate-independent
Ciclev10011472m.g	-0.035	1.023	-0.258	-0.184	AT3G52990.1		Pyruvate kinase family protein
Ciclev10011520m.g	1.129	1.083	0.140	1.421	AT2G40890.1	CYP98A3	cytochrome P450, family 98, subfamily A, polypeptide 3
Ciclev10011546m.g	0.776	-0.554	1.265	0.366	AT1G66430.1		pfkB-like carbohydrate kinase family protein
Ciclev10011549m.g	0.209	1.511	-2.713	-1.986	AT1G66250.1		O-Glycosyl hydrolases family 17 protein
Ciclev10011574m.g	0.768	1.739	0.062	1.274	AT3G54030.1		Protein kinase protein with tetratricopeptide repeat domain
Ciclev10011596m.g	0.239	0.584	-1.054	-0.071	AT2G38120.1	AUX1,MAP1,PIR1,WAV5	Transmembrane amino acid transporter family protein
Ciclev10011726m.g	0.519	1.342	-0.306	-0.295	AT2G36530.1	ENO2,LOS2	Enolase

Ciclev10011785m.g	1.213	-0.047	0.128	0.302	AT5G37600.1	ATGLN1;1,ATGSR1,GLN1;1,GSR 1	glutamine synthase clone R1
Ciclev10011989m.g	0.438	-1.144	-0.667	-1.619	AT5G15140.1		Galactose mutarotase-like superfamily protein
Ciclev10012049m.g	0.773	2.204	-0.145	-0.291	AT2G36460.1		Aldolase superfamily protein
Ciclev10012137m.g	-4.994	-0.759	-0.550	-0.503	AT3G17940.1		Galactose mutarotase-like superfamily protein
Ciclev10012205m.g	-1.860	-1.921	-2.412	-3.177	AT3G56850.1	AREB3,DPBF3	ABA-responsive element binding protein 3
Ciclev10012242m.g	-0.519	1.024	-3.362	-1.261	AT2G37770.2		NAD(P)-linked oxidoreductase superfamily protein
Ciclev10012382m.g	-2.373	-0.743	-2.603	-3.428	AT5G37820.1	NIP4;2,NLM5	NOD26-like intrinsic protein 4;2
Ciclev10013167m.g	1.744	0.862	0.055	-0.067	AT3G09870.1		SAUR-like auxin-responsive protein family
Ciclev10013397m.g	2.850	0.423	2.095	1.761	AT1G24430.1		HXXXD-type acyl-transferase family protein
Ciclev10013453m.g	-0.952	-2.384	-0.166	-1.210	AT2G01060.1		myb-like HTH transcriptional regulator family protein
Ciclev10013486m.g	2.899	5.866	-3.383	-0.349	AT3G10040.1		sequence-specific DNA binding transcription factors
Ciclev10013667m.g	-6.357	-0.161	-3.363	-0.675	AT2G14960.1	GH3.1	Auxin-responsive GH3 family protein
Ciclev10013674m.g	1.246	-0.285	0.570	0.138	AT2G36210.1		SAUR-like auxin-responsive protein family
Ciclev10013701m.g	2.731	1.896	2.377	2.129	AT2G36190.1	AtcwINV4,cwINV4	cell wall invertase 4

Ciclev10013718m.g	1.621	-0.753	0.275	-0.193	AT5G60770.1	ATNRT2.4,NRT2.4	nitrate transporter 2.4
Ciclev10013720m.g	1.889	-0.099	1.462	0.830	AT3G52720.1	ACA1,ATACA1,CAH1	alpha carbonic anhydrase 1
Ciclev10013946m.g	6.981	5.325	4.384	2.803	AT5G20810.2		SAUR-like auxin-responsive protein family
Ciclev10014137m.g	-1.112	-0.375	-1.241	-0.525	AT2G01830.2	AHK4,ATCRE1,CRE1,WOL,WOL1	CHASE domain containing histidine kinase protein
Ciclev10014537m.g	0.361	0.847	-1.539	-0.630	AT5G04885.1		Glycosyl hydrolase family protein
Ciclev10014617m.g	0.707	0.651	0.389	1.097	AT3G20770.1	AtEIN3,EIN3	Ethylene insensitive 3 family protein
Ciclev10014703m.g	1.423	3.441	-0.727	-0.288	AT5G54960.1	PDC2	pyruvate decarboxylase-2
Ciclev10014716m.g	0.773	1.109	0.440	0.984	AT3G62980.1	TIR1	F-box/RNI-like superfamily protein
Ciclev10014739m.g	1.082	1.969	-3.172	-1.748	AT3G62980.1	TIR1	F-box/RNI-like superfamily protein
Ciclev10014741m.g	-0.766	-0.507	-1.088	-1.568	AT5G48300.1	ADG1,APS1	ADP glucose pyrophosphorylase 1
Ciclev10014750m.g	-1.387	2.323	-1.302	-0.583	AT1G12000.1		Phosphofructokinase family protein
Ciclev10014770m.g	-2.466	-0.919	-0.853	0.680	AT5G47560.1	ATSDAT,ATTDT,TDT	tonoplast dicarboxylate transporter
Ciclev10014807m.g	-1.037	-0.649	-0.957	-1.146	AT5G46840.1		RNA-binding (RRM/RBD/RNP motifs) family protein
Ciclev10014963m.g	0.729	2.736	-0.295	-0.243	AT5G08570.1		Pyruvate kinase family protein
Ciclev10014983m.g	-3.125	-0.644	-2.952	-3.269	AT3G21690.1		MATE efflux family protein
Ciclev10014994m.g	0.217	2.799	-3.723	-1.388	AT1G70710.1	ATGH9B1,CEL1,GH9B1	glycosyl hydrolase 9B1

Ciclev10015005m.g	1.035	0.869	0.415	1.153	AT5G44180.1		Homeodomain-like transcriptional regulator
Ciclev10015030m.g	0.266	0.148	0.573	1.161	AT5G36890.1	BGLU42	beta glucosidase 42
Ciclev10015129m.g	0.166	2.808	-1.917	-2.580	AT5G14570.1	ATNRT2.7,NRT2.7	high affinity nitrate transporter 2.7
Ciclev10015375m.g	-0.634	0.233	-1.427	-1.113	AT2G30980.1	ASKdZeta,ATSK2-2,ATSK23,BIL1,SKdZeta	SHAGGY-related protein kinase dZeta
Ciclev10015535m.g	-3.892	0.824	-7.246	-5.813	AT5G13930.1	ATCHS,CHS,TT4	Chalcone and stilbene synthase family protein
Ciclev10015856m.g	-0.951	0.756	-2.218	-1.668	AT5G08640.1	ATFLS1,FLS,FLS1	flavonol synthase 1
Ciclev10015874m.g	0.074	-0.416	-4.945	-6.411	AT3G01500.2	ATBCA1,ATSABP3,CA1,SABP3	carbonic anhydrase 1
Ciclev10016114m.g	2.772	0.849	1.017	0.520	AT1G53240.1	mMDH1	Lactate/malate dehydrogenase family protein
Ciclev10016890m.g	0.397	1.528	-0.530	-1.016	AT4G24210.1	SLY1	F-box family protein
Ciclev10017801m.g	6.369	5.031	2.340	4.170	AT4G21760.1	BGLU47	beta-glucosidase 47
Ciclev10017968m.g	0.439	1.003	1.035	-1.557	AT5G54510.1	DFL1,GH3.6	Auxin-responsive GH3 family protein
Ciclev10018086m.g	-0.290	-1.104	-3.536	-1.398	AT4G25000.1	AMY1,ATAMY1	alpha-amylase-like
Ciclev10018889m.g	-0.022	1.344	-0.409	0.228	AT4G02280.1	ATSUS3,SUS3	sucrose synthase 3
Ciclev10018972m.g	1.319	0.143	0.210	0.573	AT3G04580.2	EIN4	Signal transduction histidine kinase, hybrid-type, ethylene sensor
Ciclev10019132m.g	0.483	0.817	-1.548	-0.513	AT2G40940.1	ERS,ERS1	ethylene response sensor 1

Ciclev10019134m.g	-0.010	0.855	0.544	1.716	AT1G12240.1	ATBETAFRUCT4,VAC-INV	Glycosyl hydrolases family 32 protein
Ciclev10019177m.g	-0.279	-0.368	1.017	0.656	AT5G24470.1	APRR5,PRR5	pseudo-response regulator 5
Ciclev10019305m.g	2.296	2.902	-0.989	1.523	AT5G20950.2		Glycosyl hydrolase family protein
Ciclev10019319m.g	-1.624	-0.179	0.835	1.020	AT5G62680.1		Major facilitator superfamily protein
Ciclev10019346m.g	-1.207	-0.211	-0.325	-0.397	AT1G32900.1		UDP-Glycosyltransferase superfamily protein
Ciclev10019349m.g	-0.045	1.351	2.825	2.019	AT1G32900.1		UDP-Glycosyltransferase superfamily protein
Ciclev10019525m.g	-1.273	-0.916	-1.403	-1.109	AT4G00490.1	BAM2,BMY9	beta-amylase 2
Ciclev10019566m.g	0.138	1.835	-0.509	0.416	AT4G17090.1	BAM3,BMY8,CT-BMY	chloroplast beta-amylase
Ciclev10019612m.g	-1.322	-0.253	-0.042	0.213	AT5G24300.1	ATSS1,SSI,SSI1	Glycogen/starch synthases, ADP-glucose type
Ciclev10019637m.g	-1.270	4.160	-2.998	-0.759	AT5G07990.1	CYP75B1,D501,TT7	Cytochrome P450 superfamily protein
Ciclev10019719m.g	-1.868	0.315	-0.884	-0.304	AT1G02850.2	BGLU11	beta glucosidase 11
Ciclev10019749m.g	1.694	0.356	-1.233	-0.136	AT1G32640.1	ATMYC2,JAI1,JIN1,MYC2,RD22BP1,ZBF1	Basic helix-loop-helix (bHLH) DNA-binding family protein
Ciclev10019786m.g	0.982	2.759	-0.770	1.121	AT2G46970.1	PIL1	phytochrome interacting factor 3-like 1
Ciclev10019840m.g	0.967	0.339	0.962	1.177	AT5G46570.1	BSK2	BR-signaling kinase 2
Ciclev10019848m.g	-0.158	0.461	0.108	1.193	AT3G18490.1		Eukaryotic aspartyl protease family protein

Ciclev10019883m.g	0.735	2.410	-3.788	1.034	AT1G71380.1	ATCEL3,ATGH9B3,CEL3	cellulase 3
Ciclev10019918m.g	-0.781	0.690	-3.601	-2.150	AT2G48020.1		Major facilitator superfamily protein
Ciclev10019938m.g	2.243	1.775	-1.070	0.898	AT1G01300.1		Eukaryotic aspartyl protease family protein
Ciclev10019943m.g	-1.328	-0.281	-0.179	-0.668	AT3G16857.1	ARR1,RR1	response regulator 1
Ciclev10019997m.g	0.599	1.676	-1.425	-0.444	AT5G56350.1		Pyruvate kinase family protein
Ciclev10020378m.g	1.343	0.132	0.491	0.175	AT3G47520.1	MDH	malate dehydrogenase
Ciclev10020390m.g	0.769	-0.123	1.056	0.625	AT5G07440.1	GDH2	glutamate dehydrogenase 2
Ciclev10020629m.g	-0.223	0.130	-1.073	-1.087	AT5G24760.1		GroES-like zinc-binding dehydrogenase family protein
Ciclev10020910m.g	0.242	1.126	-0.828	0.070	AT4G17260.1		Lactate/malate dehydrogenase family protein
Ciclev10020949m.g	1.035	1.994	0.296	0.036	AT3G59480.1		pfkB-like carbohydrate kinase family protein
Ciclev10020980m.g	0.319	1.032	0.078	-0.028	AT4G33950.1	ATOST1,OST1,P44,SNRK2-6,SNRK2.6,SRK2E	Protein kinase superfamily protein
Ciclev10021075m.g	-0.038	3.205	-3.457	-0.610	AT1G04410.1		Lactate/malate dehydrogenase family protein
Ciclev10021105m.g	0.656	1.296	0.039	0.192	AT3G59480.1		pfkB-like carbohydrate kinase family protein
Ciclev10021157m.g	0.646	0.947	-0.259	1.651	AT1G25340.1	AtMYB116,MYB116	myb domain protein 116

Ciclev10021269m.g	-0.337	-0.160	-1.967	-1.415	AT3G61610.1		Galactose mutarotase-like superfamily protein
Ciclev10021324m.g	-2.051	-0.350	-2.756	-2.224	AT4G23730.1		Galactose mutarotase-like superfamily protein
Ciclev10021622m.g	1.797	0.891	-1.183	-0.263	AT3G23240.1	ATERF1,ERF 1	ethylene response factor 1
Ciclev10021937m.g	1.197	0.748	-0.811	0.149	AT3G57040.1	ARR9,ATRR4	response regulator 9
Ciclev10022032m.g	0.604	-0.008	-2.182	-4.076	AT4G14550.1	IAA14,SLR	indole-3-acetic acid inducible 14
Ciclev10022370m.g	-3.793	1.264	-3.387	-1.147	AT5G43700.1	ATAUX2-11,IAA4	AUX/IAA transcriptional regulator family protein
Ciclev10022581m.g	1.850	1.855	0.599	1.322	AT4G22620.1		SAUR-like auxin-responsive protein family
Ciclev10022679m.g	0.328	1.543	-0.727	0.989	AT2G47485.1		
Ciclev10023271m.g	-0.052	-1.998	0.033	-0.540	AT4G24040.1	ATTRE1,TRE 1	trehalase 1
Ciclev10023390m.g	-3.290	-5.057	-2.517	-3.426	AT5G44640.1	BGLU13	beta glucosidase 13
Ciclev10023395m.g	2.356	1.451	-0.369	-1.729	AT1G27680.1	APL2	ADPGLC-PPase large subunit
Ciclev10023436m.g	1.071	0.033	1.671	1.340	AT1G03310.1	ATISA2,BE2, DBE1,ISA2	debranching enzyme 1
Ciclev10023627m.g	-4.923	-6.020	-4.028	1.306	AT1G24430.1		HXXXD-type acyl-transferase family protein
Ciclev10023789m.g	-0.041	1.086	-1.481	-0.799	AT1G05610.1	APS2	ADP-glucose pyrophosphorylase small subunit 2
Ciclev10023850m.g	1.502	1.216	0.263	-0.750	AT5G51830.1		pfkB-like carbohydrate kinase family protein

Ciclev10023880m.g	3.013	0.479	0.968	1.884	AT2G21220.1		SAUR-like auxin-responsive protein family
Ciclev10023961m.g	-0.120	0.733	-3.349	-2.157	AT3G62100.1	IAA30	indole-3-acetic acid inducible 30
Ciclev10024024m.g	-1.039	-1.130	-1.301	-0.590	AT4G24210.1	SLY1	F-box family protein
Ciclev10024030m.g	-1.243	0.770	4.391	2.384	AT2G44540.1	AtGH9B9,GH9B9	glycosyl hydrolase 9B9
Ciclev10024067m.g	1.243	2.670	-2.120	1.306	AT3G26040.1		HXXXD-type acyl-transferase family protein
Ciclev10024370m.g	0.364	1.340	0.188	-0.048	AT3G55440.1	ATCTIMC,CYTOTPI,TPI	triosephosphate isomerase
Ciclev10024450m.g	-9.603	-1.269	-10.778	-4.190	AT3G55440.1	ATCTIMC,CYTOTPI,TPI	triosephosphate isomerase
Ciclev10024457m.g	1.071	1.373	2.115	0.985	AT3G47800.1		Galactose mutarotase-like superfamily protein
Ciclev10024575m.g	1.788	4.930	-4.522	-0.124	AT5G14740.2	BETA CA2,CA18,CA2	carbonic anhydrase 2
Ciclev10024638m.g	0.769	2.554	-3.120	-0.289	AT1G73370.1	ATSUS6,SUS6	sucrose synthase 6
Ciclev10024840m.g	0.731	1.301	0.970	1.252	AT4G35830.1	ACO1	aconitase 1
Ciclev10024972m.g	1.088	1.596	-1.362	-1.003	AT4G38050.1		Xanthine/uracil permease family protein
Ciclev10025088m.g	-2.940	-1.150	-2.364	-1.919	AT4G37870.1	PCK1,PEPCK	phosphoenolpyruvate carboxykinase 1
Ciclev10025211m.g	-0.161	-1.351	-1.783	-0.590	AT2G14960.1	GH3.1	Auxin-responsive GH3 family protein
Ciclev10025255m.g	2.325	0.820	0.993	0.525	AT4G26270.1	PFK3	phosphofructokinase 3

Ciclev10025259m.g	1.009	0.433	-0.793	0.179	AT3G13790.1	ATBFRUCT1, ATCWINV1	Glycosyl hydrolases family 32 protein
Ciclev10025306m.g	1.144	-0.390	1.411	0.678	AT1G19940.1	AtGH9B5,GH9B5	glycosyl hydrolase 9B5
Ciclev10025452m.g	1.356	1.929	0.665	1.769	AT2G19860.1	ATHXK2,HXK2	hexokinase 2
Ciclev10025492m.g	1.593	2.802	1.916	1.500	AT4G36250.1	ALDH3F1	aldehyde dehydrogenase 3F1
Ciclev10025533m.g	-1.190	-0.024	0.304	-0.198	AT1G76880.1		Duplicated homeodomain-like superfamily protein
Ciclev10025685m.g	0.116	2.042	-0.515	-1.290	AT5G65140.1		Haloacid dehalogenase-like hydrolase (HAD) superfamily protein
Ciclev10025931m.g	3.321	4.265	1.710	2.183	AT3G51240.1	F3\'H,F3H,TT6	flavanone 3-hydroxylase
Ciclev10025961m.g	1.033	0.363	0.780	0.894	AT1G78080.1	RAP2.4	related to AP2 4
Ciclev10026004m.g	1.038	0.050	0.930	1.020	AT1G78290.2	SNRK2-8,SNRK2.8,SRK2C	Protein kinase superfamily protein
Ciclev10026028m.g	-3.068	-0.117	-3.488	-2.313	AT5G08640.1	ATFLS1,FLS, FLS1	flavonol synthase 1
Ciclev10026121m.g	2.548	0.619	2.233	1.533	AT5G66530.2		Galactose mutarotase-like superfamily protein
Ciclev10026151m.g	1.696	0.479	-3.657	-1.792	AT1G80760.1	NIP6,NIP6;1, NLM7	NOD26-like intrinsic protein 6;1
Ciclev10026175m.g	-0.730	0.235	-0.571	-1.003	AT3G50520.1		Phosphoglycerate mutase family protein
Ciclev10026347m.g	-1.134	-0.714	-0.907	-0.897	AT4G34050.1	CCoAOMT1	S-adenosyl-L-methionine-dependent methyltransferases superfamily protein
Ciclev10026400m.g	1.138	0.759	-2.371	0.018	AT3G15540.1	IAA19,MSG2	indole-3-acetic acid inducible 19

Ciclev10026522m.g	1.517	0.649	1.322	0.977	AT4G14550.1	IAA14,SLR	indole-3-acetic acid inducible 14
Ciclev10026558m.g	0.696	0.687	-2.503	0.957	AT5G48930.1	HCT	hydroxycinnamoyl-CoA shikimate/quinate hydroxycinnamoyl transferase
Ciclev10026661m.g	1.034	8.759	3.852	3.249	AT4G33720.1		CAP (Cysteine-rich secretory proteins, Antigen 5, and Pathogenesis-related 1 protein) superfamily protein
Ciclev10026670m.g	1.534	1.914	0.260	1.157	AT5G48930.1	HCT	hydroxycinnamoyl-CoA shikimate/quinate hydroxycinnamoyl transferase
Ciclev10026685m.g	2.759	5.199	0.063	-1.804	AT1G80100.1	AHP6,HP6	histidine phosphotransfer protein 6
Ciclev10026768m.g	3.342	0.384	0.671	0.536	AT5G53590.1		SAUR-like auxin-responsive protein family
Ciclev10027003m.g	1.057	-1.172	-0.292	-0.430	AT1G56150.1		SAUR-like auxin-responsive protein family
Ciclev10027051m.g	0.092	1.052	-0.744	-0.213	AT1G22170.1		Phosphoglycerate mutase family protein
Ciclev10027101m.g	-2.179	0.295	0.665	-3.654	AT3G16360.2	AHP4	HPT phosphotransmitter 4
Ciclev10027308m.g	-0.796	-0.618	-2.839	-0.815	AT5G48930.1	HCT	hydroxycinnamoyl-CoA shikimate/quinate hydroxycinnamoyl transferase
Ciclev10027552m.g	4.592	4.293	-1.673	-1.888	AT2G26040.1	PYL2,RCAR14	PYR1-like 2
Ciclev10027887m.g	-1.444	-0.557	-3.239	-3.526	AT5G64410.1	ATOPT4,OPT4	oligopeptide transporter 4
Ciclev10028018m.g	2.408	1.909	-2.094	-1.372	AT5G20950.1		Glycosyl hydrolase family protein

Ciclev10028048m.g	-1.287	-0.547	-0.705	-0.643	AT3G47000.1		Glycosyl hydrolase family protein
Ciclev10028056m.g	-1.050	-0.386	-0.626	-0.676	AT5G60790.1	ATGCN1,GCN1	ABC transporter family protein
Ciclev10028067m.g	1.798	-0.454	-0.545	0.270	AT2G15620.1	ATHNIR,NIR,NIR1	nitrite reductase 1
Ciclev10028173m.g	1.535	0.314	-1.099	0.588	AT5G60770.1	ATNRT2.4,NRT2.4	nitrate transporter 2.4
Ciclev10028195m.g	-2.570	0.620	-1.279	-1.156	AT4G39210.1	APL3	Glucose-1-phosphate adenylyltransferase family protein
Ciclev10028230m.g	-1.080	-0.191	-1.776	-1.187	AT5G09220.1	AAP2	amino acid permease 2
Ciclev10028271m.g	1.331	2.203	-2.816	0.940	AT2G21050.1	LAX2	like AUXIN RESISTANT 2
Ciclev10028301m.g	0.456	2.261	-2.451	-2.454	AT4G39010.1	AtGH9B18,GH9B18	glycosyl hydrolase 9B18
Ciclev10028326m.g	0.040	-1.079	0.336	-0.305	AT3G22960.1	PKP-ALPHA,PKP1	Pyruvate kinase family protein
Ciclev10028495m.g	0.871	0.545	1.467	2.046	AT1G07430.1	HAI2	highly ABA-induced PP2C gene 2
Ciclev10028504m.g	3.452	1.908	1.552	5.593	AT1G24430.1		HXXXD-type acyl-transferase family protein
Ciclev10028594m.g	-5.940	-1.636	-3.062	-1.575	AT4G38970.1	FBA2	fructose-bisphosphate aldolase 2
Ciclev10028604m.g	1.383	-0.634	-4.229	-2.397	AT5G13930.1	ATCHS,CHS,TT4	Chalcone and stilbene synthase family protein
Ciclev10028605m.g	0.848	-0.463	-2.151	2.041	AT5G13930.1	ATCHS,CHS,TT4	Chalcone and stilbene synthase family protein
Ciclev10028675m.g	-0.531	-0.625	-1.596	-1.250	AT4G34160.1	CYCD3,CYCD3;1	CYCLIN D3;1
Ciclev10028730m.g	-0.810	1.576	-2.008	-0.215	AT2G22780.1	PMDH1	peroxisomal NAD-malate

							dehydrogenase 1
Ciclev10028824m.g	-2.111	-0.251	-1.484	-0.855	AT5G60800.1		Heavy metal transport/detoxification superfamily protein
Ciclev10028905m.g	-0.023	-1.382	0.748	0.049	AT4G33580.1	ATBCA5,BCA5	beta carbonic anhydrase 5
Ciclev10029072m.g	1.804	-0.382	-0.682	0.302	AT3G19184.1		AP2/B3-like transcriptional factor family protein
Ciclev10029158m.g	-0.120	0.332	-3.264	-0.408	AT4G34050.1	CCoAOMT1	S-adenosyl-L-methionine-dependent methyltransferases superfamily protein
Ciclev10029431m.g	-1.447	-0.151	-3.105	-0.302	AT4G33720.1		CAP (Cysteine-rich secretory proteins, Antigen 5, and Pathogenesis-related 1 protein) superfamily protein
Ciclev10029459m.g	-0.298	1.083	-3.584	-5.179	AT2G14580.1	ATPRB1,PRB1	basic pathogenesis-related protein 1
Ciclev10029493m.g	-0.626	-0.402	2.723	0.832	AT1G03430.1	AHP5	histidine-containing phosphotransfer factor 5
Ciclev10029633m.g	-0.139	3.306	-3.806	-1.426	AT1G75580.1		SAUR-like auxin-responsive protein family
Ciclev10029790m.g	-1.851	-0.495	-3.170	-0.920	AT1G08080.1	ACA7,ATACA7	alpha carbonic anhydrase 7
Ciclev10029836m.g	1.835	-0.499	0.358	1.455	AT5G60770.1	ATNRT2.4,NRT2.4	nitrate transporter 2.4
Ciclev10029873m.g	2.893	-5.166	-6.053	-0.124	AT1G50060.1		CAP (Cysteine-rich secretory proteins, Antigen 5, and Pathogenesis-related 1 protein) superfamily protein
Ciclev10030029m.g	0.464	0.010	-1.354	1.356	AT2G14580.1	ATPRB1,PRB1	basic pathogenesis-related protein 1

Ciclev10030045m.g	1.381	1.716	1.723	2.749	AT5G65550.1		UDP-Glycosyltransferase superfamily protein
Ciclev10030093m.g	-10.195	0.672	-10.754	-3.261	AT5G13930.1	ATCHS,CHS,TT4	Chalcone and stilbene synthase family protein
Ciclev10030235m.g	-1.704	-1.671	-2.721	-2.950	AT3G57230.2	AGL16	AGAMOUS-like 16
Ciclev10030271m.g	-2.608	-1.532	-1.902	-1.089	AT5G65550.1		UDP-Glycosyltransferase superfamily protein
Ciclev10030358m.g	1.952	-0.324	0.126	1.586	AT5G60770.1	ATNRT2.4,NRT2.4	nitrate transporter 2.4
Ciclev10030398m.g	-1.256	0.327	-5.685	-3.118	AT5G13930.1	ATCHS,CHS,TT4	Chalcone and stilbene synthase family protein
Ciclev10030691m.g	0.327	1.055	-0.352	0.344	AT1G23870.1	ATTPS9,TPS9	trehalose-phosphatase/synthase 9
Ciclev10030911m.g	-5.273	-0.060	-3.227	-2.200	AT5G02810.1	APRR7,PRR7	pseudo-response regulator 7
Ciclev10030929m.g	-1.712	-0.791	-0.989	-1.571	AT5G45110.1	ATNPR3,NPR3	NPR1-like protein 3
Ciclev10031115m.g	-1.267	1.091	-0.487	-1.365	AT4G19660.1	ATNPR4,NPR4	NPR1-like protein 4
Ciclev10031126m.g	0.761	-0.286	-1.581	-2.167	AT1G12940.1	ATNRT2.5,NRT2.5	nitrate transporter2.5
Ciclev10031131m.g	-1.447	0.269	-0.332	-0.136	AT2G39130.1		Transmembrane amino acid transporter family protein
Ciclev10031178m.g	-3.171	-1.018	-3.243	-3.554	AT2G44480.1	BGLU17	beta glucosidase 17
Ciclev10031212m.g	1.546	1.036	-0.375	1.181	AT2G44480.1	BGLU17	beta glucosidase 17
Ciclev10031262m.g	1.385	1.466	0.831	0.613	AT5G44640.1	BGLU13	beta glucosidase 13

Ciclev10031310m.g	-8.214	-2.867	-5.813	-7.516	AT4G19660.1	ATNPR4,NPR4	NPR1-like protein 4
Ciclev10031343m.g	-0.788	-1.419	-1.159	-1.270	AT5G45110.1	ATNPR3,NPR3	NPR1-like protein 3
Ciclev10031413m.g	0.608	1.158	-1.237	0.550	AT5G01240.1	LAX1	like AUXIN RESISTANT 1
Ciclev10031441m.g	1.466	-0.215	0.052	0.171	AT1G68640.1	PAN	bZIP transcription factor family protein
Ciclev10031483m.g	-2.447	0.794	-2.532	-0.646	AT2G39710.1		Eukaryotic aspartyl protease family protein
Ciclev10031627m.g	-2.610	-0.197	-1.646	-2.024	AT5G45110.1	ATNPR3,NPR3	NPR1-like protein 3
Ciclev10031681m.g	0.503	0.870	-1.958	-0.963	AT5G07440.2	GDH2	glutamate dehydrogenase 2
Ciclev10031749m.g	-1.678	-1.104	-2.585	-2.068	AT5G45110.1	ATNPR3,NPR3	NPR1-like protein 3
Ciclev10032014m.g	1.650	2.642	0.296	0.309	AT3G04120.1	GAPC,GAPC-1,GAPC1	glyceraldehyde-3-phosphate dehydrogenase C subunit 1
Ciclev10032075m.g	1.833	1.534	0.571	0.661	AT5G23250.1		Succinyl-CoA ligase, alpha subunit
Ciclev10032517m.g	2.325	1.513	-0.219	1.838	AT5G14740.2	BETA CA2,CA18,CA2	carbonic anhydrase 2
Ciclev10032519m.g	-0.361	-0.612	1.037	1.396	AT5G13790.1	AGL15	AGAMOUS-like 15
Ciclev10032537m.g	0.663	2.172	0.195	-0.023	AT3G55440.1	ATCTIMC,CYTOTPI,TPI	triosephosphate isomerase
Ciclev10032697m.g	1.374	-0.034	0.296	-0.062	AT3G55120.1	A11,CFI,TT5	Chalcone-flavanone isomerase family protein
Ciclev10032749m.g	-2.725	0.651	-2.735	-1.573	AT5G05270.2		Chalcone-flavanone isomerase family protein

Ciclev10032781m.g	-1.112	0.447	-3.167	-1.527	AT2G38310.1	PYL4,RCAR10	PYR1-like 4
Ciclev10033008m.g	3.378	1.909	2.614	2.003	AT1G03430.1	AHP5	histidine-containing phosphotransfer factor 5
Ciclev10033363m.g	2.506	1.325	3.755	2.279	AT5G50760.1		SAUR-like auxin-responsive protein family
Ciclev10033388m.g	1.207	0.447	0.064	0.216	AT5G06800.1		myb-like HTH transcriptional regulator family protein
Ciclev10033497m.g	-0.199	0.881	0.903	1.283	AT3G26744.4	ATICE1,ICE1, SCRM	basic helix-loop-helix (bHLH) DNA-binding superfamily protein
Ciclev10033533m.g	-8.344	-2.711	-5.346	-9.726	AT5G45110.1	ATNPR3,NPR3	NPR1-like protein 3
Ciclev10033569m.g	1.694	0.791	0.855	1.252	AT5G45110.1	ATNPR3,NPR3	NPR1-like protein 3
Ciclev10033605m.g	-8.494	-1.806	-5.997	-4.039	AT5G58080.1	ARR18,RR18	response regulator 18
Ciclev10033759m.g	3.804	1.640	-1.184	-2.112	AT2G24400.1		SAUR-like auxin-responsive protein family
Ciclev10033821m.g	-1.599	-4.303	-5.271	-6.013	AT1G75290.1		NAD(P)-binding Rossmann-fold superfamily protein
Ciclev10033907m.g	1.500	2.540	1.006	0.801	AT5G48930.1	HCT	hydroxycinnamoyl-CoA shikimate/quinate hydroxycinnamoyl transferase
Ciclev10033908m.g	-0.980	-0.406	-1.945	-1.557	AT4G19660.1	ATNPR4,NPR4	NPR1-like protein 4

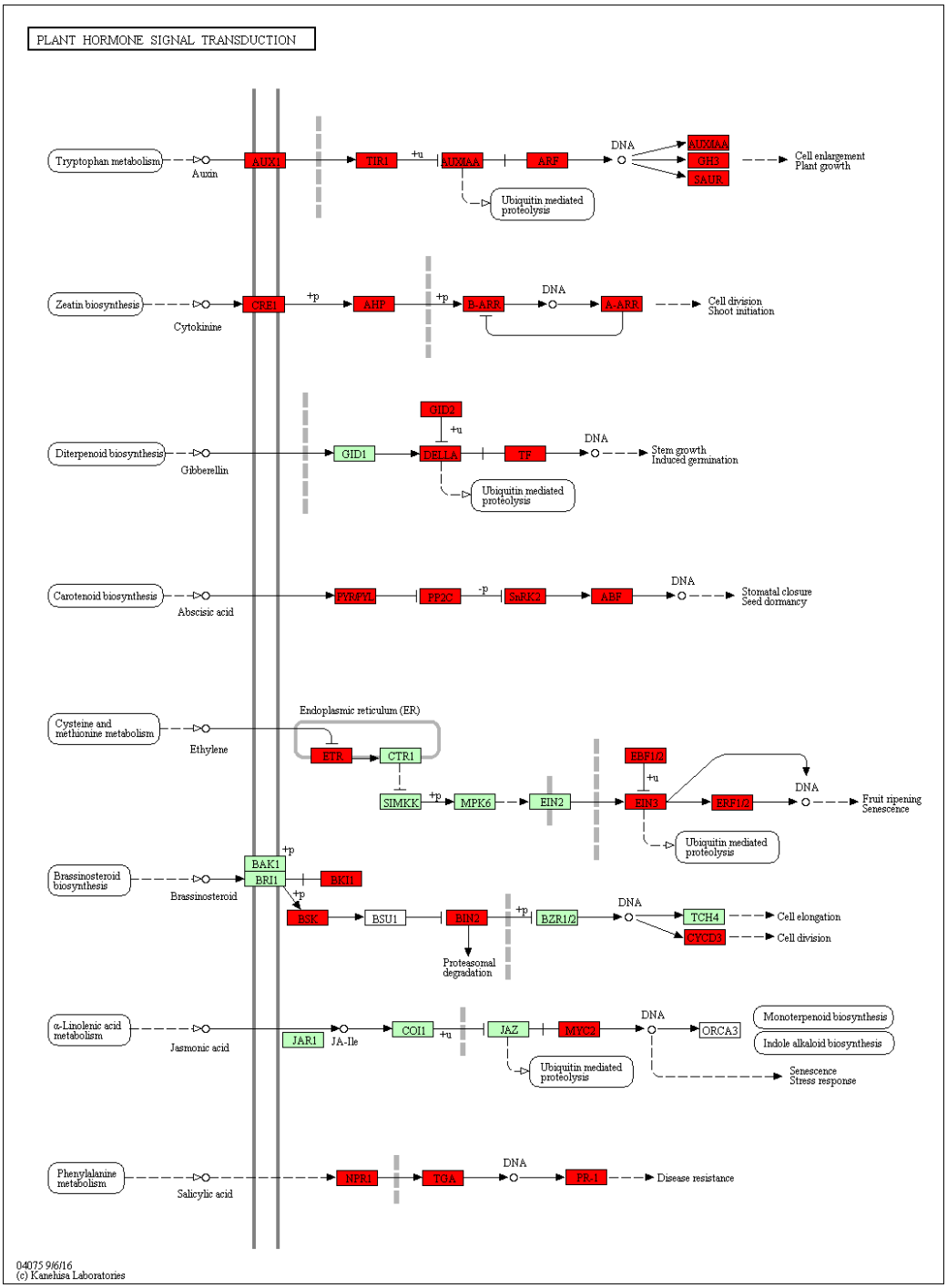

Supplemental Figure 2.3. Schematic of the 'Plant hormone signal transduction' pathway. DEGs from the comparison of trifoliate rootstock versus rough lemon rootstock highlighted in red. The map is from the Kyoto Encyclopedia of Genes and Genomes (KEGG).

General Conclusion

Citrus is one of the most widely grown and economically important fruit crops in the world. Total production of citrus in the United states in the 2018 growing season was 6.1 million tons, with California producing more than 50 percent of the United States total[1]. With over 75 percent of California's citrus production being sold to the fresh market, it is imperative to generate high quality, attractive fruit in this state's numerous growing regions. This becomes increasingly difficult due to changes in climate and emerging diseases that threaten the citrus industry[2–4].

Commercial citrus trees are rarely grown from seed and virtually all are propagated by grafting. Different citrus rootstocks are required for the profitability of the citrus industry in California, enabling certain scion varieties to be grown throughout the diverse geographical territories of this state. Grafted trees primarily provide a reduction in juvenility, greater uniformity, and rootstocks can have many effects on fruit quality, including changes in rind thickness, juice content and color, and soluble solid and acid concentrations. Furthermore, rootstocks may help the plant to be more drought tolerant or pest and disease resistant[5]. The most significant impacts of grafting are on tree growth, vigor and yield, tree nutrition, stress resistance, and fruit quality[6–9].

In the present study, four rootstocks were chosen from a rootstock trial with Washington navel orange scion in Riverside, CA to assess for various fruit quality traits; Argentina sweet orange, Schaub rough lemon, Carrizo citrange, and Rich 16-6 trifoliate orange. These rootstocks have been characterized in many previous studies and grafted trees display significant phenotypic differences in overall growth and fruit quality[6,10–16]. In

general, rough lemon rootstocks produce the highest yield and fruit size, but fruit is of lower quality, containing lower acidity and lower levels of total soluble solids, also known as the “dilution effect”[17]. On the other hand, trees on trifoliate orange produce smaller, high quality fruit with high yield on smaller trees. Carrizo citrange rootstocks produce intermediate yield with good fruit quality. Sweet orange rootstocks produce good quality fruit, but trees are very susceptible to various citrus diseases and are therefore not commonly used as a rootstock. The phenotypic fruit quality data from the rootstock trial used in this study were largely in agreement with those found in the aforementioned studies.

While the variations in fruit quality of grafted citrus trees have been well documented, the mechanisms by which rootstocks impart these traits, especially at the regulatory level, have not been elucidated. Knowledge of the root transcriptome in citrus are extremely limited, and to date, no comparative studies of citrus rootstocks have been performed and no reports have linked the genetic effects of citrus rootstocks to fruit quality. At the regulatory level, miRNAs have been found to act as master regulators of various biological and metabolic processes (Chen, 2009). Recent research has identified numerous miRNAs involved in fruit development and maturation in a variety of fruit crops, including strawberry[18,19], apple[20], grape[21], peach[22], blueberry[23], date palm[24], tomato[25] and citrus[26]. Additionally, the expression profiles of miRNAs can also be influenced by various rootstock-scion combinations and has been investigated in a few crops such as grapevine, watermelon, cucumber and tomato[27–31]. However, no information is available in citrus about the role of miRNAs underlying differences in fruit quality observed between rootstocks.

The present study aimed at identifying small RNAs that are likely causing changes in fruit quality in grafted citrus. To achieve this, an integrated study of miRNA and mRNA transcriptomes of sweet orange scions grafted onto genetically varying rootstocks was performed. Transcriptomes and miRNomes of fruit and root tissues from four different scion-rootstock combinations at four time points throughout fruit development were obtained. DEGs and DEMs were identified between rootstock genotypes and the fruit grown on these rootstocks during fruit development. The majority of the DEGs were observed in comparisons involving rough lemon rootstocks, especially when compared to trifoliate orange. This correlated well with the observed differences in fruit quality traits. Among the differentially expressed genes in fruit were several genes with functions involved in fruit quality traits, such as those relating to starch and sucrose metabolism, fructose metabolism, and hormone signaling-related genes. Several genes involved in various hormone signaling pathways, including transcription factors were DE. Mainly genes in the abscisic acid (ABA) and auxin response pathways were affected by rootstocks, genes which are known to be regulators of fruit ripening in non-climacteric fruit[32–34]. These genes were generally up-regulated in fruit grown on trifoliate rootstock compared to rough lemon, which may play a role in the ripening process.

Additionally, DEGs related to cell expansion, an important feature of fruit development, were investigated. PIP and EXP genes were down-regulated in fruit grown on trifoliate rootstock compared to rough lemon, which likely contribute to the smaller fruit size observed. This is in agreement with other fruit crops, such as grape, apple, strawberry, and tomato[35–38]. Lastly, two genes were DE in fruit that relate to sugar and acid accumulation, an important determinant of taste and flavor in citrus. A P-type H^+-ATPase was up-regulated late in the growing season and a vacuolar invertase, was down-

regulated in fruit grown on trifoliate rootstock compared to rough lemon. These two genes have been associated with acid and sugar accumulation, respectively[39–43]. The expression profiles of these genes could potentially lead to increased sugar and acid levels in fruit grown on trifoliate rootstock. This, in combination with the decreased size of fruit from scions grafted onto trifoliate rootstock provide a basis for the improved fruit quality when using this rootstock.

A much larger number of DEMS and DEGs were identified between rootstock genotypes in root tissue than in fruit, most of which were DE in comparisons involving trifoliate. Functional analysis of the DEGs revealed enrichment of genes involved in defense response, cell wall organization or biosynthesis, and many other cell wall related processes. Several genes were DE between trifoliate and rough lemon rootstocks that have been linked to an alteration of the root system architecture (RSA) in other crop species. The expression profiles of these genes typically lead to an increase in lateral roots, which could potentially cause trifoliate root systems to be better adapted to unfavorable environmental conditions. A more vigorous root system would allow for a plant to uptake water and nutrients more easily, which impacts overall growth and fruit quality of the scion[44,45]. Moreover, genes with influences on biotic and abiotic stress responses were DE between trifoliate and rough lemon rootstocks, particularly those involved in cold tolerance and pathogen defense. The increased ability of trifoliate rootstock to adapt and respond to these stressors alters water and nutrient uptake, which helps improve citrus fruit quality[46–48].

Furthermore, genes that may be responsible for phenotypic differences in grafted citrus and miRNAs that target them were validated by qRT-PCR. Largely, there was a positive

correlation between the RNA-seq and qRT-PCR data, as well as a negative correlation between miRNA and mRNA expression. This suggests that the miRNAs might play an important role in the diverse biological and metabolic processes in citrus and grafting may possibly change miRNA expression profiles to regulate plant growth and development, as well as adapt to stress. The identification of miRNAs and their target genes from this study provided new insights into miRNA-mediated regulation in grafted citrus. The results offer a basis for future investigation of mechanisms that regulate citrus fruit ripening.

The results from this study enhance our understanding of rootstock effects in grafted citrus but require additional functional validation. The gene-to-phenotype relationship of these genes could not be assessed in this work, but these results lay the groundwork for further experiments that should provide insights into the molecular mechanisms underlying improved fruit quality of citrus. The genes validated in these studies are good candidates for functional analysis and provide a better overview of the mechanisms of complex metabolic and regulatory systems of grafted citrus trees. With the emergence of the simple and affordable CRISPR/Cas9 genome editing system, the genes and miRNAs DE in this project can be modified in citrus plants to confirm the inferred effects on fruit quality[49–51]. These findings may ultimately be useful for developing rootstock varieties that will enhance fruit quality in citrus breeding programs in the future.

References

1. Citrus Fruits 2018 Summary 08/28/2018. 35 (2018).

2. Bove, J. Huanglongbing : a destructive, newly-emerging, century-old disease of citrus. *Journal of Plant Pathology* **88**, (2018).

3. Chaube, H. S. & Pundhir, V. S. *Crop diseases and their management*. (PHI Learning Pvt. Ltd., 2005).

4. Rosenzweig, C., Phillips, J., Goldberg, R., Carroll, J. & Hodges, T. Potential impacts of climate change on citrus and potato production in the US. *Agricultural Systems* **52**, 455–479 (1996).

5. Castle, W. S. A career perspective on citrus rootstocks, their development, and commercialization. *HortScience* **45**, 11–15 (2010).

6. Martínez-Cuenca, M.-R., Primo-Capella, A. & Forner-Giner, M. A. Influence of rootstock on citrus tree growth: effects on photosynthesis and carbohydrate distribution, plant size, yield, fruit quality, and dwarfing genotypes. *Plant Growth* (2016). doi:10.5772/64825

7. Simpson, C. R. *et al.* Growth response of grafted and ungrafted citrus trees to saline irrigation. *Scientia Horticulturae* **169**, 199–205 (2014).

8. Castle, W. S. Rootstock as a fruit quality factor in citrus and deciduous tree crops. *New Zealand Journal of Crop and Horticultural Science* **23**, 383–394 (1995).

9. Zhang, X., Breksa, A. P., Mishchuk, D. O. & Slupsky, C. M. Elevation, rootstock, and soil depth affect the nutritional quality of mandarin oranges. *J. Agric. Food Chem.* **59**, 2672–2679 (2011).

10. Al-Jaleel, A. & Zekri, M. Effects of rootstocks on yield and fruit quality of ‘Parent Washington Navel’ trees. *Proceedings of the Florida State Horticultural Society* **116**, 270–275 (2003).

11. Liu, X.-Y., Li, J., Liu, M.-M., Yao, Q. & Chen, J.-Z. Transcriptome profiling to understand the effect of citrus rootstocks on the growth of ‘Shatangju’ mandarin. *PLOS ONE* **12**, e0169897 (2017).

12. Roose, M. Lane Late navel orange replant trial at Lindcove. (2009).

13. Roose, M. L., Cole, D. A., Atkin, D. & Kupper, R. S. Yield and tree size of four citrus cultivars on 21 rootstocks in California. *Journal of the American Society for Horticultural Science* (1989).

14. Rouse, R. E. Citrus fruit quality and yield of six Valencia clones on 16 rootstocks in the Immokalee foundation grove. *Proceedings of the Florida State Horticultural Society* **113**, 112–114 (2000).

15. Sinclair, W. & Bartholomew, E. Effects of rootstock and environment on the composition of oranges and grapefruit. *Hilgardia* **16**, 125–176 (1944).

16. Rootstocks effects on fruit quality. *Factors affecting fruit quality. Lake Alfred: University of Florida* 24–34 (1988).

17. Barry, G. H., Castle, W. S. & Davies, F. S. Rootstocks and plant water relations affect sugar accumulation of citrus fruit via osmotic adjustment. *Journal of the American Society for Horticultural Science* **129**, 881–889 (2004).

18. Csukasi, F. *et al.* Two strawberry miR159 family members display developmental-specific expression patterns in the fruit receptacle and cooperatively regulate Fa-GAMYB. *New Phytol.* **195**, 47–57 (2012).

19. Li, D. *et al.* Developmental and stress regulation on expression of a novel miRNA, Fan-miR73, and its target ABI5 in strawberry. *Scientific Reports* **6**, 28385 (2016).

20. Qu, D. *et al.* Identification of microRNAs and their targets associated with fruit-bagging and subsequent sunlight re-exposure in the 'Granny Smith' apple exocarp using high-throughput sequencing. *Front Plant Sci* **7**, 27 (2016).

21. Paim Pinto, D. L. *et al.* The influence of genotype and environment on small RNA profiles in grapevine berry. *Front Plant Sci* **7**, (2016).

22. Zhu, H. *et al.* Unique expression, processing regulation, and regulatory network of peach (Prunus persica) miRNAs. *BMC Plant Biol.* **12**, 149 (2012).

23. Hou, Y. *et al.* Comparative analysis of fruit ripening-related miRNAs and their targets in blueberry using small RNA and degradome sequencing. *Int J Mol Sci* **18**, (2017).

24. Xin, C. *et al.* Profiling microRNA expression during multi-staged date palm (Phoenix dactylifera L.) fruit development. *Genomics* **105**, 242–251 (2015).

25. Moxon, S. *et al.* Deep sequencing of tomato short RNAs identifies microRNAs targeting genes involved in fruit ripening. *Genome Res.* **18**, 1602–1609 (2008).

26. Wu, J., Zheng, S., Feng, G. & Yi, H. Comparative analysis of miRNAs and their target transcripts between a spontaneous late-ripening sweet orange mutant and its wild-type using small RNA and degradome sequencing. *Front Plant Sci* **7**, 1416 (2016).

27. Khaldun, A. B. M. *et al.* Comparative profiling of miRNAs and target gene identification in distant-grafting between tomato and Lycium (goji berry). *Front. Plant Sci.* **7**, (2016).

28. Li, C., Li, Y., Bai, L., He, C. & Yu, X. Dynamic expression of miRNAs and their targets in the response to drought stress of grafted cucumber seedlings. *Horticultural Plant Journal* **2**, 41–49 (2016).

29. Li, C. *et al.* Grafting-responsive miRNAs in cucumber and pumpkin seedlings identified by high-throughput sequencing at whole genome level. *Physiologia Plantarum* **151**, 406–422 (2014).

30. Liu, N., Yang, J., Guo, S., Xu, Y. & Zhang, M. Genome-wide identification and comparative analysis of conserved and novel microRNAs in grafted watermelon by high-throughput sequencing. *PLOS ONE* **8**, e57359 (2013).

31. Pagliarani, C. *et al.* The accumulation of miRNAs differentially modulated by drought stress is affected by grafting in grapevine. *Plant Physiol.* **173**, 2180–2195 (2017).

32. Bassa, C., Mila, I., Bouzayen, M. & Audran-Delalande, C. Phenotypes associated with down-regulation of Sl-IAA27 support functional diversity among Aux/IAA family members in tomato. *Plant Cell Physiol* **53**, 1583–1595 (2012).

33. Leng, P., Yuan, B. & Guo, Y. The role of abscisic acid in fruit ripening and responses to abiotic stress. *J Exp Bot* **65**, 4577–4588 (2014).

34. Su, L. *et al.* The auxin Sl-IAA17 transcriptional repressor controls fruit size via the regulation of endoreduplication-related cell expansion. *Plant Cell Physiol* **55**, 1969–1976 (2014).

35. Alleva, K. *et al.* Cloning, functional characterization, and co-expression studies of a novel aquaporin (FaPIP2;1) of strawberry fruit. *J Exp Bot* **61**, 3935–3945 (2010).

36. Doligez, A. *et al.* New stable QTLs for berry weight do not colocalize with QTLs for seed traits in cultivated grapevine (Vitis vinifera L.). *BMC Plant Biology* **13**, 16 (2013).

37. Hu, C.-G., Hao, Y.-J., Honda, C., Kita, M. & Moriguchi, T. Putative PIP1 genes isolated from apple: expression analyses during fruit development and under osmotic stress. *J Exp Bot* **54**, 2193–2194 (2003).

38. Marowa, P., Ding, A. & Kong, Y. Expansins: roles in plant growth and potential applications in crop improvement. *Plant Cell Rep* **35**, 949–965 (2016).

39. Aprile, A. *et al.* Expression of the H+-ATPase AHA10 proton pump is associated with citric acid accumulation in lemon juice sac cells. *Funct Integr Genomics* **11**, 551–563 (2011).

40. Huang, D., Zhao, Y., Cao, M., Qiao, L. & Zheng, Z.-L. Integrated systems biology analysis of transcriptomes reveals candidate genes for acidity control in developing fruits of sweet orange (Citrus sinensis L. Osbeck). *Front. Plant Sci.* **7**, (2016).

41. Lester, G. E., Arias, L. S. & Gomez-Lim, M. Muskmelon fruit soluble acid invertase and sucrose phosphate synthase activity and polypeptide profiles during growth and maturation. *Journal of the American Society for Horticultural Science* **126**, 33–36 (2001).

42. Ohyama, A. *et al.* Suppression of acid invertase activity by antisense RNA modifies the sugar composition of tomato fruit. *Plant Cell Physiol* **36**, 369–376 (1995).

43. Shi, C.-Y. *et al.* Citrus PH5-like H+-ATPase genes: identification and transcript analysis to investigate their possible relationship with citrate accumulation in fruits. *Front. Plant Sci.* **6**, (2015).

44. Malamy, J. E. Intrinsic and environmental response pathways that regulate root system architecture. *Plant, Cell & Environment* **28**, 67–77 (2005).

45. Malamy, J. E. & Ryan, K. S. Environmental regulation of lateral root initiation in Arabidopsis. *Plant Physiology* **127**, 899–909 (2001).

46. Zekri, M. & Parsons, L. R. Salinity tolerance of citrus rootstocks: effects of salt on root and leaf mineral concentrations. *Plant Soil* **147**, 171–181 (1992).

47. Obreza, T. A. & Schumann, A. Keeping water and nutrients in the Florida citrus tree root zone. *HortTechnology* **20**, 67–73 (2010).

48. Panigrahi, P. & Srivastava, A. K. Water and nutrient management effects on water use and yield of drip irrigated citrus in vertisol under a sub-humid region. *Journal of Integrative Agriculture* **16**, 1184–1194 (2017).

49. Belhaj, K., Chaparro-Garcia, A., Kamoun, S., Patron, N. J. & Nekrasov, V. Editing plant genomes with CRISPR/Cas9. *Current Opinion in Biotechnology* **32**, 76–84 (2015).

50. Bortesi, L. & Fischer, R. The CRISPR/Cas9 system for plant genome editing and beyond. *Biotechnology Advances* **33**, 41–52 (2015).

51. Jia, H., Zou, X., Orbovic, V. & Wang, N. Genome editing in citrus tree with CRISPR/Cas9. in *Plant Genome Editing with CRISPR Systems: Methods and Protocols* (ed. Qi, Y.) 235–241 (Springer New York, 2019). doi:10.1007/978-1-4939-8991-1_17